MATCH
Communications in Mathematical and in Computer Chemistry

MATCH Commun. Math. Comput. Chem. **88** (2022) 239–318
ISSN: 0340–6253
doi: 10.46793/match.88-2.239F

Klein Four-Group as the Factor Group for Elucidating *RS*-Stereoisomerism of Cubane Derivatives. The Factor-Group Method for Type-Itemized Enumeration of Stereoisograms

Shinsaku Fujita[a,*]

[a] *Shonan Institute of Chemoinformatics and Mathematical Chemistry, Kaneko 479-7 Ooimachi, Ashigara-Kami-Gun, Kanagawa-Ken, 258-0019 Japan*

shinsaku_fujita@nifty.com

(Received February 8, 2022)

Abstract

Van't Hoff's way (asymmetry, stereogenicity) and Le Bel's way (dissymmetry, chirality) are compared from the viewpoint of two ways for investigating organic stereochemistry, where cubane derivatives of the point group $\boldsymbol{O}_h$ are selected as probes. For emphasizing Le Bel's way, combinatorial enumerations of 3D structures under point groups are first discussed to develop Fujita's proligand method and Fujita's USCI approach. The foundations of these enumerations are applied to support synthetic studies of stereoisomers for emphasizing van't Hoff's way after the proposal of Fujita's stereoisogram approach based on *RS*-stereoisomeric groups, e.g., $\boldsymbol{O}_{h\widetilde{\sigma}\widehat{I}}$. Importance of the proligand-promolecule model is emphasized in enumerations under point groups (Fujita's proligand method and Fujita's USCI approach) as well as in enumerations of *RS*-stereoisomeric groups (Fujita's stereoisogram approach). After the five types (type I to type V) of stereoisograms are classified into three categories (i.e.,

*Corresponding author.

Category 1 (types I/IV), Category 2 (types II/III/V), and the coexistence case), the half-size-subgroup method and the factor-group method have been developed for type-itemized enumerations of stereoisograms. Type-V stereoisograms for characterizing "extended pseudoasymmetry" are discussed by assigning their configuration numbers and *CA*-descriptors.

1 Introduction

1.1 Van't Hoff's way and Le Bel's way for investigating organic stereochemistry

The concept of *stereoisograms* proposed by the author (Fujita) [1–3] aims at excluding serious conceptual confusions, which have been caused by the two different ways derived from two founders of organic stereochemistry, i.e., van't Hoff's way based on "asymmetry" [4, 5] (later replaced by the term "stereogenicity" in the Mislow-Siegel's article [6]) and Le Bel's way based on "dissymmetry" [7, 8] (later replaced by the term "chirality" in the lecture by Lord Kelvin [9]), ever since the beginning of organic stereochemistry. In this paper, inherent inconsistency between van't Hoff's way and Le Bel's way during the practices of the conventional stereochemistry will be discussed by paying attention to dynamic and static aspects.

1.2 Syntheses of stereoisomers. Emphasis on van't Hoff's way in dynamic aspects of stereochemistry

The term "stereogenic" originally aims at representing generation of stereoisomers [6], the number of which may be two *or more*, so that pairwise nature is not included as intrinsic nature. Hence, the pairwise use of stereogenic/non-stereogenic or stereogenic/astereogenic is beyond the scope of the assumption in contrast to the pairwise use of chirality/achirality.

As a result of lacking pairwise nature, during practices under the conventional organic stereochemistry, Mislow-Siegel's stereogenicity has been adopted in the form of "stereogenic units", which may be classified into two *or more* units, so as to be categorized into stereogenic centers (atoms),

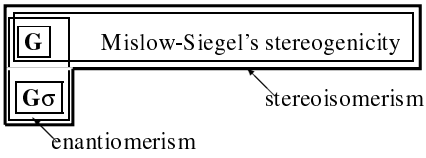

Figure 1. Conventional stereochemistry based on enantiomerism, Mislow-Siegel's stereogenicity, and stereoisomerism.

stereogenic axes, stereogenic planes, and so on [10]. In particular, an "asymmetric atom (chirality centre)" is adopted as the traditional example of a stereogenic unit in IUPAC recommendations 1996 [10].

So long as we examine the usage described in IUPAC recommendations 1996 [10], chirality is treated as a subordinate concept to Mislow-Siegel's stereogenicity to specify the nature of stereogenic units. After preparing the terms "chirotopic/achirotopic centers" [6], some achiral cases $\boldsymbol{G}\sigma$ are treated under the term "pseudoasymmetry" as exceptional cases of "asymmetry", and accordingly as exceptional cases of Mislow-Siegel's stereogenicity (Figure 1).

According to IUPAC recommendations 1996 [10], the term "chirotopic" is defined to be "the description of an atom (or point, group, face, etc. in a molecular model) that resides within a chiral" environment, while the term "achirotopic" is defined to be "one that resides within an achiral environment has been called achirotopic." Thus, chirotopic/achirotopic centers are subordinate concepts of Mislow-Siegel's stereogenicity. More pictorially speaking, the vertical frame of the enantiomerism is redrawn horizontally in Figure 1, so as to be completely involved in the horizontal frame of Mislow-Siegel's stereogenicity. This treatment would reinforce the viewpoint about the naming "pseudoasymmetry" for specifying some achiral cases $\boldsymbol{G}\sigma$ ("asymmetry" modified with "pseudo"). .

In spite of preparing the terms "chirotopic/achirotopic centers" [6] for the purposes of further discussions concerning "pseudoasymmetry", the relationship between chirality and Mislow-Siegel's stereogenicity has provided us with some sources of misunderstanding.

In addition to "pseudoasymmetry" [11,12], we are able to perceive that there have appeared several fundamental terms with inaccurate or ambigu-

ous interpretations, such as "*R/S* vs. *r/s*" in the *RS*-nomenclature (the CIP system) [13,14], "stereogenicity" [15], and "prochirality" [16,17]. The details of inaccuracy or ambiguity have been discussed respectively in the references cited above after the proposal of the concept of stereoisograms.

1.3 Combinatorial enumeration of 3D structures under point groups. Emphasis on Le Bel's way in static aspects of stereochemistry

Before starting discussions on stereoisograms and *RS*-stereoisomeric groups, several fundamental aspects on symmetry-itemized enumerations and gross enumerations of 3D structures under point groups should be pointed out by comparing the counterparts for enumerations of graphs. These fundamental aspects for the proligand-promolecule model and for the USCI approach will be extended to cover Fujita's stereoisogram approach.

1. The proligand-promolecule model based on a given skeleton [18,19].

   A proligand is an abstract ligand (substituent) which is characterized to be chiral or achiral in isolation, but to have no concrete 3D structure even if chiral. A promolecule is an abstract molecule which is constructed by putting a set of such proligands on the substitution positions of an appropriate skeleton belonging to a given point group $\boldsymbol{G}$. The presence of achiral and chiral proligands is a crucial point during 3D structural enumeration. On the other hand, the conventional graph enumeration does not depend on such proligand-promolecule model but postulates the presence of achiral ligands (and no chiral ligands), as found in Pólya's graph enumerations [20,21].

2. The concept of sphericity of an orbit and chirality fittingness [22–24].

   The substitution positions of the skeleton are separated into orbits (equivalence classes), each of which belongs to a coset representation $(\boldsymbol{G}_i\backslash)\boldsymbol{G}$ under the subgroup $\boldsymbol{G}_i$ of $\boldsymbol{G}$ during a substitution process. Symmetry-itemized enumerations based on tables of marks (mark tables) [25] have been extended to treat both achiral and chiral proligands on the basis of the *sphericity* of an orbit [22,23]. Thus, each

orbit is controlled by its *sphericity* due to the coset representation $(\boldsymbol{G}_i\backslash)\boldsymbol{G}$, so as to be classified into a *homospheric orbit* (if both $\boldsymbol{G}$ and $\boldsymbol{G}_i$ are achiral), an *enantiospheric orbit* (if $\boldsymbol{G}$ is achiral and $\boldsymbol{G}_i$ is chiral), and a *hemispheric orbit* (if both $\boldsymbol{G}$ and $\boldsymbol{G}_i$ are chiral) [22]. Each orbit has *chirality fittingness* according to its sphericity, so that a homospheric orbit permits the substitution of a set of achiral proligands, an enantiospheric orbit permits the substitution of a set of the same achiral proligands or pairs of enantiomeric proligands, as well as a hemispheric orbit permits the substitution of a set of same achiral or chiral proligands. Thus, chirality fittingness due to sphericity controls symmetry-itemized enumeration [23, 24].

3. The concept of the USCI-CF of an orbit [22–24].

   Each orbit is controlled by the USCI-CF (unit subduced cycle index with chirality fittingness), which is derived by the subduction of coset representation [22, 23]. The USCI-CF table corresponding to a mark table can be used to symmetry-itemized enumerations, where four enumeration methods are developed under the collective name *Fujita's USCI approach*: (1) the partial-cycle-index (PCI) method by using *partial cycle indices with chirality fittingness* (PCI-CFs) [26, 27], (2) the fixed-point matrix (FPM) method [28–30], (3) the elementary-superposition (ES) method [31], and (4) the partial-superposition (PS) method [26,31]. The symmetry-itemized enumerations based on a cubane as an $\boldsymbol{O}_h$-skeleton have been conducted by means of the FPM method [32], the PCI method [33], and the ES method [34].

4. The concept of sphericity of a cycle and chirality fittingness [35].

   Pólya's Theorem [36] has been extended to cover 3D structures along with graphs, where the proligand-promolecule model is adopted to create the concept of *sphericity of a cycle* [35]. Thereby, *cycle indices with chirality fittingness* (CI-CFs) have been developed to establish the proligand method [37] for gross enumerations of 3D structures, e.g., extended sphericity indices of cycles for stereochemical extension of Pólya's coronas [38], the use of different sets of sphericity

indices for combinatorial enumeration of nonrigid stereoisomers [39], and combinatorial enumeration of planted 3D trees as stereochemical models of monosubstituted alkanes [40].

The applicabilities of Fujita's proligand method and related methods [37] have been studied by using a cubane skeleton of $\boldsymbol{O}_h$-point group as a probe [41]; i.e., gross enumerations of cubane derivatives by Fujita's proligand method [41], by Fujita's markaracter method [42], by Fujita's characteristic-monomial method [43], by Fujita's extended-superposition method [44], and by Fujita's double-coset-representation method [45].

5. Emphasis on equivalence relationships and equivalence classes (orbits).

   IUPAC 1996 [10] defines *stereoisomerism* as "Isomerism *due to differences* in the spatial arrangement of atoms *without any differences* in connectivity or bond multiplicity between the isomers. (the expression "differences" is stressed as an italicized form by the author.)" This definition is not an equivalence relationship, because there always appear two different entities, i.e., the original entity and the isomeric entity. As a result, it is unable to deal with one-membered equivalence class (orbit).

   Orbits in a molecule [24] and orbits among molecules [46] are linked with each other to accomplish combinatorial enumeration of stereoisomers [47]. Thereby, the concept of mandalas based on Fujita's proligand method has been formulated as a novel way of combinatorial enumerations through the concepts of coset representations and sphericities [48].

6. The application of the GAP system after the development of combined-permutation representations (CPRs) as computer-oriented utilities [49].

   The GAP (Groups, Algorithms, Programming) system [50] released in 1988 (the current version is GAP 4.11.1 released on 02 March 2021) provides us with various useful functions, e.g., `TableOfMarks` for gen-

erating mark tables of permutation groups. To apply GAP functions to enumeration practices under point groups, the author (Fujita) has developed *combined-permutation representations* (CPRs) [49]. CPRs have been applied to calculate cycle indices with chirality fittingness (CI-CFs), which have been used for enumerating 3D structures of ligancy 4 by Fujita's proligand method [49]. CPRs have also been applied to calculate CI-CFs of various $\mathbf{O}_h$-skeletons, which have been used to their gross enumerations [51].

For the purpose of symmetry-itemized enumerations, concordant generation of standard mark tables and standard USCI-CF tables has been executed by using CPRs [52]. This procedure has been applied to the generation of standard mark tables and standard USCI-CF tables by starting from various $\boldsymbol{O}_h$-skeletons [53]. The resulting USCI-CFs are used to calculate PCI-CFs and to execute symmetry-itemized enumerations of $\boldsymbol{O}_h$-derivatives.

The items pointed out above are mainly concerned with symmetry-itemized enumerations and gross enumerations of 3D structures under point groups, where enantiomerism (enantiomeric relationship) or the pairwise nature of chirality/achirality is emphasized. Thus, during the above discussions on rather *static aspects* of stereochemistry, we have laid stress on the geometric nature of 3D structures. This means that "chirality" linked with enantiomerism (i.e., Le Bel's way for chirality) has been selected as a basis.

1.4 Dynamic aspects compared to static aspects in organic stereochemistry

By starting from the above items discussed on the geometric nature of 3D structures (*static aspects*), the stereoisomeric nature of 3D structures should be discussed by focusing rather *dynamic aspects* of stereochemistry. It should be noted, however, when we survey the procedures of studies on stereochemistry, actual procedures of studies are opposite (dynamic $\rightarrow$ static). Thus, we first consider what is synthesized (van't Hoff's way

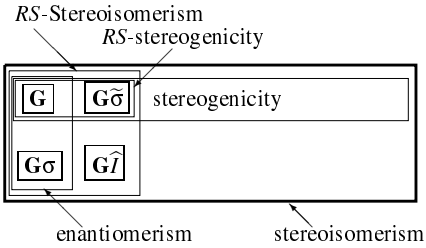

Figure 2. Fujita's stereoisogram approach based on enantiomerism, *RS*-stereogenicity, *RS*-stereoisomerism, and stereoisomerism.

(asymmetry)) and then examine the geometric properties of the synthesized matter at issue (such as chirality and its Cahn-Ingold-Prelog (CIP) *RS*-descriptor). Hence, it is natural that van't Hoff's way (asymmetry) for treating stereoisomerism became a mainstream stereochemistry. According to this trend, Mislow-Siegel's stereogenicity [6] has been mainly adopted as a successor of van't Hoff's way (asymmetry).

Because Mislow-Siegel's stereogenicity has been defined in the fundamental step of terminology, the alternation of its meaning accompanies wide-range re-examination of terminology. However, the *ad-hoc* modification of Mislow-Siegel's stereogenicity (such as the term "pseudoasymmetry") has been found to be unexpected influences on stereochemical terminology, as discussed above (Figure 1). Hence, the essential modification (Figure 2) should be added to the fundamental of Mislow-Siegel's stereogenicity.

To cover the overlooked aspects in Mislow-Siegel's stereogenicity, the author (Fujita) has coined a term *RS-stereogenicity*, which specifies the net interaction between chirality and Mislow-Siegel's stereogenicity (Figure 2). Fujita's *RS*-stereogenicity [1, 15] is a *substantial and meaningful restriction* of Mislow-Siegel's stereogenicity [6], so that the static aspect (Le Bel's way) and the dynamic aspect (van't Hoff's way) are integrated after *sclerality/asclerality* is added as the third aspect for specifying a pair of holantimers. Thus, chirality/achirality (for specifying a pair of enantiomers) and *RS*-stereogenicity/*RS*-astereogenicity (for specifying a pair of *RS*-diastereomers) are regarded as two kinds of handedness and inte-

grated into *RS-stereoisomerism* [54]. Group-theoretically speaking, this integration of three kinds of half-size subgroups (i.e., point groups for specifying chirality/achirality, *RS*-stereogenic groups for specifying *RS*-stereogenicity/*RS*-astereogenicity, and *LR*-permutation groups for specifying sclerality/asclerality) is formulated to give *RS*-stereoisomeric groups. Note that *LR* is the abbreviation of the term *ligand-reflection*. It is an important perspective that the integrations into *RS*-stereoisomeric groups are illustrated by *stereoisograms* as diagrammatic expressions.

1.5 *RS*-stereoisomerism vs stereoisomerism

Before stating the targets of the present article, it is useful to compare between Figure 1 and Figure 2 more detailedly.

According to IUPAC Recommendations 2013 (P-92.1.1) [55] which is based on Mislow-Siegel's stereogenicity, the term "stereogenic units" is defined that "A stereogenic unit (i.e. a unit generating stereoisomerism) is a grouping within a molecular entity that may be considered to generate stereoisomerism." and that (a) a chirality center, (b) a chirality axis, (c) a chirality plane, (d) pseudoasymmetric center, axis or plane, (e) cis/-trans isomers containing a double bond, and (f) an enantiomorphic double bond are listed as the basic types of stereogenic units. As a result, the Mislow-Siegel's stereogenicity of Figure 1 has no description on multiple appearance of such stereogenic units.

For example, a facial stereoisomer and a meridional stereoisomer shown in Figure 3 are explained as two permutation derivatives of a *single* octahedral stereogenic unit controlled by the stereoisomeric group $\boldsymbol{S}^{[6]}_{\boldsymbol{O}_{h\widetilde{\sigma}\widehat{I}}}$, if we obey Figure 1. There is no participation of the *RS*-stereoisomeric group $\boldsymbol{O}_{h\widetilde{\sigma}\widehat{I}}$ in the case of Figure 1.

On the other hand, if we obey Figure 2, Figure 3 is regarded to be controlled by the *RS*-stereoisomeric group $\boldsymbol{O}_{h\widetilde{\sigma}\widehat{I}}$ (order $|\boldsymbol{O}_{h\widetilde{\sigma}\widehat{I}}| = 96$) and the stereoisomeric group $\boldsymbol{S}^{[6]}_{\boldsymbol{O}_{h\widetilde{\sigma}\widehat{I}}}$ (order $|\boldsymbol{S}^{[6]}_{\boldsymbol{O}_{h\widetilde{\sigma}\widehat{I}}}| = 1440$). Hence, fifteen ($= |\boldsymbol{S}^{[6]}_{\boldsymbol{O}_{h\widetilde{\sigma}\widehat{I}}}|/|\boldsymbol{O}_{h\widetilde{\sigma}\widehat{I}}| = 1440/96$) cosets, i.e., $\boldsymbol{O}_{h\widetilde{\sigma}\widehat{I}}\backslash\boldsymbol{S}^{[6]}_{\boldsymbol{O}_{h\widetilde{\sigma}\widehat{I}}}$, are generated to give Figure 2, which constructs maximum number of fifteen stereoisomers. Each of them is controlled by a stereoisogram corresponding to

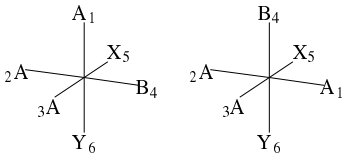

1 fac **2** mer

Figure 3. Stereoisomers but not *RS*-Stereoisomers. Two isomers of octahedral complexes, i.e., a *fac*-isomer having three A's in the facial position and a *mer*-isomer having three A's in the meridional position, are stereoisomeric but not *RS*-stereoisomeric.

a quadruplet of *RS*-stereoisomers according to the coset decomposition $\boldsymbol{O}_{h\tilde{\sigma}\hat{I}}\backslash\boldsymbol{S}^{[6]}\boldsymbol{O}_{h\tilde{\sigma}\hat{I}}$. In the case of a facial octahedral complex **1** and a meridional octahedral complex **2** with the composition A_3BXY, the author (Fujita) [56, 57] has reported the type-itemized enumerations of octahedral complexes, which indicate the presence of one type-I stereoisogram (one facial stereoisomer) and three type-IV stereoisograms (three meridional stereoisomers). Each stereoisogram corresponds to a quadruplet of *RS*-stereoisomers for representing *RS*-stereoisomerism, so that the one type-I stereoisogram (one facial stereoisomer, e.g., **1**) and the three type-IV stereoisograms (three meridional stereoisomers, e,g., **2**) just fill up the frame of stereoisomerism shown in Figure 2.

In the case of a cubane skeleton, the *RS*-stereoisomerism and the stereoisomerism overlap each other. In other words, one stereoisogram for representing the *RS*-stereoisomerism is sufficient to fill up the frame of stereoisomerism shown in Figure 2.

1.6 Targets of the present article

Targets of the present article are the discussions on the concepts of stereoisograms and *RS*-stereoisomerism, where chirality and *RS*-stereogenicity as two kinds of handedness are integrated by adding sclerality as the third aspect. Throughout the present article, a cubane skeleton is selected as a representative probe for extending the point group $\boldsymbol{O}_h$ into

an *RS*-stereoisomeric group $\boldsymbol{O}_{h\widetilde{\sigma}\widehat{I}}$. This course of investigation lays stress on three half-size subgroups of *RS*-stereoisomeric group $\boldsymbol{O}_{h\widetilde{\sigma}\widehat{I}}$, so that the *half-size-subgroup method* has been proposed as one method for type-itemized enumerations of stereoisograms [58]. On the other hand, the coset decomposition of the *RS*-stereoisomeric group $\boldsymbol{O}_{h\widetilde{\sigma}\widehat{I}}$ by the subgroup $\boldsymbol{O}$ is examined from the viewpoint of a factor group $\boldsymbol{O}\backslash\boldsymbol{O}_{h\widetilde{\sigma}\widehat{I}}$, which is isomorphic to the Klein four-group. Thereby, another method for type-itemized enumeration of stereoisograms (named the *factor-group method*) will be developed and accomplished by means of CPRs under the GAP system. Because the half-size-subgroup method has been reported in details in the previous article [58], it will be reported here by way of introduction and comparison to the factor group method. In particular, the main target of the present article is the proposal and detailed discussions on the factor-group method, where the above-described foundations obtained during the enumerations of stereoisomers under point groups (Fujita's USCI approach based on the proligand-promolecule model) are extended to develop Fujita's stereoisogram approach.

2 *RS*-stereoisomeric group $\boldsymbol{O}_{h\widetilde{\sigma}\widehat{I}}$

2.1 Elementary stereoisogram for a cubane skeleton

We start from the point groups $\boldsymbol{O}$ and $\boldsymbol{O}_h$ for discussing geometric properties of a cubane skeleton **3**. The point group $\boldsymbol{O}_h$ (order 48) consists of a subgroup $\boldsymbol{O}$ (**A**: order or size 24) and a coset $\boldsymbol{O}\sigma$ (**B**: size 24) as shown by Eq. 1:

$$\boldsymbol{O}_h = \underbrace{\boldsymbol{O}}_{\mathbf{A}} + \underbrace{\boldsymbol{O}\sigma}_{\mathbf{B}}, \tag{1}$$

where the symbol σ represents an appropriate reflection (e.g., $\sigma_{h(1)}$), which is represented with a overline (e.g., $\sigma_{h(1)} \sim \overline{(1,5)(2,6)(3,7)(4,8)}$).

Under the GAP system, the point group $\boldsymbol{O}$ (`O_cube`) is created by using a set of generators `gen_O_cube` (containing a four-fold rotation and a three-fold rotation for a cubane skeleton), while the point group $\boldsymbol{O}_h$ (`Oh_cube`) is created by using a set of generators `gen_Oh_cube` (containing an additional

reflection $\sigma \sim (1,5)(2,6)(3,7)(4,8)(9,10)$ with a 2-cycle $(9,10)$) as follows:

```
gap> gen_O_cube := [ (1,2,3,4)(5,6,7,8), (2,4,5)(3,8,6) ];;
gap> O_cube := Group(gen_O_cube);;
gap> Display(Size(O_cube));
24
gap> gen_Oh_cube := [ (1,2,3,4)(5,6,7,8), (2,4,5)(3,8,6), (1,5)(2,6)(3,7)(4,8)(9,10)];;
gap> Oh_cube := Group(gen_Oh_cube);;
gap> Display(Size(Oh_cube));
48
```

The *RS*-stereoisomeric group $\boldsymbol{O}_{h\widetilde{\sigma}\widehat{I}}$ (`OhsI_cube`) is defined according to Eq. 2, where an *RS*-permutation $\widetilde{\sigma}$ ($\in \boldsymbol{O}\widetilde{\sigma} \subset \boldsymbol{O}_h\widetilde{\sigma}$) is created by deleting the mirror operation from the reflection σ ($\in \boldsymbol{O}\sigma \subset \boldsymbol{O}_h$). Note that the second term of Eq. 2 is further converted as follows:

$\boldsymbol{O}_h\boldsymbol{O}\widetilde{\sigma} = (\boldsymbol{O} + \boldsymbol{O}\sigma)\boldsymbol{O}\widetilde{\sigma} = \boldsymbol{O}\widetilde{\sigma} + \boldsymbol{O}\sigma\widetilde{\sigma} = \boldsymbol{O}\widetilde{\sigma} + \boldsymbol{O}\widehat{I}$.

Hence, Eq. 2 is converted into Eq. 3, which represents the *RS*-stereoisomeric group $\boldsymbol{O}_{h\widetilde{\sigma}\widehat{I}}$ in the form of a coset decomposition of $\boldsymbol{O}_{h\widetilde{\sigma}\widehat{I}}$ by the subgroup $\boldsymbol{O}$.

$$\boldsymbol{O}_{h\widetilde{\sigma}\widehat{I}} = \underbrace{\boldsymbol{O}_h}_{\mathbf{AB}} + \underbrace{\boldsymbol{O}_h\boldsymbol{O}\widetilde{\sigma}}_{\mathbf{CD}} \tag{2}$$

$$= \underbrace{\boldsymbol{O}}_{\mathbf{A}} + \underbrace{\boldsymbol{O}\sigma}_{\mathbf{B}} + \underbrace{\boldsymbol{O}\widetilde{\sigma}}_{\mathbf{C}} + \underbrace{\boldsymbol{O}\widehat{I}}_{\mathbf{D}} \tag{3}$$

The construction of the *RS*-stereoisomeric group $\boldsymbol{O}_{h\widetilde{\sigma}\widehat{I}}$ (`OhsI_cube`) by Eq. 3 is illustrated as an elementary stereoisogram shown in Figure 4, where each coset of Eq. 3 is shown by an appropriately selected skeleton [59].

According to the GAP system, the *RS*-permutation $(1,5)(2,6)(3,7)(4,8)$ is added to a set of generators `gen_Oh_cube` for the point group $\boldsymbol{O}_h$, where the GAP function `Concatenation` is used to generate a set of generators `gen_OhsI_cube` for the *RS*-stereoisomeric group $\boldsymbol{O}_{h\widetilde{\sigma}\widehat{I}}$ (`OhsI_cube`).

```
gap> gen_O_cube := [ (1,2,3,4)(5,6,7,8), (2,4,5)(3,8,6) ];;
gap> O_cube := Group(gen_O_cube);;
gap> gen_Oh_cube := [ (1,2,3,4)(5,6,7,8), (2,4,5)(3,8,6), (1,5)(2,6)(3,7)(4,8)(9,10)];;
gap> Oh_cube := Group(gen_Oh_cube);;
gap> gen_OhsI_cube := Concatenation(gen_Oh_cube, [(1,5)(2,6)(3,7)(4,8)]);;
gap> OhsI_cube := Group(gen_OhsI_cube);;
gap> Display(Size(OhsI_cube));
96
gap>
```

The application of the GAP function `CosetDecomposition` produces the four cosets collected in Eq. 3 in the form of list formats `CD_OhsI_O` of

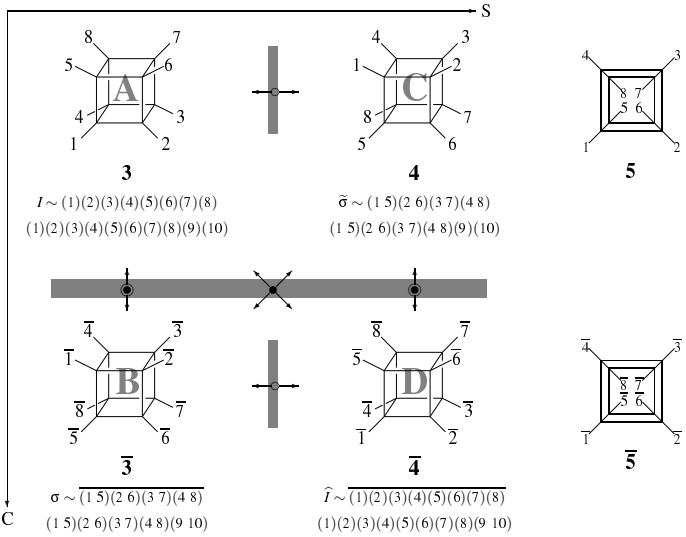

Figure 4. Elementary stereoisogram for a cubane skeleton. The respective skeletons are tentatively linked with double-headed arrows [59].

the GAP system.

```
gap> #Coset Decomposition
gap> CD_OhsI_O := CosetDecomposition(OhsI_cube,O_cube);;
gap> Display(CD_OhsI_O[1]);
[ (), (2,4,5)(3,8,6), (2,5,4)(3,6,8), (1,2)(3,5)(4,6)(7,8), (1,2,3,4)(5,6,7,8),
  (1,2,6,5)(3,7,8,4), (1,3,6)(4,7,5), (1,3)(2,4)(5,7)(6,8), (1,3,8)(2,7,5),
  (1,4,3,2)(5,8,7,6), (1,4,8,5)(2,3,7,6), (1,4)(2,8)(3,5)(6,7), (1,5,6,2)(3,4,8,7),
  (1,5,8,4)(2,6,7,3), (1,5)(2,8)(3,7)(4,6), (1,6,3)(4,5,7), (1,6)(2,5)(3,8)(4,7),
  (1,6,8)(2,7,4), (1,7)(2,3)(4,6)(5,8), (1,7)(2,6)(3,5)(4,8),
  (1,7)(2,8)(3,4)(5,6), (1,8,6)(2,4,7), (1,8,3)(2,5,7), (1,8)(2,7)(3,6)(4,5) ]
gap> Display(CD_OhsI_O[2]);
[ ( 3, 6)( 4, 5), ( 2, 5)( 3, 8), ( 2, 4)( 6, 8), ( 1, 2)( 3, 4)( 5, 6)( 7, 8),
  ( 1, 2, 6, 7, 8, 4)( 3, 5), ( 1, 2, 3, 7, 8, 5)( 4, 6), ( 1, 6)( 4, 7),
  ( 1, 6, 8, 3)( 2, 5, 7, 4), ( 1, 6, 3, 8)( 2, 7, 4, 5), ( 1, 5, 8, 7, 3, 2)( 4, 6),
  ( 1, 5)( 2, 6)( 3, 7)( 4, 8), ( 1, 5, 6, 7, 3, 4)( 2, 8),
  ( 1, 4, 8, 7, 6, 2)( 3, 5), ( 1, 4)( 2, 3)( 5, 8)( 6, 7),
  ( 1, 4, 3, 7, 6, 5)( 2, 8), ( 1, 3)( 5, 7), ( 1, 3, 8, 6)( 2, 4, 7, 5),
  ( 1, 3, 6, 8)( 2, 7, 5, 4), ( 1, 7)( 2, 6, 5, 8, 4, 3), ( 1, 7)( 2, 3, 4, 8, 5, 6),
  ( 1, 7)( 2, 8)( 3, 5)( 4, 6), ( 1, 8, 3, 6)( 2, 5, 4, 7),
  ( 1, 8, 6, 3)( 2, 4, 5, 7), ( 1, 8)( 2, 7) ]
gap> Display(CD_OhsI_O[3]);
[ ( 9,10), ( 2, 4, 5)( 3, 8, 6)( 9,10), ( 2, 5, 4)( 3, 6, 8)( 9,10),
  ( 1, 2)( 3, 5)( 4, 6)( 7, 8)( 9,10), ( 1, 2, 3, 4)( 5, 6, 7, 8)( 9,10),
  ( 1, 2, 6, 5)( 3, 7, 8, 4)( 9,10), ( 1, 3, 6)( 4, 7, 5)( 9,10),
  ( 1, 3)( 2, 4)( 5, 7)( 6, 8)( 9,10), ( 1, 3, 8)( 2, 7, 5)( 9,10),
  ( 1, 4, 3, 2)( 5, 8, 7, 6)( 9,10), ( 1, 4, 8, 5)( 2, 3, 7, 6)( 9,10),
  ( 1, 4)( 2, 8)( 3, 5)( 6, 7)( 9,10), ( 1, 5, 6, 2)( 3, 4, 8, 7)( 9,10),
  ( 1, 5, 8, 4)( 2, 6, 7, 3)( 9,10), ( 1, 5)( 2, 8)( 3, 7)( 4, 6)( 9,10),
  ( 1, 6, 3)( 4, 5, 7)( 9,10), ( 1, 6)( 2, 5)( 3, 8)( 4, 7)( 9,10),
  ( 1, 6, 8)( 2, 7, 4)( 9,10),
  ( 1, 7)( 2, 3)( 4, 6)( 5, 8)( 9,10), ( 1, 7)( 2, 6)( 3, 5)( 4, 8)( 9,10),
  ( 1, 7)( 2, 8)( 3, 4)( 5, 6)( 9,10), ( 1, 8, 6)( 2, 4, 7)( 9,10),
```

```
  ( 1, 8, 3)( 2, 5, 7)( 9,10), ( 1, 8)( 2, 7)( 3, 6)( 4, 5)( 9,10) ]
gap> Display(CD_OhsI_O[4]);
[ ( 3, 6)( 4, 5)( 9,10), ( 2, 5)( 3, 8)( 9,10), ( 2, 4)( 6, 8)( 9,10),
  ( 1, 2)( 3, 4)( 5, 6)( 7, 8)( 9,10), ( 1, 2, 6, 7, 8, 4)( 3, 5)( 9,10),
  ( 1, 2, 3, 7, 8, 5)( 4, 6)( 9,10), ( 1, 6)( 4, 7)( 9,10),
  ( 1, 6, 8, 3)( 2, 5, 7, 4)( 9,10), ( 1, 6, 3, 8)( 2, 7, 4, 5)( 9,10),
  ( 1, 5, 8, 7, 3, 2)( 4, 6)( 9,10), ( 1, 5)( 2, 6)( 3, 7)( 4, 8)( 9,10),
  ( 1, 5, 6, 7, 3, 4)( 2, 8)( 9,10), ( 1, 4, 8, 7, 6, 2)( 3, 5)( 9,10),
  ( 1, 4)( 2, 3)( 5, 8)( 6, 7)( 9,10), ( 1, 4, 3, 7, 6, 5)( 2, 8)( 9,10),
  ( 1, 3)( 5, 7)( 9,10), ( 1, 3, 8, 6)( 2, 4, 7, 5)( 9,10),
  ( 1, 3, 6, 8)( 2, 7, 5, 4)( 9,10), ( 1, 7)( 2, 6, 5, 8, 4, 3)( 9,10),
  ( 1, 7)( 2, 3, 4, 8, 5, 6)( 9,10), ( 1, 7)( 2, 8)( 3, 5)( 4, 6)( 9,10),
  ( 1, 8, 3, 6)( 2, 5, 4, 7)( 9,10),
  ( 1, 8, 6, 3)( 2, 4, 5, 7)( 9,10), ( 1, 8)( 2, 7)( 9,10) ]
gap>
```

These cosets of the RS-stereoisomeric group $\boldsymbol{O}_{h\widetilde{\sigma}\widehat{I}}$ construct a basis for an elementary stereoisogram for a cubane skeleton, as shown in Figure 4. Thus, the first pair of square brackets (`CD_OhsI_O[1]`) shows the coset $\underbrace{\boldsymbol{O}}_{\mathbf{A}}$ for controlling the reference skeleton **3**, the second pair of square brackets (`CD_OhsI_O[2]`) shows the coset $\underbrace{\boldsymbol{O}\widetilde{\sigma}}_{\mathbf{C}}$ for controlling an RS-diastereomeric skeleton **4**, the third pair of square brackets (`CD_OhsI_O[3]`) shows the coset $\underbrace{\boldsymbol{O}\widehat{I}}_{\mathbf{D}}$ for controlling a ligand-reflection (LR) skeleton $\overline{\mathbf{4}}$, and finally the 4th pair of square brackets (`CD_OhsI_O[4]`) shows the coset $\underbrace{\boldsymbol{O}\sigma}_{\mathbf{B}}$ for controlling the mirror-numbered skeleton $\overline{\mathbf{3}}$.

In the elementary stereoisogram shown by Figure 4, a horizontal gray line represents a mirror plane, which causes reflection between **3** and $\overline{\mathbf{3}}$ or between **4** and $\overline{\mathbf{4}}$. On the other hand, a vertical gray line represents a graphical inversion, where the pair of RS-diastereomeric skeletons (**3** and **4**) can be converted to each other by the intervention of a graph **5**, while the pair of RS-diastereomeric mirror-skeletons ($\overline{\mathbf{3}}$ and $\overline{\mathbf{4}}$) can be converted to each other by the intervention of a mirror graph ($\overline{\mathbf{5}}$).

2.2 Construction of half-size subgroups of the *RS*-stereoisomeric group $\boldsymbol{O}_{h\widetilde{\sigma}\widehat{I}}$.

Along with the point group $\boldsymbol{O}_h$ (Eq. 1) as a half-size subgroup (size or order 48, appearing in the vertical directions of a stereoisogram), the RS-stereoisomeric group $\boldsymbol{O}_{h\widetilde{\sigma}\widehat{I}}$ (Eq. 3, size 96) has two other half-size sub-

groups, i.e., RS-stereogenic group $\boldsymbol{O}_{\widetilde{\sigma}}$ (size 48, appearing in the horizontal directions of a stereoisogram) and LR-permutation group $\boldsymbol{O}_{\widehat{I}}$ (size 48, appearing in the diagonal directions of s stereoisogram).

$$\boldsymbol{O}_{\widetilde{\sigma}} = \underbrace{\boldsymbol{O}}_{\mathbf{A}} + \underbrace{\boldsymbol{O}\widetilde{\sigma}}_{\mathbf{C}} \tag{4}$$

$$\boldsymbol{O}_{\widehat{I}} = \underbrace{\boldsymbol{O}}_{\mathbf{A}} + \underbrace{\boldsymbol{O}\widehat{I}}_{\mathbf{D}}, \tag{5}$$

where the symbol $\widetilde{\sigma}$ represents an appropriate RS-permutation selected from the coset $\underbrace{\boldsymbol{O}\widetilde{\sigma}}_{\mathbf{C}}$ (e.g., $\widetilde{\sigma}_{h(1)}$ ($\sim (1,5)(2,6)(3,7)(4,8)$)), while the symbol $\widehat{I}$ represents an appropriate LR-permutation selected from the coset $\underbrace{\boldsymbol{O}\widehat{I}}_{\mathbf{D}}$ (e.g., $\widehat{I}$ ($\sim \overline{(1)(2)(3)(4)(5)(6)(7)(8)}$)).

Under the GAP system, a set of generator (`gen_Os_cube`) is used to generate the RS-permutation group $\boldsymbol{O}_{\widetilde{\sigma}}$ (`Os_cube`, Eq. 4), while a set of generators (`gen_OI_cube`) is used to generate the LR-permutation group $\boldsymbol{O}_{\widehat{I}}$ (`OI_cube`, Eq. 5).

```
gap> gen_Os_cube := [ (1,2,3,4)(5,6,7,8), (2,4,5)(3,8,6), (1,5)(2,6)(3,7)(4,8)];;
gap> Os_cube := Group(gen_Os_cube);;
gap> Display(Size(Os_cube));
48
gap> gen_OI_cube := [ (1,2,3,4)(5,6,7,8), (2,4,5)(3,8,6), (9,10)];;
gap> OI_cube := Group(gen_OI_cube);;
gap> Display(Size(OI_cube));
48
gap> gen_OhsI_cube := [ (1,2,3,4)(5,6,7,8), (2,4,5)(3,8,6), (1,5)(2,6)(3,7)(4,8),
     ↪ (9,10)];;
gap> OhsI_cube := Group(gen_OhsI_cube);;
gap> Display(Size(OhsI_cube));
96
gap>
```

Among the four cosets of the RS-stereoisomeric group $\boldsymbol{O}_{h\widetilde{\sigma}\widehat{I}}$ described above, the first coset (`CD_OhsI_O[1]`) and the second coset (`CD_OhsI_O[2]`) produces the RS-permutation group `Os_cube`, i.e., $\underbrace{\boldsymbol{O}}_{\mathbf{A}} + \underbrace{\boldsymbol{O}\widetilde{\sigma}}_{\mathbf{C}}$ (Eq. 4). On the other hand, the first coset (`CD_OhsI_O[1]`) and the third coset (`CD_OhsI_O[3]`) produces the LR-permutation group `OI_cube`, i.e., $\underbrace{\boldsymbol{O}}_{\mathbf{A}}$ +

$\underbrace{\boldsymbol{O}\widehat{I}}_{\mathbf{D}}$ (Eq. 5).

3 Factor group of the *RS*-stereoisomeric group $\boldsymbol{O}_{h\widetilde{\sigma}\widehat{I}}$

Because the coset decomposition of the *RS*-stereoisomeric group $\boldsymbol{O}_{h\widetilde{\sigma}\widehat{I}}$ by the subgroup $\boldsymbol{O}$ (Eq. 3) can produce a factor group $\boldsymbol{O}\backslash\boldsymbol{O}_{h\widetilde{\sigma}\widehat{I}}$, because the subgroup $\boldsymbol{O}$ is a normal subgroup of $\boldsymbol{O}_{h\widetilde{\sigma}\widehat{I}}$.

$$\boldsymbol{O}\backslash\boldsymbol{O}_{h\widetilde{\sigma}\widehat{I}} = \{\underbrace{\boldsymbol{O}}_{\mathbf{A\ 1}}, \quad \underbrace{\boldsymbol{O}\sigma}_{\mathbf{B\ 2}}, \quad \underbrace{\boldsymbol{O}\widetilde{\sigma}}_{\mathbf{C\ 3}}, \quad \underbrace{\boldsymbol{O}\widehat{I}}_{\mathbf{D\ 4}}\} \tag{6}$$

For example, any two cosets in Eq. 6 can be multiplied to give another coset, e.g., $\boldsymbol{O}\widetilde{\sigma}\ \boldsymbol{O}\sigma = \boldsymbol{O}\boldsymbol{O}\widetilde{\sigma}\sigma = \boldsymbol{O}\widehat{I}$, because $\boldsymbol{O}$ is normal and has commutative nature.

Because the four skeletons collected in Figure 4 can be regarded to correspond to the four cosets collected in Eq. 6, the stereoisogram (Figure 4) can be regarded as a matrix shown as the first formula corresponding to the factor group $\boldsymbol{O}\backslash\boldsymbol{O}_{h\widetilde{\sigma}\widehat{I}}$, as shown in the left-hand side of Eq. 7. Hence, the multiplication by $\boldsymbol{O}\sigma$, for example, results in a transformation into another matrix, as shown in the right-hand side of Eq. 7. This result is converted into a permutation (1 2)(3 4).

$$\underbrace{\begin{pmatrix} \underbrace{\boldsymbol{O}}_{\mathbf{A\ 1}} & \underbrace{\boldsymbol{O}\widetilde{\sigma}}_{\mathbf{C\ 3}} \\ \underbrace{\boldsymbol{O}\sigma}_{\mathbf{B\ 2}} & \underbrace{\boldsymbol{O}\widehat{I}}_{\mathbf{D\ 4}} \end{pmatrix}}_{\boldsymbol{O}\backslash\boldsymbol{O}_{h\widetilde{\sigma}\widehat{I}}} \boldsymbol{O}\sigma = \left(\begin{array}{cc} \underbrace{\boldsymbol{O}\sigma}_{\mathbf{B\ 2}} & \underbrace{\boldsymbol{O}\widehat{I}}_{\mathbf{D\ 4}} \\ \hline \underbrace{\boldsymbol{O}}_{\mathbf{A\ 1}} & \underbrace{\boldsymbol{O}\widetilde{\sigma}}_{\mathbf{C\ 3}} \end{array}\right) \sim (1\ 2)(3\ 4) \tag{7}$$

In a similar way to Eq. 7, the four cosets contained in Eq. 6 satisfy the multiplication table shown by Figure 5. Note that the $\underbrace{\boldsymbol{O}\sigma}_{\mathbf{B\ 2}}$-row in Figure 5 represents the same multiplication as Eq. 7. The gray alphabets **A–D** attached with under-braces show the four *RS*-stereoisomers collected in

	$\underbrace{\mathbf{O}}_{\mathbf{A\,1}}$	$\underbrace{\mathbf{O}\sigma}_{\mathbf{B\,2}}$	$\underbrace{\mathbf{O}\widetilde{\sigma}}_{\mathbf{C\,3}}$	$\underbrace{\mathbf{O}\widehat{I}}_{\mathbf{D\,4}}$
$\underbrace{\mathbf{O}}_{\mathbf{A\,1}}$	$\underbrace{\mathbf{O}}_{\mathbf{A\,1}}$	$\underbrace{\mathbf{O}\sigma}_{\mathbf{B\,2}}$	$\underbrace{\mathbf{O}\widetilde{\sigma}}_{\mathbf{C\,3}}$	$\underbrace{\mathbf{O}\widehat{I}}_{\mathbf{D\,4}}$
$\underbrace{\mathbf{O}\sigma}_{\mathbf{B\,2}}$	$\underbrace{\mathbf{O}\sigma}_{\mathbf{B\,2}}$	$\underbrace{\mathbf{O}}_{\mathbf{A\,1}}$	$\underbrace{\mathbf{O}\widehat{I}}_{\mathbf{D\,4}}$	$\underbrace{\mathbf{O}\widetilde{\sigma}}_{\mathbf{C\,3}}$
$\underbrace{\mathbf{O}\widetilde{\sigma}}_{\mathbf{C\,3}}$	$\underbrace{\mathbf{O}\widetilde{\sigma}}_{\mathbf{C3}}$	$\underbrace{\mathbf{O}\widehat{I}}_{\mathbf{D\,4}}$	$\underbrace{\mathbf{O}}_{\mathbf{A\,1}}$	$\underbrace{\mathbf{O}\sigma}_{\mathbf{B\,2}}$
$\underbrace{\mathbf{O}\widehat{I}}_{\mathbf{D\,4}}$	$\underbrace{\mathbf{O}\widehat{I}}_{\mathbf{D\,4}}$	$\underbrace{\mathbf{O}\widetilde{\sigma}}_{\mathbf{C\,3}}$	$\underbrace{\mathbf{O}\sigma}_{\mathbf{B\,2}}$	$\underbrace{\mathbf{O}}_{\mathbf{A\,1}}$

Figure 5. Multiplication table of the factor group $\boldsymbol{O}\backslash\boldsymbol{O}_{h\widetilde{\sigma}\widehat{I}}$,

the elementary stereoisogram (Figure 4).

By referring to Eq. 7 and the multiplication table (Figure 5), the factor group $\boldsymbol{O}\backslash\boldsymbol{O}_{h\widetilde{\sigma}\widehat{I}}$ (Eq. 6) can be regarded to be a Klein 4-group, which has 5 subgroups up to conjugacy. Thereby, the factor group can be discussed in terms of a non-redundant set of subgroups (SSG):

$$\begin{aligned}&\mathrm{SSG}_{\boldsymbol{O}\backslash\boldsymbol{O}_{h\widetilde{\sigma}\widehat{I}}} = \\ &\{\underbrace{\boldsymbol{O}\ (\mathbf{A})}_{1},\quad \underbrace{\boldsymbol{O}_{h}\ (\mathbf{AB})}_{2},\quad \underbrace{\boldsymbol{O}_{\widetilde{\sigma}}\ (\mathbf{AC})}_{3},\quad \underbrace{\boldsymbol{O}_{\widehat{I}}\ (\mathbf{AD})}_{4},\quad \underbrace{\boldsymbol{O}_{h\widetilde{\sigma}\widehat{I}}\ (\mathbf{ABCD})}_{5}\}\end{aligned} \tag{8}$$

where the subgroups are aligned and numbered sequentially in the ascending order of their orders (sizes).

The first subgroup $\underbrace{\boldsymbol{O}\ (\mathbf{A})}_{1}$ collected in Eq. 8 constructs the factor group $\boldsymbol{O}\backslash\boldsymbol{O}_{h\widetilde{\sigma}\widehat{I}}$, which show the following multiplication results by referring to Figure 5. Note that Eq. 11 represent the same multiplication as Eq. 7

$$\boldsymbol{O}\backslash\boldsymbol{O}_{h\widetilde{\sigma}\widehat{I}} = \left\{ \underbrace{\boldsymbol{O}}_{\mathbf{A}\ 1}, \underbrace{\boldsymbol{O}\sigma}_{\mathbf{B}\ 2}, \underbrace{\boldsymbol{O}\widetilde{\sigma}}_{\mathbf{C}\ 3}, \underbrace{\boldsymbol{O}\widehat{I}}_{\mathbf{D}\ 4} \right\} \quad \textit{Permutation} \quad \begin{matrix}\text{SSG}\\ 1\ 2\,3\,4\,5\end{matrix} \tag{9}$$

$$\boldsymbol{O}\backslash\boldsymbol{O}_{h\widetilde{\sigma}\widehat{I}}\,\boldsymbol{O} = \underbrace{\boldsymbol{O}}_{\mathbf{A}\ 1}, \underbrace{\boldsymbol{O}\sigma}_{\mathbf{B}\ 2}, \underbrace{\boldsymbol{O}\widetilde{\sigma}}_{\mathbf{C}\ 3}, \underbrace{\boldsymbol{O}\widehat{I}}_{\mathbf{D}\ 4} \quad \sim (1)(2)(3)(4) \quad \circ\ \circ\ \circ\ \circ\ \circ \tag{10}$$

$$\boldsymbol{O}\backslash\boldsymbol{O}_{h\widetilde{\sigma}\widehat{I}}\,\boldsymbol{O}\sigma = \underbrace{\boldsymbol{O}\sigma}_{\mathbf{B}\ 2}, \underbrace{\boldsymbol{O}}_{\mathbf{A}\ 1}, \underbrace{\boldsymbol{O}\widehat{I}}_{\mathbf{D}\ 4}, \underbrace{\boldsymbol{O}\widetilde{\sigma}}_{\mathbf{C}\ 3} \quad \sim (1\ \ 2)(3\ \ 4) \quad \mathrm{x}\ \circ\ \mathrm{x}\ \mathrm{x}\ \circ \tag{11}$$

$$\boldsymbol{O}\backslash\boldsymbol{O}_{h\widetilde{\sigma}\widehat{I}}\,\boldsymbol{O}\widetilde{\sigma} = \underbrace{\boldsymbol{O}\widetilde{\sigma}}_{\mathbf{C}\ 3}, \underbrace{\boldsymbol{O}\widehat{I}}_{\mathbf{D}\ 4}, \underbrace{\boldsymbol{O}}_{\mathbf{A}\ 1}, \underbrace{\boldsymbol{O}\sigma}_{\mathbf{B}\ 2} \quad \sim (1\ \ 3)(2\ \ 4) \quad \mathrm{x}\ \mathrm{x}\ \circ\ \mathrm{x}\ \circ \tag{12}$$

$$\boldsymbol{O}\backslash\boldsymbol{O}_{h\widetilde{\sigma}\widehat{I}}\,\boldsymbol{O}\widehat{I} = \underbrace{\boldsymbol{O}\widehat{I}}_{\mathbf{D}\ 4}, \underbrace{\boldsymbol{O}\widetilde{\sigma}}_{\mathbf{C}\ 3}, \underbrace{\boldsymbol{O}\sigma}_{\mathbf{B}\ 2}, \underbrace{\boldsymbol{O}}_{\mathbf{A}\ 1} \quad \sim (1\ \ 4)(2\ \ 3) \quad \mathrm{x}\ \mathrm{x}\ \mathrm{x}\ \circ\ \circ \tag{13}$$

list of marks [4,0,0,0,0]

By referring to $\mathrm{SSG}_{\boldsymbol{O}\backslash\boldsymbol{O}_{h\widetilde{\sigma}\widehat{I}}}$ (Eq. 8), the list of permutations shown in the last parts of Eqs. 10–13 produces the list of marks [4,0,0,0,0], which is aligned according to the ascending order of sizes of subgroups ((**A** 1) → (**AB** 2) → (**AC** 2) → (**AD** 2) → (**ABCD** 4)) shown below each brace in Eq. 8. For example, the subgroup $\boldsymbol{O}$ (**A** 1) consists of one permutation {(1)(2)(3)(4)} so as to give the mark 4 (i.e., 4 fixed cosets); the subgroup $\boldsymbol{O}_h$ (**AB** 2) consists of two permutations {(1)(2)(3)(4), (1 2)(3 4)} so as to give the mark 0 (i.e., no fixed coset); and so on.

The second subgroup $\underbrace{\boldsymbol{O}_h\ (\mathbf{AB})}_{2}$ collected in Eq. 8 constructs the factor group $\boldsymbol{O}_h\backslash\boldsymbol{O}_{h\widetilde{\sigma}\widehat{I}}$, which show the following multiplication results by referring to Figure 5:

$$\boldsymbol{O}_h\backslash\boldsymbol{O}_{h\widetilde{\sigma}\widehat{I}} = \left\{ \underbrace{(\boldsymbol{O}+\boldsymbol{O}\sigma)}_{\mathbf{AB}\ 1}, \underbrace{(\boldsymbol{O}\widetilde{\sigma}+\boldsymbol{O}\widehat{I})}_{\mathbf{CD}\ 2} \right\} \quad \textit{Permutation} \quad \begin{matrix}\text{SSG}\\ 1\ 2\,3\,4\,5\end{matrix} \tag{14}$$

$$\boldsymbol{O}_h\backslash\boldsymbol{O}_{h\widetilde{\sigma}\widehat{I}}\,\boldsymbol{O} = \underbrace{(\boldsymbol{O}+\boldsymbol{O}\sigma)}_{\mathbf{AB}\ 1}, \underbrace{(\boldsymbol{O}\widetilde{\sigma}+\boldsymbol{O}\widehat{I})}_{\mathbf{CD}\ 2} \quad \sim (1)(2) \quad \circ\ \circ\ \circ\ \circ\ \circ \tag{15}$$

$$\boldsymbol{O}_h\backslash\boldsymbol{O}_{h\widetilde{\sigma}\widehat{I}}\,\boldsymbol{O}\sigma = \underbrace{(\boldsymbol{O}+\boldsymbol{O}\sigma)}_{\mathbf{AB}\ 1}, \underbrace{(\boldsymbol{O}\widetilde{\sigma}+\boldsymbol{O}\widehat{I})}_{\mathbf{CD}\ 2} \quad \sim (1)(2) \quad \mathrm{x}\ \circ\ \mathrm{x}\ \mathrm{x}\ \circ \tag{16}$$

$$\boldsymbol{O}_h\backslash\boldsymbol{O}_{h\widetilde{\sigma}\widehat{I}}\,\boldsymbol{O}\widetilde{\sigma} = \underbrace{(\boldsymbol{O}\widetilde{\sigma}+\boldsymbol{O}\widehat{I})}_{\mathbf{CD}\ 2}, \underbrace{(\boldsymbol{O}+\boldsymbol{O}\sigma)}_{\mathbf{AB}\ 1} \quad \sim (1\ \ 2) \quad \mathrm{x}\ \mathrm{x}\ \circ\ \mathrm{x}\ \circ \tag{17}$$

$$\boldsymbol{O}_h\backslash\boldsymbol{O}_{h\widetilde{\sigma}\widehat{I}}\,\boldsymbol{O}\widehat{I} = \underbrace{(\boldsymbol{O}\widetilde{\sigma}+\boldsymbol{O}\widehat{I})}_{\mathbf{CD}\ 2}, \underbrace{(\boldsymbol{O}+\boldsymbol{O}\sigma)}_{\mathbf{AB}\ 1} \quad \sim (1\ \ 2) \quad \mathrm{x}\ \mathrm{x}\ \mathrm{x}\ \circ\ \circ \tag{18}$$

list of marks [2,2,0,0,0]

In a similar way, the list of permutations shown in the last parts of Eqs. 15–18 produces the list of marks [2,2,0,0,0] by referring to $\mathrm{SSG}_{\boldsymbol{O}\backslash\boldsymbol{O}_{h\widetilde{\sigma}\widehat{I}}}$ (Eq. 8).

The third subgroup $\underbrace{\boldsymbol{O}_{\widetilde{\sigma}}\ (\mathbf{AC})}_{3}$ collected in Eq. 8 constructs the factor group $\boldsymbol{O}_{\widetilde{\sigma}}\backslash\boldsymbol{O}_{h\widetilde{\sigma}\widehat{I}}$, which show the following multiplication results by

referring to Figure 5:

$$\boldsymbol{O}_{\bar{\sigma}}\backslash\boldsymbol{O}_{h\bar{\sigma}\hat{I}} = \left\{ \underbrace{(\boldsymbol{O}+\boldsymbol{O}\tilde{\sigma})}_{\text{AC 1}}, \underbrace{(\boldsymbol{O}\sigma+\boldsymbol{O}\hat{I})}_{\text{BD 2}} \right\} \quad \textit{Permutation} \quad \begin{matrix}\text{SSG}\\ 1\ 2\,3\,4\,5\end{matrix} \tag{19}$$

$$\boldsymbol{O}_{\bar{\sigma}}\backslash\boldsymbol{O}_{h\bar{\sigma}\hat{I}}\,\boldsymbol{O} = \underbrace{(\boldsymbol{O}+\boldsymbol{O}\tilde{\sigma})}_{\text{AC 1}}, \underbrace{(\boldsymbol{O}\sigma+\boldsymbol{O}\hat{I})}_{\text{BD 2}} \quad \sim(1)(2) \quad \circ\ \circ\circ\circ\circ \tag{20}$$

$$\boldsymbol{O}_{\bar{\sigma}}\backslash\boldsymbol{O}_{h\bar{\sigma}\hat{I}}\,\boldsymbol{O}\sigma = \underbrace{(\boldsymbol{O}\sigma+\boldsymbol{O}\hat{I})}_{\text{BD 2}}, \underbrace{(\boldsymbol{O}+\boldsymbol{O}\tilde{\sigma})}_{\text{AC 1}} \quad \sim(1\ \ 2) \quad \mathrm{x}\circ\mathrm{x}\,\mathrm{x}\circ \tag{21}$$

$$\boldsymbol{O}_{\bar{\sigma}}\backslash\boldsymbol{O}_{h\bar{\sigma}\hat{I}}\,\boldsymbol{O}\tilde{\sigma} = \underbrace{(\boldsymbol{O}+\boldsymbol{O}\tilde{\sigma})}_{\text{AC 1}}, \underbrace{(\boldsymbol{O}\sigma+\boldsymbol{O}\hat{I})}_{\text{BD 2}} \quad \sim(1)(2) \quad \mathrm{x}\,\mathrm{x}\circ\mathrm{x}\circ \tag{22}$$

$$\boldsymbol{O}_{\bar{\sigma}}\backslash\boldsymbol{O}_{h\bar{\sigma}\hat{I}}\,\boldsymbol{O}\hat{I} = \underbrace{(\boldsymbol{O}\sigma+\boldsymbol{O}\hat{I})}_{\text{BD 2}}, \underbrace{(\boldsymbol{O}+\boldsymbol{O}\tilde{\sigma})}_{\text{AC 1}} \quad \sim(1\ \ 2) \quad \mathrm{x}\,\mathrm{x}\,\mathrm{x}\circ\circ \tag{23}$$

list of marks [2,0,2,0,0]

In a similar way, the list of permutations shown in the last parts of Eqs. 20–23 produces the list of marks [2,0,2,0,0] by referring to $\mathrm{SSG}_{\boldsymbol{O}\backslash\boldsymbol{O}_{h\tilde{\sigma}\hat{I}}}$ (Eq. 8).

The 4th subgroup $\underbrace{\boldsymbol{O}_{\hat{I}}\ (\mathbf{AD})}_{4}$ collected in Eq. 8 constructs the factor group $\boldsymbol{O}_{\hat{I}}\backslash\boldsymbol{O}_{h\tilde{\sigma}\hat{I}}$, which show the following multiplication results by referring to Figure 5:

$$\boldsymbol{O}_{\hat{I}}\backslash\boldsymbol{O}_{h\bar{\sigma}\hat{I}} = \left\{ \underbrace{(\boldsymbol{O}+\boldsymbol{O}\tilde{\sigma})}_{\text{AC 1}}, \underbrace{(\boldsymbol{O}\sigma+\boldsymbol{O}\hat{I})}_{\text{BD 2}} \right\} \quad \textit{Permutation} \quad \begin{matrix}\text{SSG}\\ 1\ 2\,3\,4\,5\end{matrix} \tag{24}$$

$$\boldsymbol{O}_{\hat{I}}\backslash\boldsymbol{O}_{h\bar{\sigma}\hat{I}}\,\boldsymbol{O} = \underbrace{(\boldsymbol{O}+\boldsymbol{O}\hat{I})}_{\text{AD 1}}, \underbrace{(\boldsymbol{O}\sigma+\boldsymbol{O}\tilde{\sigma})}_{\text{BC 2}} \quad \sim(1)(2) \quad \circ\ \circ\circ\circ\circ \tag{25}$$

$$\boldsymbol{O}_{\hat{I}}\backslash\boldsymbol{O}_{h\bar{\sigma}\hat{I}}\,\boldsymbol{O}\sigma = \underbrace{(\boldsymbol{O}\sigma+\boldsymbol{O}\tilde{\sigma})}_{\text{BC 2}}, \underbrace{(\boldsymbol{O}+\boldsymbol{O}\hat{I})}_{\text{AD 1}} \quad \sim(1\ \ 2) \quad \mathrm{x}\circ\mathrm{x}\,\mathrm{x}\circ \tag{26}$$

$$\boldsymbol{O}_{\hat{I}}\backslash\boldsymbol{O}_{h\bar{\sigma}\hat{I}}\,\boldsymbol{O}\tilde{\sigma} = \underbrace{(\boldsymbol{O}\sigma+\boldsymbol{O}\tilde{\sigma})}_{\text{BC 2}}, \underbrace{(\boldsymbol{O}+\boldsymbol{O}\hat{I})}_{\text{AD 1}} \quad \sim(1\ \ 2) \quad \mathrm{x}\,\mathrm{x}\circ\mathrm{x}\circ \tag{27}$$

$$\boldsymbol{O}_{\hat{I}}\backslash\boldsymbol{O}_{h\bar{\sigma}\hat{I}}\,\boldsymbol{O}\hat{I} = \underbrace{(\boldsymbol{O}+\boldsymbol{O}\hat{I})}_{\text{AD 1}}, \underbrace{(\boldsymbol{O}\sigma+\boldsymbol{O}\tilde{\sigma})}_{\text{BC 2}} \quad \sim(1)(2) \quad \mathrm{x}\,\mathrm{x}\,\mathrm{x}\circ\circ \tag{28}$$

list of marks [2,0,0,2,0]

The resulting list of permutations shown in the last parts of Eqs. 25–28 similarly produces the list of marks [2,0,0,2,0] by referring to $\mathrm{SSG}_{\boldsymbol{O}\backslash\boldsymbol{O}_{h\tilde{\sigma}\hat{I}}}$ (Eq. 8).

The 5th subgroup $\underbrace{\boldsymbol{O}_{h\tilde{\sigma}\hat{I}}\ (\mathbf{ABCD})}_{5}$ is the *RS*-stereoisomeric group itself as collected in Eq. 8. It constructs the factor group $\boldsymbol{O}_{h\tilde{\sigma}\hat{I}}\backslash\boldsymbol{O}_{h\tilde{\sigma}\hat{I}}$, which show the following multiplication results by referring to Figure 5:

$$\boldsymbol{O}_{h\widetilde{\sigma}\widehat{I}}\backslash\boldsymbol{O}_{h\widetilde{\sigma}\widehat{I}} = \left\{ \underbrace{(\boldsymbol{O}+\boldsymbol{O}\sigma+\boldsymbol{O}\widetilde{\sigma}+\boldsymbol{O}\widehat{I})}_{\mathbf{ABCD\ 1}} \right\} \quad \textit{Permutation} \quad \begin{matrix}\text{SSG}\\ 1\ 2\ 3\ 4\ 5\end{matrix} \tag{29}$$

$$\boldsymbol{O}_{h\widetilde{\sigma}\widehat{I}}\backslash\boldsymbol{O}_{h\widetilde{\sigma}\widehat{I}}\ \boldsymbol{O} = \underbrace{(\boldsymbol{O}+\boldsymbol{O}\sigma+\boldsymbol{O}\widetilde{\sigma}+\boldsymbol{O}\widehat{I})}_{\mathbf{ABCD\ 1}} \quad \sim(1) \quad \circ\ \circ\ \circ\ \circ\ \circ \tag{30}$$

$$\boldsymbol{O}_{h\widetilde{\sigma}\widehat{I}}\backslash\boldsymbol{O}_{h\widetilde{\sigma}\widehat{I}}\ \boldsymbol{O}\sigma = \underbrace{(\boldsymbol{O}\sigma+\boldsymbol{O}+\boldsymbol{O}\widehat{I}+\boldsymbol{O}\widetilde{\sigma})}_{\mathbf{ABCD\ 1}} \quad \sim(1) \quad \mathrm{x}\ \circ\ \mathrm{x}\ \mathrm{x}\ \circ \tag{31}$$

$$\boldsymbol{O}_{h\widetilde{\sigma}\widehat{I}}\backslash\boldsymbol{O}_{h\widetilde{\sigma}\widehat{I}}\ \boldsymbol{O}\widetilde{\sigma} = \underbrace{(\boldsymbol{O}\widetilde{\sigma}+\boldsymbol{O}\widehat{I}+\boldsymbol{O}+\boldsymbol{O}\sigma)}_{\mathbf{ABCD\ 1}} \quad \sim(1) \quad \mathrm{x}\ \mathrm{x}\ \circ\ \mathrm{x}\ \circ \tag{32}$$

$$\boldsymbol{O}_{h\widetilde{\sigma}\widehat{I}}\backslash\boldsymbol{O}_{h\widetilde{\sigma}\widehat{I}}\ \boldsymbol{O}\widehat{I} = \underbrace{(\boldsymbol{O}\widehat{I}+\boldsymbol{O}\widetilde{\sigma}+\boldsymbol{O}\sigma+\boldsymbol{O})}_{\mathbf{ABCD\ 1}} \quad \sim(1) \quad \mathrm{x}\ \mathrm{x}\ \mathrm{x}\ \circ\ \circ \tag{33}$$

list of marks [1,1,1,1,1]

Note that, although the sequence of **A–D** in each product is different from another product, the set of **A–D** is fixed to give the unit permutation (1). Hence, the resulting list of permutations shown in the last parts of Eqs. 30–33 similarly produces the list of marks [1,1,1,1,1] by referring to $\text{SSG}_{\boldsymbol{O}\backslash\boldsymbol{O}_{h\widetilde{\sigma}\widehat{I}}}$ (Eq. 8).

According to the SSG (Eq. 8), the lists of marks calculated above are aligned to give the corresponding mark table as a left triangular matrix:

$$\texttt{tom\_matrix} = \begin{matrix}\boldsymbol{O}\backslash\boldsymbol{O}_{h\widetilde{\sigma}\widehat{I}}\\ \boldsymbol{O}_{h}\backslash\boldsymbol{O}_{h\widetilde{\sigma}\widehat{I}}\\ \boldsymbol{O}_{\widetilde{\sigma}}\backslash\boldsymbol{O}_{h\widetilde{\sigma}\widehat{I}}\\ \boldsymbol{O}_{\widehat{I}}\backslash\boldsymbol{O}_{h\widetilde{\sigma}\widehat{I}}\\ \boldsymbol{O}_{h\widetilde{\sigma}\widehat{I}}\backslash\boldsymbol{O}_{h\widetilde{\sigma}\widehat{I}}\end{matrix} \begin{pmatrix} 4 & 0 & 0 & 0 & 0\\ 2 & 2 & 0 & 0 & 0\\ 2 & 0 & 2 & 0 & 0\\ 2 & 0 & 0 & 2 & 0\\ 1 & 1 & 1 & 1 & 1 \end{pmatrix} \tag{34}$$

The GAP function `FactorGroup` can be used to obtain the factor group of the *RS*-stereoisomeric group $\boldsymbol{O}_{h\widetilde{\sigma}\widehat{I}}$ by the subgroup $\boldsymbol{O}$, i.e., $\boldsymbol{O}\backslash\boldsymbol{O}_{h\widetilde{\sigma}\widehat{I}}$ (Eq. 6). The size (order) of the resulting factor group `Group([ f1, f2 ])` (named `FG_OhsI_O` here) is calculated to be 4, which can be regarded to be a Klein 4-group and has 5 subgroups up to conjugacy. Note that the sequence of the subgroups of the factor group `FG_OhsI_O` (`Group([ f1, f2 ])`) is calculated to be `[ <identity> of ..., f1, f2, f1*f2 ]`, where `<identity> of ...` corresponds to $\boldsymbol{O}$, `f1` corresponds to $\boldsymbol{O}_{\widehat{I}}$, `f2` corresponds to $\boldsymbol{O}_{\widetilde{\sigma}}$, and `f1*f2` corresponds to $\boldsymbol{O}_{h}$. See that the output of `hom` indicates the correspondence between

$$[(1,2,3,4)(5,6,7,8),(2,4,5)(3,8,6),(1,5)(2,6)(3,7)(4,8),(9,10)]$$

and

```
[ <identity> of ..., <identity> of ..., f2,f1 ].
```

The mark table named `tom_FG_OhsI_O` is obtained by using the GAP function `TableOfMarks` and is found to be identical with Eq. 34 (note that the order of appearance of rows and columns is not equal to Eq. 34).

```
gap> gen_O_cube := [ (1,2,3,4)(5,6,7,8), (2,4,5)(3,8,6) ];;
gap> O_cube := Group(gen_O_cube);;
gap> gen_OhsI_cube := [ (1,2,3,4)(5,6,7,8), (2,4,5)(3,8,6), (1,5)(2,6)(3,7)(4,8),
     ↪ (9,10)];;
gap> OhsI_cube := Group(gen_OhsI_cube);;
gap> FG_OhsI_O := FactorGroup(OhsI_cube,O_cube);
<pc group with 2 generators>
gap> Display(Size(FG_OhsI_O));
4
gap> Display(Elements(FG_OhsI_O));
[ <identity> of ..., f1, f2, f1*f2 ]
gap> StructureDescription(last);
"C2 x C2"
gap> hom:=NaturalHomomorphismByNormalSubgroup(OhsI_cube,O_cube);
[ (1,2,3,4)(5,6,7,8), (2,4,5)(3,8,6), (1,5)(2,6)(3,7)(4,8), (9,10) ] ->
[ <identity> of ..., <identity> of ..., f2,f1 ]
gap> Display(ImagesSource(hom));
Group( [ f1, f2 ] )
gap> tom_FG_OhsI_O := TableOfMarks(FG_OhsI_O);
TableOfMarks( C2 x C2 )
gap> Display(tom_FG_OhsI_O);
1: 4
2: 2 2
3: 2 . 2
4: 2 . . 2
5: 1 1 1 1 1

gap>
```

4 Type-itemized enumerations

4.1 CI-CFs of half-size subgroups of the *RS*-stereoisomeric group $O_{h\widetilde{\sigma}\widehat{I}}$ and related CI-CFs.

For the purpose of enumeration based on Fujita's proligand method, CI-CFs have been calculated by means of the newly-defined GAP function `CalcConjClassCICF`, which is stored in `CICFgenCC.gapfunc`. The CI-CFs for the gross enumerations of cubane derivatives have been reported

previously [59].

$$\text{CI-CF}(\boldsymbol{O}, b_d) = \tfrac{1}{24}b_1^8 + \tfrac{1}{3}b_1^2b_3^2 + \tfrac{3}{8}b_2^4 + \tfrac{1}{4}b_4^2 \tag{35}$$

$$\text{CI-CF}(\boldsymbol{O}_h, \$_d) = \tfrac{1}{48}b_1^8 + \tfrac{1}{8}a_1^4c_2^2 + \tfrac{1}{6}b_1^2b_3^2 + \tfrac{3}{16}b_2^4 + \tfrac{1}{12}c_2^4 + \tfrac{1}{8}b_4^2 + \tfrac{1}{6}c_2c_6 + \tfrac{1}{8}c_4^2 \tag{36}$$

$$\text{CI-CF}(\boldsymbol{O}_{\tilde{\sigma}}, b_d) = \tfrac{1}{48}b_1^8 + \tfrac{1}{8}b_1^4b_2^2 + \tfrac{1}{6}b_1^2b_3^2 + \tfrac{13}{48}b_2^4 + \tfrac{1}{6}b_2b_6 + \tfrac{1}{4}b_4^2 \tag{37}$$

$$\text{CI-CF}(\boldsymbol{O}_{\hat{I}}, \$_d) = \tfrac{1}{48}b_1^8 + \tfrac{1}{48}a_1^8 + \tfrac{1}{6}b_1^2b_3^2 + \tfrac{3}{16}b_2^4 + \tfrac{1}{6}a_1^2a_3^2 + \tfrac{3}{16}c_2^4 + \tfrac{1}{8}b_4^2 + \tfrac{1}{8}c_4^2 \tag{38}$$

$$\begin{aligned}\text{CI-CF}(\boldsymbol{O}_{h\tilde{\sigma}\hat{I}}, \$_d) = {} & \tfrac{1}{96}b_1^8 + \tfrac{13}{96}b_2^4 + \tfrac{1}{12}b_1^2b_3^2 + \tfrac{1}{8}b_4^2 + \tfrac{1}{16}b_1^4b_2^2 + \tfrac{1}{12}b_2b_6 \\ & + \tfrac{13}{96}c_2^4 + \tfrac{1}{16}a_1^4c_2^2 + \tfrac{1}{8}c_4^2 + \tfrac{1}{12}c_2c_6 + \tfrac{1}{96}a_1^8 + \tfrac{1}{12}a_1^2a_3^2.\end{aligned} \tag{39}$$

The CI-CF for the point group $\boldsymbol{O}$ (CI-CF$(\boldsymbol{O}, b_d)$ (Eq. 35)) is calculated by referring to the permutations listed in `CD_OhsI_O[1]`. The CI-CF for the point group $\boldsymbol{O}_h$ (CI-CF$(\boldsymbol{O}_h, \$_d)$ (Eq. 36)) is calculated by referring to the permutations listed in `CD_OhsI_O[1]` and `CD_OhsI_O[4]`, where each 2-cycle (9,10) indicates a reflection operation. The CI-CF for the *RS*-permuation group $\boldsymbol{O}_{\tilde{\sigma}}$ (CI-CF$(\boldsymbol{O}_{\tilde{\sigma}}, b_d)$ (Eq. 37)) is calculated by referring to the permutations listed in `CD_OhsI_O[1]` and `CD_OhsI_O[2]`. Similarly, the CI-CF for the *LR*-permuation group $\boldsymbol{O}_{\hat{I}}$ (CI-CF$(\boldsymbol{O}_{\hat{\sigma}}, \$_d)$ (Eq. 38)) is calculated by referring to the permutations listed in `CD_OhsI_O[1]` and `CD_OhsI_O[3]`, where each 2-cycle (9,10) indicates a reflection operation. And finally, the CI-CF for the *RS*-stereoisomeric group $\boldsymbol{O}_{h\tilde{\sigma}\hat{I}}$ (CI-CF$(\boldsymbol{O}_{h\tilde{\sigma}\hat{I}}, \$_d)$ (Eq. 39)) is calculated by referring to the permutations listed from `CD_OhsI_O[1]` to `CD_OhsI_O[4]`, where each 2-cycle (9,10) indicates a reflection operation.

In the present article, a novel method on the basis of the factor group will be proposed as an alternative type-itemized enumerations of cubane derivatives. By referring to the factor group $\boldsymbol{O}\backslash\boldsymbol{O}_{h\tilde{\sigma}\hat{I}}$ (Eq. 6), the CI-CFs for the respective cosets (**A**, **B**, **C**, and **D**) can be calculated from Eq. 35 to Eq. 38, e.g., 2CI-CF$(\boldsymbol{O}_h, \$_d)$ − CI-CF$(\boldsymbol{O}, b_d)$ (Eq. 41) for the coset **B**.

$$\text{CI-CF}(\mathbf{A}) = \text{CI-CF}(\boldsymbol{O}, b_d) = \tfrac{1}{24}b_1^8 + \tfrac{1}{3}b_1^2b_3^2 + \tfrac{3}{8}b_2^4 + \tfrac{1}{4}b_4^2 \tag{40}$$

$$\text{CI-CF}(\mathbf{B}) = 2\text{CI-CF}(\boldsymbol{O}_h, \$_d) - \text{CI-CF}(\boldsymbol{O}, b_d) = \tfrac{1}{4}a_1^4c_2^2 + \tfrac{1}{4}c_4^2 + \tfrac{1}{6}c_2^4 + \tfrac{1}{3}c_2c_6. \tag{41}$$

$$\text{CI-CF}(\mathbf{C}) = 2\text{CI-CF}(\boldsymbol{O}_{\tilde{\sigma}}, b_d) - \text{CI-CF}(\boldsymbol{O}, b_d) = \tfrac{1}{4}b_1^4b_2^2 + \tfrac{1}{4}b_4^2 + \tfrac{1}{6}b_2^4 + \tfrac{1}{3}b_2b_6, \tag{42}$$

$$\text{CI-CF}(\mathbf{D}) = 2\text{CI-CF}(\boldsymbol{O}_{\hat{I}}, \$_d) - \text{CI-CF}(\boldsymbol{O}, b_d) = \tfrac{1}{24}a_1^8 + \tfrac{1}{3}a_1^2a_3^2 + \tfrac{3}{8}c_2^4 + \tfrac{1}{4}c_4^2. \tag{43}$$

These CI-CFs can be calculated alternatively by referring to `CD_OhsI_O[1]` to `CD_OhsI_O[4]`, because these cosets (**A**–**D**) are concretely obtained as shown above. It should be noted that CI-CF(**A**) (Eq. 40) and CI-CF(**D**)

(Eq. 43) (as well as CI-CF(**B**) (Eq. 41) and CI-CF(**C**) (Eq. 42)) have the same cycle structures, if the differences due to chirality fittingness are neglected. This parallelism comes from the fact that the permutations listed in `CD_OhsI_O[1]` (for **A**) have the same structures as those of `CD_OhsI_O[3]` (for **D**) if the 2-cycle (9,10) is neglected, as well as from the fact that the permutations listed in `CD_OhsI_O[2]` (for **C**) have the same structures as those of `CD_OhsI_O[4]` (for **B**) if the 2-cycle (9,10) is neglected.

4.2 Ligand inventories and ligand-inventory functions

The CI-CFs (Eqs. 35–39) calculated under the subgroups of $\boldsymbol{O}_{h\widetilde{\sigma}\widehat{I}}$ are used in the type-itemized enumerations of cubane derivatives (the half-size-subgroup method). On the other hand, the CI-CFs for the respective cosets (**A**, **B**, **C**, and **D**) (Eqs. 40–43) are used in the type-itemized enumerations of cubane derivatives (the factor-group method) by referring to the factor group $\boldsymbol{O}\backslash\boldsymbol{O}_{h\widetilde{\sigma}\widehat{I}}$ (Eq. 6). For the sake of simplicity, a set of eight proligands is selected from the following inventory of proligands:

$$\boldsymbol{L} = \{\mathrm{H}, \mathrm{A}, \mathrm{B}, \mathrm{X}, \mathrm{Y}, \mathrm{Z};\ \mathrm{p}, \overline{\mathrm{p}};\ \mathrm{q}, \overline{\mathrm{q}}\} \tag{44}$$

where H, A, B, X, Y, and Z are achiral proligands in isolation, while a pair of p and $\overline{\mathrm{p}}$ (or q and $\overline{\mathrm{q}}$) represents an enantiomeric pair of chiral proligands in isolation. The corresponding ligand-inventory functions are obtained according to Eqs. 5–7 in Theorem 1 of Ref. [35].

$$a_d = \mathrm{H}^d + \mathrm{A}^d + \mathrm{B}^d + \mathrm{X}^d + \mathrm{Y}^d + \mathrm{Z}^d \tag{45}$$

$$b_d = \mathrm{H}^d + \mathrm{A}^d + \mathrm{B}^d + \mathrm{X}^d + \mathrm{Y}^d + \mathrm{Z}^d + \mathrm{p}^d + \overline{\mathrm{p}}^d + \mathrm{q}^d + \overline{\mathrm{q}}^d \tag{46}$$

$$c_d = \mathrm{H}^d + \mathrm{A}^d + \mathrm{B}^d + \mathrm{X}^d + \mathrm{Y}^d + \mathrm{Z}^d + 2\mathrm{p}^{d/2}\overline{\mathrm{p}}^{d/2} + 2\mathrm{q}^{d/2}\overline{\mathrm{q}}^{d/2} \tag{47}$$

Note that the methodology of Fujita's USCI approach is applied to the enumerations of stereoisograms after an appropriate reinterpretation. The ligand-inventory functions (Eqs. 45–47) are introduced into the CI-CFs (Eqs. 35–39) or the CI-CFs (Eqs. 40–43). The resulting equations are expanded to give generating functions, in which the coefficient of

each term $\mathrm{H}^h\mathrm{A}^a\mathrm{B}^b\mathrm{X}^x\mathrm{Y}^y\mathrm{Z}^z\mathrm{p}^p\overline{\mathrm{p}}^{\overline{p}}\mathrm{q}^q\overline{\mathrm{q}}^{\overline{q}}$ represents the number of fixed 3D-structures with the composition $\mathrm{C}_8\mathrm{H}_h\mathrm{A}_a\mathrm{B}_b\mathrm{X}_x\mathrm{Y}_y\mathrm{Z}_z\mathrm{p}_p\overline{\mathrm{p}}_{\overline{p}}\mathrm{q}_q\overline{\mathrm{q}}_{\overline{q}}$, where each orbit (equivalence class) of 3D-structures is counted once under the respective subgroup.

Such a mode of substitution is represented by a substitution pattern represented by a partition $[h, a, b, x, y, z; p, \overline{p}, q, \overline{q}]$, because the coefficients appear symmetrically. The symmetrical appearance permits us to presume $h \geq a \geq w \geq x \geq y \geq z$; $p \geq q$, $p \geq \overline{p}$, and $q \geq \overline{q}$ without losing generality. Appendix A shows a typical procedure for Fujita's proligand method applied extendedly to *RS*-stereoisomeric group $\boldsymbol{O}_{h\widetilde{\sigma}\widehat{I}}$ by using the combined-permutation representation (CPR). Each substitution pattern marked by an asterisk (e.g., [7,0,0,0,0,0;1,0,0,0]* for H^7p) has the counterpart of opposite chirality sense (e.g., [7,0,0,0,0,0;0,1,0,0]* for $\mathrm{H}^7\overline{\mathrm{p}}$), so that the corresponding coefficient should be duplicated to generate the number of cubane derivatives.

Several examples of outputs by Appendix A are listed as follows:

```
list_partitions[1] := [ 8, 0, 0, 0, 0, 0, 0, 0, 0, 0 ];
 list_FP[1] := [ 1, 1, 1, 1, 1, 1, 1, 1, 1, E];
                    ####Category 1 (1st/4th = 1)
list_partitions[2] := [ 7, 1, 0, 0, 0, 0, 0, 0, 0, 0 ];
 list_FP[2] := [ 1, 1, 1, 1, 1, 1, 1, 1, 1, E];
list_partitions[3] := [ 6, 2, 0, 0, 0, 0, 0, 0, 0, 0 ];
 list_FP[3] := [ 3, 3, 3, 3, 3, 3, 3, 3, 3, E];
(omitted)
list_partitions[20] := [ 7, 0, 0, 0, 0, 0, 1, 0, 0, 0 ];
 list_FP[20] := [ 1, 1/2, 1, 1/2, 1/2, 1, 0, 1, 0, E];
                    #####Category 2 (1st/4th = 2)
list_partitions[21] := [ 6, 1, 0, 0, 0, 0, 1, 0, 0, 0 ];
 list_FP[21] := [ 3, 3/2, 3, 3/2, 3/2, 3, 0, 3, 0, E];
list_partitions[22] := [ 6, 0, 0, 0, 0, 0, 2, 0, 0, 0 ];
 list_FP[22] := [ 3, 3/2, 3, 3/2, 3/2, 3, 0, 3, 0, E];
(omitted)
list_partitions[40] := [ 4, 2, 1, 0, 0, 0, 1, 0, 0, 0 ];
 list_FP[40] := [ 35, 35/2, 22, 35/2, 11, 35, 0, 9, 0, E];
list_partitions[41] := [ 4, 2, 0, 0, 0, 0, 1, 1, 0, 0 ];
 list_FP[41] := [ 35, 23, 22, 22, 16, 35, 11, 9, 9, E];
                   #### Category 3 (1st/4th =/ 1,2)
(omitted)
```

in which the j-th symbol `list_partitions[j]` shows the respective substitution pattern according to $[h, a, b, x, y, z; p, \overline{p}, q, \overline{q}]$ and the j-th symbol `list_FP[j]` shows the respective list of fixed points according to the se-

Table 1. Numbers of Cubane Derivatives Under the Subgroups of *RS*-Stereoisomeric Group (Category 1)

j	list1_partitions	list1_FP									
		[$\boldsymbol{O}$, (Eq. 35)	$\boldsymbol{O}_h$, (Eq. 36)	$\boldsymbol{O}_{\widetilde{\sigma}}$, (Eq. 37)	$\boldsymbol{O}_{\widehat{I}}$, (Eq. 38)	$\boldsymbol{O}_{h\widetilde{\sigma}\widehat{I}}$, (Eq. 39)	A, (Eq. 40)	B, (Eq. 41)	C, (Eq. 42)	D, (Eq. 43)	E]
1	[8, 0, 0, 0, 0, 0, 0, 0, 0, 0]	[1,	1,	1,	1,	1,	1,	1,	1,	1,	E]
2	[7, 1, 0, 0, 0, 0, 0, 0, 0, 0]	[1,	1,	1,	1,	1,	1,	1,	1,	1,	E]
3	[6, 2, 0, 0, 0, 0, 0, 0, 0, 0]	[3,	3,	3,	3,	3,	3,	3,	3,	3,	E]
4	[6, 1, 1, 0, 0, 0, 0, 0, 0, 0]	[3,	3,	3,	3,	3,	3,	3,	3,	3,	E]
5	[5, 3, 0, 0, 0, 0, 0, 0, 0, 0]	[3,	3,	3,	3,	3,	3,	3,	3,	3,	E]
6	[5, 2, 1, 0, 0, 0, 0, 0, 0, 0]	[7,	6,	6,	7,	6,	7,	5,	5,	7,	E]
7	[5, 1, 1, 1, 0, 0, 0, 0, 0, 0]	[14,	10,	10,	14,	10,	14,	6,	6,	14,	E]
8	[4, 4, 0, 0, 0, 0, 0, 0, 0, 0]	[7,	6,	6,	7,	6,	7,	5,	5,	7,	E]
9	[4, 3, 1, 0, 0, 0, 0, 0, 0, 0]	[13,	10,	10,	13,	10,	13,	7,	7,	13,	E]
10	[4, 2, 2, 0, 0, 0, 0, 0, 0, 0]	[22,	16,	16,	22,	16,	22,	10,	10,	22,	E]
11	[4, 2, 1, 1, 0, 0, 0, 0, 0, 0]	[35,	22,	22,	35,	22,	35,	9,	9,	35,	E]
12	[4, 1, 1, 1, 1, 0, 0, 0, 0, 0]	[70,	38,	38,	70,	38,	70,	6,	6,	70,	E]
13	[3, 3, 2, 0, 0, 0, 0, 0, 0, 0]	[24,	17,	17,	24,	17,	24,	10,	10,	24,	E]
14	[3, 3, 1, 1, 0, 0, 0, 0, 0, 0]	[48,	30,	30,	48,	30,	48,	12,	12,	48,	E]
15	[3, 2, 2, 1, 0, 0, 0, 0, 0, 0]	[70,	42,	42,	70,	42,	70,	14,	14,	70,	E]
16	[3, 2, 1, 1, 1, 0, 0, 0, 0, 0]	[140,	76,	76,	140,	76,	140,	12,	12,	140,	E]
17	[2, 2, 2, 2, 0, 0, 0, 0, 0, 0]	[114,	68,	68,	114,	68,	114,	22,	22,	114,	E]
18	[2, 2, 2, 1, 1, 0, 0, 0, 0, 0]	[210,	114,	114,	210,	114,	210,	18,	18,	210,	E]
19	[2, 2, 1, 1, 1, 1, 0, 0, 0, 0]	[420,	216,	216,	420,	216,	420,	12,	12,	420,	E]
20	[6, 0, 0, 0, 0, 0, 1, 1, 0, 0]	[3,	3,	3,	3,	3,	3,	3,	3,	3,	E]
21	[3, 1, 1, 1, 1, 1, 0, 0, 0, 0]	[280,	140,	140,	280,	140,	280,	0,	0,	280,	E]
22	[0, 0, 0, 0, 0, 0, 4, 4, 0, 0]	[7,	6,	6,	7,	6,	7,	5,	5,	7,	E]

quence [$\boldsymbol{O}$, $\boldsymbol{O}_h$, $\boldsymbol{O}_{\widetilde{\sigma}}$, $\boldsymbol{O}_{\widehat{I}}$, $\boldsymbol{O}_{h\widetilde{\sigma}\widehat{I}}$, A, B, C, D, and E], where the last symbol E is a tentative output corresponding to a value of $\boldsymbol{O}_{h\widetilde{\sigma}\widehat{I}}$.

For the sake of convenience, the output data due to Appendix A are separated into Category 1 (Table 1), Category 2 (Tables 2 and 3), and Category 3 (Table 4), where the respective rows are renumbered according to each category (the leftmost column of each row). For example, `list_partitions[1]` and `list_FP[1]` explained above (Category 1) are printed as `list1_partitions[1]` and `list1_FP[1]` in Table 1; `list_partitions[20]` and `list_FP[20]` explained above (Category 2) are printed as `list2_partitions[1]` and `list2_FP[1]` in Table 2 (and also in Table 3); as well as `list_partitions[41]` and `list_FP[41]` explained above (Category 3) are printed as `list3_partitions[2]` and `list3_FP[2]` in Table 4.

Category 1 is determined if the ratio $\boldsymbol{O}/\boldsymbol{O}_{\widehat{I}}$ (the 1st value /4th value in `list_FP[j]`) is equal to 1, so that we put E = B (the 7th value) for subsequent calculations. Table 1 collects the data of Category 1, where the list numbers are changed for use of Category 1, i.e., `list1_partitions[j]` and `list1_FP[j]`.

On the other hand, Category 2 is determined if the ratio $\boldsymbol{O}/\boldsymbol{O}_{\widehat{I}}$ (the 1st value /4th value in `list_FP[j]`) is equal to 2, so that we put E = 0 for subsequent calculations. Tables 2 and 3 collect several data of Cat-

Table 2. Numbers of Cubane Derivatives Under the Subgroups of *RS*-Stereoisomeric Group (Category 2, Part 1)

j	list2_partitions	list2_FP [$\boldsymbol{O}$, (Eq. 35)	$\boldsymbol{O}_h$, (Eq. 36)	$\boldsymbol{O}_{\tilde{\sigma}}$, (Eq. 37)	$\boldsymbol{O}_{\widehat{I}}$, (Eq. 38)	$\boldsymbol{O}_{h\tilde{\sigma}\widehat{I}}$, (Eq. 39)	A, (Eq. 40)	B, (Eq. 41)	C, (Eq. 42)	D, (Eq. 43)	E]
1	[7, 0, 0, 0, 0, 0, 1, 0, 0, 0]	1,	1/2,	1,	1/2,	1/2,	1,	0,	1,	0,	0]
2	[6, 1, 0, 0, 0, 0, 1, 0, 0, 0]	3,	3/2,	3,	3/2,	3/2,	3,	0,	3,	0,	0]
3	[6, 0, 0, 0, 0, 0, 2, 0, 0, 0]	3,	3/2,	3,	3/2,	3/2,	3,	0,	3,	0,	0]
4	[6, 0, 0, 0, 0, 0, 1, 0, 1, 0]	3,	3/2,	3,	3/2,	3/2,	3,	0,	3,	0,	0]
5	[5, 2, 0, 0, 0, 0, 1, 0, 0, 0]	7,	7/2,	6,	7/2,	3,	7,	0,	5,	0,	0]
6	[5, 1, 1, 0, 0, 0, 1, 0, 0, 0]	14,	7,	10,	7,	5,	14,	0,	6,	0,	0]
7	[5, 1, 0, 0, 0, 0, 2, 0, 0, 0]	7,	7/2,	6,	7/2,	3,	7,	0,	5,	0,	0]
8	[5, 1, 0, 0, 0, 0, 1, 1, 0, 0]	14,	9,	10,	7,	6,	14,	4,	6,	0,	0]
9	[5, 1, 0, 0, 0, 0, 1, 0, 1, 0]	14,	7,	10,	7,	5,	14,	0,	6,	0,	0]
10	[5, 0, 0, 0, 0, 0, 3, 0, 0, 0]	3,	3/2,	3,	3/2,	3/2,	3,	0,	3,	0,	0]
11	[5, 0, 0, 0, 0, 0, 2, 1, 0, 0]	7,	7/2,	6,	7/2,	3,	7,	0,	5,	0,	0]
12	[5, 0, 0, 0, 0, 0, 1, 1, 1, 0]	14,	7,	10,	7,	5,	14,	0,	6,	0,	0]
13	[4, 0, 0, 0, 0, 0, 4, 0, 0, 0]	7,	7/2,	6,	7/2,	3,	7,	0,	5,	0,	0]
14	[4, 3, 0, 0, 0, 0, 1, 0, 0, 0]	13,	13/2,	10,	13/2,	5,	13,	0,	7,	0,	0]
15	[4, 0, 0, 0, 0, 0, 3, 1, 0, 0]	13,	13/2,	10,	13/2,	5,	13,	0,	7,	0,	0]
16	[4, 0, 0, 0, 0, 0, 3, 0, 1, 0]	13,	13/2,	10,	13/2,	5,	13,	0,	7,	0,	0]
17	[4, 2, 0, 0, 0, 0, 2, 0, 0, 0]	22,	11,	16,	11,	8,	22,	0,	10,	0,	0]
18	[4, 0, 0, 0, 0, 0, 2, 0, 2, 0]	22,	11,	16,	11,	8,	22,	0,	10,	0,	0]
19	[4, 2, 1, 0, 0, 0, 1, 0, 0, 0]	35,	35/2,	22,	35/2,	11,	35,	0,	9,	0,	0]
20	[4, 2, 0, 0, 0, 0, 1, 0, 1, 0]	35,	35/2,	22,	35/2,	11,	35,	0,	9,	0,	0]
21	[4, 0, 0, 0, 0, 0, 2, 1, 1, 0]	35,	35/2,	22,	35/2,	11,	35,	0,	9,	0,	0]
22	[4, 0, 0, 0, 0, 0, 2, 0, 1, 1]	35,	35/2,	22,	35/2,	11,	35,	0,	9,	0,	0]
23	[4, 1, 1, 1, 0, 0, 1, 0, 0, 0]	70,	35,	38,	35,	19,	70,	0,	6,	0,	0]
24	[4, 1, 1, 0, 0, 0, 1, 1, 0, 0]	70,	41,	38,	35,	22,	70,	12,	6,	0,	0]
25	[4, 1, 1, 0, 0, 0, 2, 0, 0, 0]	35,	35/2,	22,	35/2,	11,	35,	0,	9,	0,	0]
26	[4, 1, 0, 0, 0, 0, 1, 1, 1, 0]	70,	35,	38,	35,	19,	70,	0,	6,	0,	0]
27	[3, 3, 1, 0, 0, 0, 1, 0, 0, 0]	48,	24,	30,	24,	15,	48,	0,	12,	0,	0]
28	[3, 3, 0, 0, 0, 0, 1, 1, 0, 0]	48,	28,	30,	24,	17,	48,	8,	12,	0,	0]
29	[3, 3, 0, 0, 0, 0, 1, 0, 1, 0]	48,	24,	30,	24,	15,	48,	0,	12,	0,	0]
30	[3, 3, 0, 0, 0, 0, 2, 0, 0, 0]	24,	12,	17,	12,	17/2,	24,	0,	10,	0,	0]
31	[3, 2, 2, 0, 0, 0, 1, 0, 0, 0]	70,	35,	42,	35,	21,	70,	0,	14,	0,	0]
32	[3, 2, 0, 0, 0, 0, 2, 1, 0, 0]	70,	35,	42,	35,	21,	70,	0,	14,	0,	0]
33	[3, 2, 1, 1, 0, 0, 1, 0, 0, 0]	140,	70,	76,	70,	38,	140,	0,	12,	0,	0]
34	[3, 2, 1, 0, 0, 0, 1, 1, 0, 0]	140,	78,	76,	70,	42,	140,	16,	12,	0,	0]
35	[3, 2, 0, 0, 0, 0, 1, 1, 1, 0]	140,	70,	76,	70,	38,	140,	0,	12,	0,	0]
36	[3, 1, 1, 1, 1, 0, 1, 0, 0, 0]	280,	140,	140,	140,	70,	280,	0,	0,	0,	0]
37	[3, 1, 1, 1, 0, 0, 1, 1, 0, 0]	280,	152,	140,	140,	76,	280,	24,	0,	0,	0]
38	[3, 1, 1, 1, 0, 0, 1, 0, 1, 0]	280,	140,	140,	140,	70,	280,	0,	0,	0,	0]
39	[3, 1, 1, 0, 0, 0, 1, 1, 1, 0]	280,	140,	140,	140,	70,	280,	0,	0,	0,	0]
40	[3, 1, 0, 0, 0, 0, 1, 1, 1, 1]	280,	144,	140,	140,	72,	280,	8,	0,	0,	0]

egory 2, where the list numbers are changed for use of Category 2, i.e., `list2_partitions[j]` and `list2_FP[j]`.

Category 3 is determined if the ratio $\boldsymbol{O}/\boldsymbol{O}_{\widehat{I}}$ in `list_FP[j]` is neither equal to 1 nor equal to 2, so that E is calculated by a special procedure for subsequent calculations. Table 4 collects several data of Category 3. where the list numbers are changed for use of Category 3, i.e., `list3_partitions[j]` and `list3_FP[j]`.

4.3 Total features of type-itemized enumerations

By type-itemized enumerations under the *RS*-stereoisomeric group $\boldsymbol{O}_{h\tilde{\sigma}\widehat{I}}$, there emerge five types of stereoisograms shown in Figure 6, which is cited

Table 3. Numbers of Cubane Derivatives Under the Subgroups of *RS*-Stereoisomeric Group (Category 2, Part 2)

j	list2_partitions	list2_FP									
		[$\boldsymbol{O}$, (Eq. 35)	$\boldsymbol{O}_h$, (Eq. 36)	$\boldsymbol{O}_{\tilde{\sigma}}$, (Eq. 37)	$\boldsymbol{O}_{\tilde{I}}$, (Eq. 38)	$\boldsymbol{O}_{h\tilde{\sigma}\tilde{I}}$, (Eq. 39)	A, (Eq. 40)	B, (Eq. 41)	C, (Eq. 42)	D, (Eq. 43)	E]
41	[3, 0, 0, 0, 0, 0, 3, 2, 0, 0]	[24,	12,	17,	12,	17/2,	24,	0,	10,	0,	0]
42	[3, 0, 0, 0, 0, 0, 3, 1, 1, 0]	[48,	24,	30,	24,	15,	48,	0,	12,	0,	0]
43	[3, 0, 0, 0, 0, 0, 3, 0, 1, 1]	[48,	24,	30,	24,	15,	48,	0,	12,	0,	0]
44	[3, 0, 0, 0, 0, 0, 2, 2, 1, 0]	[70,	35,	42,	35,	21,	70,	0,	14,	0,	0]
45	[3, 0, 0, 0, 0, 0, 2, 1, 1, 1]	[140,	70,	76,	70,	38,	140,	0,	12,	0,	0]
46	[2, 2, 2, 0, 0, 0, 2, 0, 0, 0]	[114,	57,	68,	57,	34,	114,	0,	22,	0,	0]
47	[2, 0, 0, 0, 0, 0, 3, 2, 1, 0]	[70,	35,	42,	35,	21,	70,	0,	14,	0,	0]
48	[2, 0, 0, 0, 0, 0, 3, 1, 2, 0]	[70,	35,	42,	35,	21,	70,	0,	14,	0,	0]
49	[2, 0, 0, 0, 0, 0, 3, 1, 1, 1]	[140,	70,	76,	70,	38,	140,	0,	12,	0,	0]
50	[2, 0, 0, 0, 0, 0, 2, 2, 2, 0]	[114,	57,	68,	57,	34,	114,	0,	22,	0,	0]
51	[2, 0, 0, 0, 0, 0, 2, 1, 2, 1]	[210,	105,	114,	105,	57,	210,	0,	18,	0,	0]
52	[2, 2, 2, 1, 0, 0, 1, 0, 0, 0]	[210,	105,	114,	105,	57,	210,	0,	18,	0,	0]
53	[2, 2, 2, 0, 0, 0, 1, 0, 1, 0]	[210,	105,	114,	105,	57,	210,	0,	18,	0,	0]
54	[2, 2, 1, 0, 0, 0, 2, 1, 0, 0]	[210,	105,	114,	105,	57,	210,	0,	18,	0,	0]
55	[2, 2, 1, 0, 0, 0, 2, 0, 1, 0]	[210,	105,	114,	105,	57,	210,	0,	18,	0,	0]
56	[2, 2, 0, 0, 0, 0, 2, 1, 1, 0]	[210,	105,	114,	105,	57,	210,	0,	18,	0,	0]
57	[2, 2, 1, 1, 1, 0, 1, 0, 0, 0]	[420,	210,	216,	210,	108,	420,	0,	12,	0,	0]
58	[2, 2, 1, 1, 0, 0, 2, 0, 0, 0]	[210,	105,	114,	105,	57,	210,	0,	18,	0,	0]
59	[2, 2, 1, 1, 0, 0, 1, 1, 0, 0]	[420,	222,	216,	210,	114,	420,	24,	12,	0,	0]
60	[2, 2, 1, 1, 0, 0, 1, 0, 1, 0]	[420,	210,	216,	210,	108,	420,	0,	12,	0,	0]
61	[2, 2, 1, 0, 0, 0, 1, 1, 1, 0]	[420,	210,	216,	210,	108,	420,	0,	12,	0,	0]
62	[2, 1, 1, 1, 1, 0, 2, 0, 0, 0]	[420,	210,	216,	210,	108,	420,	0,	12,	0,	0]
63	[2, 1, 1, 1, 0, 0, 2, 1, 0, 0]	[420,	210,	216,	210,	108,	420,	0,	12,	0,	0]
64	[2, 1, 1, 1, 0, 0, 2, 0, 1, 0]	[420,	210,	216,	210,	108,	420,	0,	12,	0,	0]
65	[2, 1, 1, 1, 1, 1, 1, 0, 0, 0]	[840,	420,	420,	420,	210,	840,	0,	0,	0,	0]
66	[2, 1, 1, 1, 1, 0, 1, 1, 0, 0]	[840,	432,	420,	420,	216,	840,	24,	0,	0,	0]
67	[2, 1, 1, 1, 1, 0, 1, 0, 1, 0]	[840,	420,	420,	420,	210,	840,	0,	0,	0,	0]
68	[2, 1, 1, 1, 0, 0, 1, 1, 1, 0]	[840,	420,	420,	420,	210,	840,	0,	0,	0,	0]
69	[2, 1, 1, 0, 0, 0, 1, 1, 1, 1]	[840,	432,	420,	420,	216,	840,	24,	0,	0,	0]
70	[1, 1, 1, 1, 1, 1, 2, 0, 0, 0]	[840,	420,	420,	420,	210,	840,	0,	0,	0,	0]
71	[1, 1, 1, 1, 1, 0, 3, 0, 0, 0]	[280,	140,	140,	140,	70,	280,	0,	0,	0,	0]
72	[1, 1, 1, 1, 1, 0, 2, 1, 0, 0]	[840,	420,	420,	420,	210,	840,	0,	0,	0,	0]
73	[1, 1, 1, 1, 1, 0, 2, 0, 1, 0]	[840,	420,	420,	420,	210,	840,	0,	0,	0,	0]
74	[1, 1, 1, 1, 0, 0, 2, 1, 1, 0]	[840,	420,	420,	420,	210,	840,	0,	0,	0,	0]
75	[1, 1, 1, 0, 0, 0, 2, 1, 1, 1]	[840,	420,	420,	420,	210,	840,	0,	0,	0,	0]
76	[1, 1, 1, 1, 1, 1, 1, 1, 0, 0]	[1680,	840,	840,	840,	420,	1680,	0,	0,	0,	0]
77	[1, 1, 1, 1, 1, 0, 1, 1, 1, 0]	[1680,	840,	840,	840,	420,	1680,	0,	0,	0,	0]
78	[1, 1, 1, 1, 0, 0, 1, 1, 1, 1]	[1680,	864,	840,	840,	432,	1680,	48,	0,	0,	0]
79	[0, 0, 0, 0, 0, 0, 0, 6, 2, 0, 0]	[3,	3/2,	3,	3/2,	3/2,	3,	0,	3,	0,	0]
80	[0, 0, 0, 0, 0, 0, 0, 4, 3, 1, 0]	[13,	13/2,	10,	13/2,	5,	13,	0,	7,	0,	0]
81	[0, 0, 0, 0, 0, 0, 0, 4, 2, 2, 0]	[22,	11,	16,	11,	8,	22,	0,	10,	0,	0]
82	[0, 0, 0, 0, 0, 0, 0, 4, 2, 1, 1]	[35,	35/2,	22,	35/2,	11,	35,	0,	9,	0,	0]
83	[0, 0, 0, 0, 0, 0, 0, 3, 2, 2, 1]	[70,	35,	42,	35,	21,	70,	0,	14,	0,	0]
84	[0, 0, 0, 0, 0, 0, 0, 3, 1, 3, 1]	[48,	24,	30,	24,	15,	48,	0,	12,	0,	0]

Table 4. Numbers of Cubane Derivatives Under the Subgroups of *RS*-Stereoisomeric Group (Category 3: Coexistence of Category 1 and 2)

j	list3_partitions	list3_FP									
		[$\boldsymbol{O}$, (Eq. 35)	$\boldsymbol{O}_h$, (Eq. 36)	$\boldsymbol{O}_{\tilde{\sigma}}$, (Eq. 37)	$\boldsymbol{O}_{\tilde{I}}$, (Eq. 38)	$\boldsymbol{O}_{h\tilde{\sigma}\tilde{I}}$, (Eq. 39)	A, (Eq. 40)	B, (Eq. 41)	C, (Eq. 42)	D, (Eq. 43)	E]
1	[4, 0, 0, 0, 0, 0, 2, 2, 0, 0]	[22,	14,	16,	16,	12,	22,	6,	10,	10,	E]
2	[4, 2, 0, 0, 0, 0, 1, 1, 0, 0]	[35,	23,	22,	22,	16,	35,	11,	9,	9,	E]
3	[4, 0, 0, 0, 0, 0, 1, 1, 1, 1]	[70,	40,	38,	44,	26,	70,	10,	6,	18,	E]
4	[2, 2, 0, 0, 0, 0, 2, 2, 0, 0]	[114,	64,	68,	66,	42,	114,	14,	22,	18,	E]
5	[2, 0, 0, 0, 0, 0, 2, 2, 1, 1]	[210,	113,	114,	123,	70,	210,	16,	18,	36,	E]
6	[2, 2, 2, 0, 0, 0, 1, 1, 0, 0]	[210,	118,	114,	114,	68,	210,	26,	18,	18,	E]
7	[2, 2, 0, 0, 0, 0, 1, 1, 1, 1]	[420,	224,	216,	228,	124,	420,	28,	12,	36,	E]

from the previous report [15] after necessary data for type-itemization are added.

Because a type-I stereoisogram (type index $[-,-,a]$) has equality symbols along the diagonal directions (i.e., ascleral), double-headed arrows along the vertical directions (i.e., chiral), and double-headed arrows along the horizontal directions (i.e., RS-stereogenic), the numbers of fixed points under the subgroups ($\boldsymbol{O}$, $\boldsymbol{O}_h$, $\boldsymbol{O}_{\widetilde{\sigma}}$, $\boldsymbol{O}_{\widehat{I}}$, and $\boldsymbol{O}_{h\widetilde{\sigma}\widehat{I}}$) are obtained as shown below the type-I stereoisogram. Note that such a fixed point is altered according to equivalence class of each subgroup. For example, one pair of enantiomers or one achiral derivative is counted once as a "fixed point" (an "equivalence class" or an "orbit") under the point group $\boldsymbol{O}_h$. Such numbers of fixed points are aligned to give a list for the type I (mat_I = [2,1,1,2,1]).

In a similar way, other types correspond to respective lists, i.e., mat_II = [2,1,2,1,1] for type-II (type index $[-,a,-]$), mat_III = [4,2,2,2,1] for type-III (type index $[-,-,-]$), mat_IV = [1,1,1,1,1] for type-IV (type index $[a,a,a]$), and mat_V = [2,2,1,1,1] for type-V (type index $[a,-,-]$).

These lists (mat_I to mat_V) shown in the bottoms of the respective stereoisograms of Figure 6 are collected into `type_matrix` as a 5×5 matrix as follows:

$$\text{type\_matrix} = \begin{array}{c} \backslash \\ \text{I} \\ \text{II} \\ \text{III} \\ \text{IV} \\ \text{V} \end{array} \begin{array}{c} \begin{array}{ccccc} \boldsymbol{O} & \boldsymbol{O}_h & \boldsymbol{O}_{\widetilde{\sigma}} & \boldsymbol{O}_{\widehat{I}} & \boldsymbol{O}_{h\widetilde{\sigma}\widehat{I}} \end{array} \\ \left(\begin{array}{ccccc} 2, & 1, & 1, & 2, & 1 \\ 2, & 1, & 2, & 1, & 1 \\ 4, & 2, & 2, & 2, & 1 \\ 1, & 1, & 1, & 1, & 1 \\ 2, & 2, & 1, & 1, & 1 \end{array} \right) \end{array} \tag{48}$$

The list $[3,3,3,3,3]$ for $[\boldsymbol{O}, \boldsymbol{O}_h, \boldsymbol{O}_{\widetilde{\sigma}}, \boldsymbol{O}_{\widehat{I}}, \boldsymbol{O}_{h\widetilde{\sigma}\widehat{I}}]$ can be obtained by the multiplication of $[0,0,0,3,0]$ (the presence of 3 type-IV stereoisograms) by `type_matrix` under the GAP system:

```
gap> type_matrix :=
> [[2,1,1,2,1],
> [2,1,2,1,1],
> [4,2,2,2,1],
```

<table>
<tr><th></th><th>RS-astereogenic</th><th>RS-stereogenic</th></tr>
<tr><td rowspan="2">chiral</td><td></td><td>Type I: $[-,-,a]$
chiral/RS-stereogenic/ascleral
 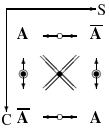

O two promolecules
$\mathbf{O}_h$ one pair of enantiomers
$\mathbf{O}_{\tilde{\sigma}}$ one pair of RS-diasteromers
$\mathbf{O}_{\tilde{I}}$ two ascleral promolecules
$\mathbf{O}_{h\tilde{\sigma}\tilde{I}}$ one quadruplet of RS-stereoisomers
mat_I = [2,1,1,2,1]</td></tr>
<tr><td>Type II: $[-,a,-]$
chiral/RS-astereogenic/scleral
 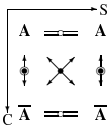

O two promolecules
$\mathbf{O}_h$ one pair of enantiomers
$\mathbf{O}_{\tilde{\sigma}}$ two RS-astereogenic promolecules
$\mathbf{O}_{\tilde{I}}$ one pair of holantimers
$\mathbf{O}_{h\tilde{\sigma}\tilde{I}}$ one quadruplet of RS-stereoisomers
mat_II = [2,1,2,1,1]</td><td>Type III: $[-,-,-]$
chiral/RS-stereogenic/scleral
 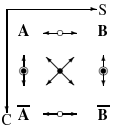

O four promolecules
$\mathbf{O}_h$ two pairs of enantiomers
$\mathbf{O}_{\tilde{\sigma}}$ two pairs of RS-diastereomers
$\mathbf{O}_{\tilde{I}}$ two pairs of holantimers
$\mathbf{O}_{h\tilde{\sigma}\tilde{I}}$ one quadruplet of RS-stereoisomers
mat_III = [4,2,2,2,1]</td></tr>
<tr><td>achiral</td><td>Type IV: $[a,a,a]$
achiral/RS-astereogenic/ascleral
 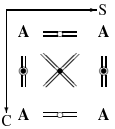

O one promolecule
$\mathbf{O}_h$ one achiral promolecule
$\mathbf{O}_{\tilde{\sigma}}$ one RS-astereogenic promolecule
$\mathbf{O}_{\tilde{I}}$ one ascleral promolecule
$\mathbf{O}_{h\tilde{\sigma}\tilde{I}}$ one quadruplet of RS-stereoisomers
mat_IV = [1,1,1,1,1]</td><td>Type V: $[a,-,-]$
achiral/RS-stereogenic/scleral
 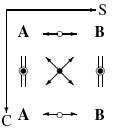

O two promolecules
$\mathbf{O}_h$ two achiral promolecules
$\mathbf{O}_{\tilde{\sigma}}$ one pair of RS-diastereomers
$\mathbf{O}_{\tilde{I}}$ one pair of holantimers
$\mathbf{O}_{h\tilde{\sigma}\tilde{I}}$ one quadruplet of RS-stereoisomers
mat_V = [2,2,1,1,1]</td></tr>
</table>

Figure 6. Stereoisograms for representing *RS*-stereoisomers of five types [15].

```
> [1,1,1,1,1],
> [2,2,1,1,1]];;
gap> [0,0,0,3,0]*type_matrix;
[ 3, 3, 3, 3, 3 ]
gap>
```

However, the inverse calculation is impossible, because the matrix `type_matrix` is singular, where the corresponding determinant is equal to zero. This means that the inverse matrix cannot be calculated, as testified as follows:

```
gap> Determinant(type_matrix);
0
gap> type_matrix^(-1);
fail
gap>
```

4.4 Half-size-subgroup method for type-itemized enumerations

Although the half-size-subgroup method for type-itemized enumerations has been described in a previous report [58], the essential points should be described briefly so as to be compared with those of the present new method (the factor-group method).

4.4.1 Half-size-subgroup method applied to category-1 cases

By examining the data of the previous subsections, we find that the enumeration results under the LR-permutation group $\boldsymbol{O}_{\hat{I}}$ are remarkable to understand total features of type-itemized enumerations. The Category 1 for a stereoisogram is defined if the number of fixed points under $\boldsymbol{O}$ (the first value of `list_FP[j]`) is equal to the number of fixed points under the LR-permutation group $\boldsymbol{O}_{\hat{I}}$.

Table 1 collects several data of Category 1, in which the ratio $\boldsymbol{O}/\boldsymbol{O}_{\hat{I}}$ (the 1st value /4th value in `list1_FP[j]`) is equal to 1, so that we put E = B (the 7th value).

By examining the type-I row and type-IV row in the type matrix (48), the $\boldsymbol{O}$-column and the $\boldsymbol{O}_{\widehat{I}}$-column have the same value (i.e., $\boldsymbol{O}/\boldsymbol{O}_{\widehat{I}} = 1$). This means that any number of type-I stereoisograms and any number of type-IV stereoisograms are possible to give the Category 1 ($\boldsymbol{O}/\boldsymbol{O}_{\widehat{I}} = 1$), if the absence of type-II, type-III, and type-IV is guaranteed.

The list $[3, 3, 3, 3, 3]$ for $[\boldsymbol{O},\ \boldsymbol{O}_h,\ \boldsymbol{O}_{\widetilde{\sigma}},\ \boldsymbol{O}_{\widehat{I}},\ \boldsymbol{O}_{h\widetilde{\sigma}\widehat{I}}]$ is extracted from the first to 5th values in the intersection between $[6, 2, 0, 0, 0, 0, 0, 0, 0, 0]$-row and `list1_FP` in Table 1. As another example, the list $[7, 6, 6, 7, 6]$ for $[\boldsymbol{O},\ \boldsymbol{O}_h,\ \boldsymbol{O}_{\widetilde{\sigma}},\ \boldsymbol{O}_{\widehat{I}},\ \boldsymbol{O}_{h\widetilde{\sigma}\widehat{I}}]$ is extracted from the first to 5th values in the intersection between $[5, 2, 1, 0, 0, 0, 0, 0, 0, 0]$-row and `list1_FP` in Table 1.

A tentative non-singular matrix `type_matrixX` is formulated from the singular matrix `type_matrix` by changing the value 1 at the intersection between th 2nd row and the 4th column into 0. Thereby, the following results are obtained.

```
gap> type_matrixX :=
> [[2,1,1,2,1],
> [2,1,2,0,1],
> [4,2,2,2,1],
> [1,1,1,1,1],
> [2,2,1,1,1]];;
gap> [3,3,3,3,3]*type_matrixX^(-1);
[ 0, 0, 0, 3, 0 ]
gap> [7,6,6,7,6]*type_matrixX^(-1);
[ 1, 0, 0, 5, 0 ]
gap>
```

The resulting list [I, II, III, IV, V] = [0, 0, 0, 3, 0] indicates the presence of three cubane derivatives having a type-IV stereoisogram, which have composition H_6A_2. On the other hand, the resulting list [I, II, III, IV, V] = [1, 0, 0, 5, 0] indicates the presence of one cubane derivative having a type-I stereoisogram and five cubane derivatives having type-IV stereoisograms, both of which have composition H_5A_2B.

More primitively speaking, the list [I, 0, 0, IV, 0] gives the following

simultaneous linear equations for the former case:

$$\begin{aligned} \text{for } \boldsymbol{O},\, \boldsymbol{O}_{\widehat{I}}: &\quad 2\mathrm{I} + \mathrm{IV} = 3 \\ \text{for } \boldsymbol{O}_h,\, \boldsymbol{O}_{\widetilde{\sigma}},\, \boldsymbol{O}_{h\widetilde{\sigma}\widehat{I}}: &\quad \mathrm{I} + \mathrm{IV} = 3 \\ \text{Result:} &\quad \mathrm{I} = 0 \text{ and } \mathrm{IV} = 3: \\ &\quad \text{i.e., [I, II, III, IV, V]} = [0,0,0,3,0]. \end{aligned} \tag{49}$$

and for the latter case:

$$\begin{aligned} \text{for } \boldsymbol{O},\, \boldsymbol{O}_{\widehat{I}}: &\quad 2\mathrm{I} + \mathrm{IV} = 7 \\ \text{for } \boldsymbol{O}_h,\, \boldsymbol{O}_{\widetilde{\sigma}},\, \boldsymbol{O}_{h\widetilde{\sigma}\widehat{I}}: &\quad \mathrm{I} + \mathrm{IV} = 6 \\ \text{Result:} &\quad \mathrm{I} = 1 \text{ and } \mathrm{IV} = 5: \\ &\quad \text{i.e., [I, II, III, IV, V]} = [1,0,0,5,0]. \end{aligned} \tag{50}$$

These results are consistent with the data calculated above by using the non-singular matrix `type_matrixX`.

Similar procedures can be applied to the data of Category 1 listed in Table 1, where the presence of cubane derivatives having type-I and type-IV stereoisograms. The results have been reported in a previous paper [58].

4.4.2 Half-size-subgroup method applied to category-2 cases

Let us examine the partition $[4, 1, 1, 0, 0, 0, 1, 1, 0, 0]$ appearing in the 24th row of Table 2, which indicates that $\boldsymbol{O}/\boldsymbol{O}_{\widehat{I}}$ (the 1st value /the 4th value) is equal to $70/35 = 2$. This value means a Category-2 case.

The list $[70, 41, 38, 35, 22]$ for $[\boldsymbol{O},\, \boldsymbol{O}_h,\, \boldsymbol{O}_{\widetilde{\sigma}},\, \boldsymbol{O}_{\widehat{I}},\, \boldsymbol{O}_{h\widetilde{\sigma}\widehat{I}}]$ is extracted from the first to 5th values in the intersection between $[4, 1, 1, 0, 0, 0, 1, 1, 0, 0]$-row and `list2_FP` in Table 2.

As discussed in the previous article [58], another non-singular matrix `type_matrixY` is tentatively formulated by starting from the singular matrix `type_matrix`, where the value 1 at the intersection between the 1st row and the 5th column is changed into 0. Thereby, the following results are obtained.

```
gap> type_matrixY :=
> [[2,1,1,2,0],
> [2,1,2,1,1],
> [4,2,2,2,1],
> [1,1,1,1,1],
> [2,2,1,1,1]];;
gap> [70,41,38,35,22]*type_matrixY^(-1);
[ 0, 3, 13, 0, 6 ]
gap>
```

The resulting list [I, II, III, IV, V] = [0, 3, 13, 0, 6] indicates that the composition $H_4ABp\overline{p}$ permits the presence of three cubane derivatives having a type-II stereoisogram, 13 cubane derivatives having a type-III stereoisogram, and 6 cubane derivatives having a type-V stereoisogram. Their formulas will be shown below for illustrating the corresponding results of the factor-group method.

Similar procedures can be applied to the data of Category 2 listed in Tables 2 and 3, where the presence of cubane derivatives having type-II, type-III, and type-V stereoisograms. The results have been reported in a previous paper [58].

4.5 Factor-group method for type-itemized enumerations

4.5.1 Factor-group method applied to category-1 cases

The respective numbers of fixed points corresponding to the respective cosets (**A**, **B**, **C**, and **D**) (Eqs. 40–43) have been calculated by using the CI-CFs for the factor group $\boldsymbol{O}\backslash\boldsymbol{O}_{h\widetilde{\sigma}\widehat{I}}$ (Eq. 6). They are listed as the five values of `list1_FP[j]` in the latter half of each row of Table 1, which can be used as a list for type-itemized enumeration under the factor group $\boldsymbol{O}\backslash\boldsymbol{O}_{h\widetilde{\sigma}\widehat{I}}$. Each value shown in the **A**-column is regarded as the number of fixed points under $\underbrace{\boldsymbol{O}\ (\mathbf{A})}_{1}$, each value shown in the **B**-column is regarded as the number of fixed points under $\underbrace{\boldsymbol{O}_h\ (\mathbf{AB})}_{2}$, each value shown in the **C**-column is regarded as the number of fixed points under $\underbrace{\boldsymbol{O}_{\widetilde{\sigma}}\ (\mathbf{AC})}_{3}$, and each value

shown in the D-column is regarded as the number of fixed points under $\underbrace{\boldsymbol{O}_{\widehat{I}}}_{4}$ (AD). By referring to the non-redundant set of subgroups $\mathrm{SSG}_{\boldsymbol{O}\backslash\boldsymbol{O}_{h\widetilde{\sigma}\widehat{I}}}$ (Eq. 8), the E-column is the number of fixed points under $\underbrace{\boldsymbol{O}_{h\widetilde{\sigma}\widehat{I}}}_{5}$ (ABCD), which is estimated by the relationship E = B in the case of Category 1. This is because Category 1 means that the ascleral property results in the absence of type-V stereoisograms to assure B = E.

The extracted list [A, B, C, D, E] is regarded to be `list1_FPCat1A`, which is represented in the calculation process as follows:

```
list1_FPCat1A :=
[list1_FP[j][6],list1_FP[j][7],list1_FP[j][8], list1_FP[j][9], list1_FP[j][10]];.
```

This list is multiplied by the inverse of a mark table `tom_matrix` as a left triangular matrix.

For the sake of convenience, the type-itemized calculations based on the factor group (mark table: `tom_matrix`) is referred to under the name *the factor-group method*. Several calculation data ($j = 20 \cdots 22$) are shown below as the examples of the GAP calculation:

```
gap> tom_matrix :=
> [[4,0,0,0,0],
> [2,2,0,0,0],
> [2,0,2,0,0],
> [2,0,0,2,0],
> [1,1,1,1,1]];;
gap> list1_partitions :=[];;
gap> list1_FP := [];;
gap> #selected data
gap> list1_III_V_II_I_Vtype := [];;
gap> list1_partitions[20] := [ 6, 0, 0, 0, 0, 0, 1, 1, 0, 0 ];
[ 6, 0, 0, 0, 0, 0, 1, 1, 0, 0 ]
gap> list1_FP[20] := [ 3, 3, 3, 3, 3, 3, 3, 3, 3, 3];
[ 3, 3, 3, 3, 3, 3, 3, 3, 3, 3 ]
gap> list1_partitions[21] := [ 3, 1, 1, 1, 1, 1, 0, 0, 0, 0 ];
[ 3, 1, 1, 1, 1, 1, 0, 0, 0, 0 ]
gap> list1_FP[21] := [ 280, 140, 140, 280, 140, 280, 0, 0, 280,0];
[ 280, 140, 140, 280, 140, 280, 0, 0, 280, 0 ]
gap> list1_partitions[22] := [ 0, 0, 0, 0, 0, 0, 4, 4, 0, 0 ];
[ 0, 0, 0, 0, 0, 0, 4, 4, 0, 0 ]
gap> list1_FP[22] := [ 7, 6, 6, 7, 6, 7, 5, 5, 7, 5];
[ 7, 6, 6, 7, 6, 7, 5, 5, 7, 5 ]
gap> #type-itemized enumeration
gap> for j in [20..22] do
> Print("list1_partitions[", j, "] := ", list1_partitions[j], "; \n");
```

Table 5. Type-Itemized Enumerations by the Factor-Group Method (Category 1)

j	list1_partitions	list1_FPCat1 $\left[\underset{\text{(Eq. 40)}}{\text{A}}, \underset{\text{(Eq. 41)}}{\text{B}}, \underset{\text{(Eq. 42)}}{\text{C}}, \underset{\text{(Eq. 43)}}{\text{D}}, \text{E}\right]$	[III_V_II_I_IV]type
1	[8, 0, 0, 0, 0, 0, 0, 0, 0, 0]	[1, 1, 1, 1, 1]	[0, 0, 0, 0, 1]
2	[7, 1, 0, 0, 0, 0, 0, 0, 0, 0]	[1, 1, 1, 1, 1]	[0, 0, 0, 0, 1]
3	[6, 2, 0, 0, 0, 0, 0, 0, 0, 0]	[3, 3, 3, 3, 3]	[0, 0, 0, 0, 3]
4	[6, 1, 1, 0, 0, 0, 0, 0, 0, 0]	[3, 3, 3, 3, 3]	[0, 0, 0, 0, 3]
5	[5, 3, 0, 0, 0, 0, 0, 0, 0, 0]	[3, 3, 3, 3, 3]	[0, 0, 0, 0, 3]
6	[5, 2, 1, 0, 0, 0, 0, 0, 0, 0]	[7, 5, 5, 7, 5]	[0, 0, 0, 1, 5]
7	[5, 1, 1, 1, 0, 0, 0, 0, 0, 0]	[14, 6, 6, 14, 6]	[0, 0, 0, 4, 6]
8	[4, 4, 0, 0, 0, 0, 0, 0, 0, 0]	[7, 5, 5, 7, 5]	[0, 0, 0, 1, 5]
9	[4, 3, 1, 0, 0, 0, 0, 0, 0, 0]	[13, 7, 7, 13, 7]	[0, 0, 0, 3, 7]
10	[4, 2, 2, 0, 0, 0, 0, 0, 0, 0]	[22, 10, 10, 22, 10]	[0, 0, 0, 6, 10]
11	[4, 2, 1, 1, 0, 0, 0, 0, 0, 0]	[35, 9, 9, 35, 9]	[0, 0, 0, 13, 9]
12	[4, 1, 1, 1, 1, 0, 0, 0, 0, 0]	[70, 6, 6, 70, 6]	[0, 0, 0, 32, 6]
13	[3, 3, 2, 0, 0, 0, 0, 0, 0, 0]	[24, 10, 10, 24, 10]	[0, 0, 0, 7, 10]
14	[3, 3, 1, 1, 0, 0, 0, 0, 0, 0]	[48, 12, 12, 48, 12]	[0, 0, 0, 18, 12]
15	[3, 2, 2, 1, 0, 0, 0, 0, 0, 0]	[70, 14, 14, 70, 14]	[0, 0, 0, 28, 14]
16	[3, 2, 1, 1, 1, 0, 0, 0, 0, 0]	[140, 12, 12, 140, 12]	[0, 0, 0, 64, 12]
17	[2, 2, 2, 2, 0, 0, 0, 0, 0, 0]	[114, 22, 22, 114, 22]	[0, 0, 0, 46, 22]
18	[2, 2, 2, 1, 1, 0, 0, 0, 0, 0]	[210, 18, 18, 210, 18]	[0, 0, 0, 96, 18]
19	[2, 2, 1, 1, 1, 1, 0, 0, 0, 0]	[420, 12, 12, 420, 12]	[0, 0, 0, 204, 12]
20	[6, 0, 0, 0, 0, 0, 1, 1, 0, 0]	[3, 3, 3, 3, 3]	[0, 0, 0, 0, 3]
21	[3, 1, 1, 1, 1, 1, 0, 0, 0, 0]	[280, 0, 0, 280, 0]	[0, 0, 0, 140, 0]
22	[0, 0, 0, 0, 0, 0, 4, 4, 0, 0]	[7, 5, 5, 7, 5]	[0, 0, 0, 1, 5]

```
> list1_FPCat1A := [list1_FP[j][6],list1_FP[j][7],list1_FP[j][8],list1_FP[j][9],
      ↪ list1_FP[j][10]];
> list_temp := list1_FPCat1A * tom_matrix^(-1);
> Print("list1_III_V_II_I_Vtype[", j, "] := ", list_temp, "; \n");
> od;
list1_partitions[20] := [ 6, 0, 0, 0, 0, 0, 1, 1, 0, 0 ];
list1_III_V_II_I_Vtype[20] := [ 0, 0, 0, 0, 3 ];
list1_partitions[21] := [ 3, 1, 1, 1, 1, 1, 0, 0, 0, 0 ];
list1_III_V_II_I_Vtype[21] := [ 0, 0, 0, 140, 0 ];
list1_partitions[22] := [ 0, 0, 0, 0, 0, 0, 4, 4, 0, 0 ];
list1_III_V_II_I_Vtype[22] := [ 0, 0, 0, 1, 5 ];
gap>
```

The total data for Category 1 (`[III_V_II_I_IV]type`, $j = 1 \cdots 22$) has been obtained on the basis of the factor-group method due to the five values `list1_FPCat1[j]` ($j = 1 \cdots 22$) extracted from the latter half of each row of Table 1 (listed as `list1_FP`, $j = 1 \cdots 22$). The resulting values are collected in Table 5. They are consistent with the values of the half-size-subgroup method in the preceding subsubsection and in the previous article [58].

4.5.2 Examples of calculation data of category 1

To examine the validity of the factor-group method proposed in the present article, let us testify several data of type-itemized enumerations of Category 1 collected in Table 5.

Cubane Derivatives with Composition H_5A_3.

The [III_V_II_I_IV]type[5] list $[0, 0, 0, 0, 3]$ appearing in the 5th row of Table 5 indicates the presence of three type-IV cubane derivatives with `list1_partitions`[5] (H_5A_3). Their stereoisograms are depicted in Figure 7. Each of them is degenerated into one achiral derivative: $([\mathbf{6}])_{\mathrm{IV}}$, $([\mathbf{8}])_{\mathrm{IV}}$, or $([\mathbf{10}])_{\mathrm{IV}}$.

The symmetry-itemized enumeration [33] under the point group $\boldsymbol{O}_h$ has indicated the presence of two $\mathbf{C}_s'$-derivatives and one $\mathbf{C}_{3v}$-derivative. The derivatives $([\mathbf{6}])_{\mathrm{IV}}$ and $([\mathbf{8}])_{\mathrm{IV}}$ belong to $\mathbf{C}_s'$-point group, where the respective mirror plane is determined to be the plane 1-2-7-8 in $([\mathbf{6}])_{\mathrm{IV}}$ and the plane 2-4-8-6 in $([\mathbf{8}])_{\mathrm{IV}}$. The three-fold axis is determined to run through 1 an 7 in the $\mathbf{C}_{3v}$-derivative ($([\mathbf{10}])_{\mathrm{IV}}$-derivative), where the projection along this line is depicted in the formula **12**.

Cubane Derivatives with Composition H_5A_2B.

The [III_V_II_I_IV]type[6] list $[0, 0, 0, 1, 5]$ appearing in the 6th row of Table 5 indicates the presence of one type-I and five type-IV cubane derivatives with `list1_partitions`[6] (H_5A_2B). Because each of the latter five type-IV stereoisograms are degenerated into one achiral derivative, they are depicted to be $([\mathbf{15}])_{\mathrm{IV}}$, $([\mathbf{16}])_{\mathrm{IV}}$, $([\mathbf{17}])_{\mathrm{IV}}$, $([\mathbf{18}])_{\mathrm{IV}}$, and $([\mathbf{19}])_{\mathrm{IV}}$. One type-I stereoisogram, which is fully depicted in Figure 8, can be represented by the corresponding simplified stereoisogram, i.e., $([\mathbf{13}\ \ \overline{\mathbf{13}}])_{\mathrm{I}}$.

The symmetry-itemized enumeration [33] under the point group $\boldsymbol{O}_h$ has indicated the presence of one $\mathbf{C}_1$-derivative and five $\mathbf{C}_s'$-derivatives with the composition H_5A_2B.

The $\mathbf{C}_s'$-point group assigned to the derivatives $([\mathbf{15}])_{\mathrm{IV}}$ and $([\mathbf{16}])_{\mathrm{IV}}$ are characterized by the respective mirror plane determined to be the plane 2486. On the other hand, the $\mathbf{C}_s'$-point group assigned to the derivatives $([\mathbf{17}])_{\mathrm{IV}}$. $([\mathbf{18}])_{\mathrm{IV}}$, and $([\mathbf{19}])_{\mathrm{IV}}$ are characterized by the respective mirror plane determined to be the plane 1375. The two kinds of $\mathbf{C}_s'$-point groups are conjugate to each other under the point group $\boldsymbol{O}_h$.

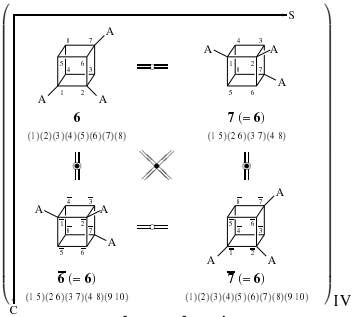

$[a,a,a]$, $\mathbf{C}_s'$,

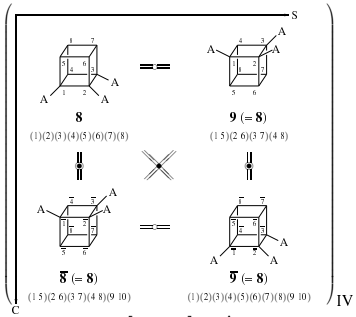

$[a,a,a]$, $\mathbf{C}_s'$

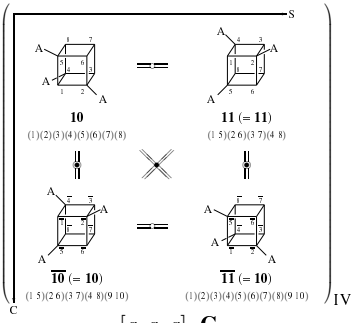

$[a,a,a]$, $\mathbf{C}_{3v}$

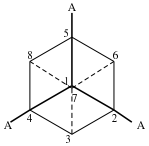

12

Figure 7. Stereoisograms of cubane derivative with the composition H_5A_3. The type index $[a,a,a]$ is assigned to such a type-IV stereoisogram, which is specified to be achiral, *RS*-astereogenic, and ascleral.

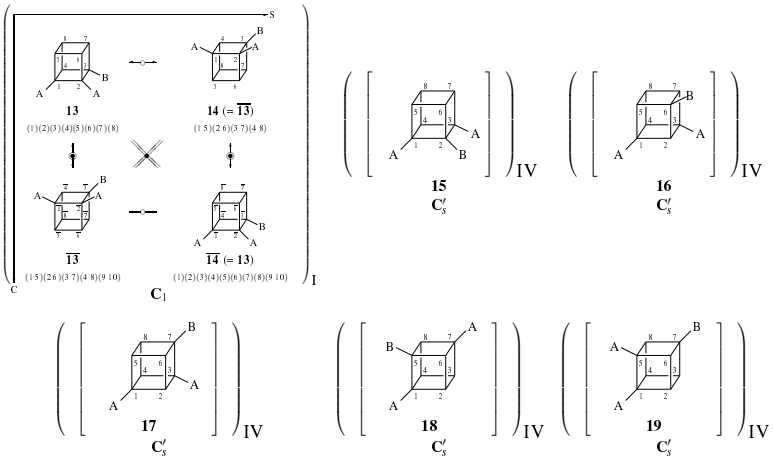

Figure 8. Type-I stereoisogram (full form) of a cubane derivative with the composition H_5A_2B and Simplified type-IV stereoisograms of cubane derivatives with the composition H_5A_2B.

In the previous paper [59], the author (Fujita) has applied the *C/A*-descriptors for a cube (*CU-8*) [60], which is adopted in the indexing system of Chemical Abstracts [61]. For the procedure of assigning the *C/A*-descriptors to cubane derivatives, see Section 4.3.1 of the previous paper [59]. According to Fujita's stereoisogram approach [54], a pair of *C/A*-descriptors has been clarified to be assigned to a pair of *RS*-diastereomers (due to *RS*-stereogenicity as the second kind of handedness), not to a pair of enantiomers (due to chirality as the first kind of handedness).

Let us examine the assignment of *C/A*-descriptors to the type-I stereoisogram shown in Figure 8, which is characterized by a type index $[-, -, a]$ (chirality, *RS*-stereogenicity, and asclerality) to show the presence of diagonal equality symbols. Figure 9 indicates the assignment of *C/A*-descriptors to the type-I cubane derivative (the reference promolecule **13**) with the composition H_5A_2B. According to Fujita's stereoisogram approach (see Figure 2), a pair of *C/A*-descriptors is considered to be assigned to a pair of *RS*-diastereomers **13**/**14** (due to *RS*-stereogenicity), not to a pair of enantiomers **13**/$\overline{\mathbf{13}}$ (due to chirality). Thereby, *CU*-8-13132333-*C* is given to **13**, while *CU*-8-13132333-*A* is given to **14** (= $\overline{\mathbf{13}}$). In the case of a type-I stereoisograms, its asclerality $[-, -, a]$ results in the incorpora-

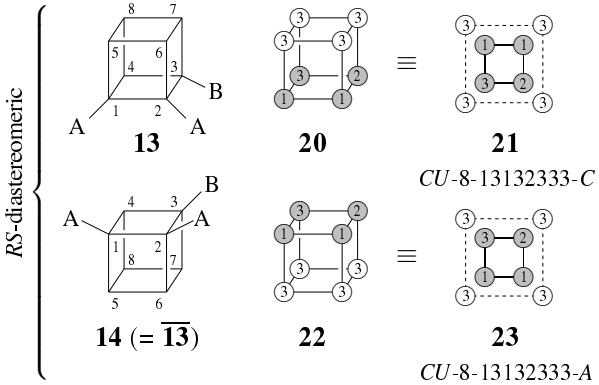

Figure 9. Assignment of *C/A*-descriptors to a pair of *RS*-diastereomers **13/14** with the composition H_5A_2B, which is characterized by a type-I stereoisogram. The pair of *RS*-diastereomers **13/14** is coincident with a pair of enantiomers **13**/$\overline{\mathbf{13}}$. The priority sequence is presumed to be A① > B② > H③.

tion between an enantiomeric relationship **13**/$\overline{\mathbf{13}}$ and *RS*-diastereomeric relationship **13/14**, so that the *C/A*-descriptors are regarded to be given to a pair of enantiomers (Figure 1) under the conventional stereochemistry. Even in Fujita's stereoisogram approach, this case is treated as being chirality-faithful because of the parallelism of *C/A*-descriptors between *RS*-stereogenicity and chirality.

Note that the conventional stereochemistry adopts chirality as a sole kind of handedness, and disregards *RS*-stereogenicity until now. This treatment under the sole kind of handedness means that the vertical frame of the enantiomerism is redrawn horizontally in Figure 1, so as to be completely involved in the horizontal frame of Mislow-Siegel's stereogenicity. As a result, the cases of type-III and the cases of type-V are treated in accordance with the type-I cases (e.g., Figure 9). Such treatments that nullify the presence of *RS*-stereogenicity as the second kind handedness have been main roots of misunderstandings in the conventional stereochemistry.

4.5.3 The factor-group method applied to category-2 cases

The Category 2 for a stereoisogram is defined if the number of fixed points under $\boldsymbol{O}$ (the first value of `list_FP[j]`) is obtained by the duplication of the number of fixed points under the LR-permutation group $\boldsymbol{O}_{\widehat{I}}$ (i.e., $\boldsymbol{O}/\boldsymbol{O}_{\widehat{I}} = 2$).

Tables 2 and 3 collect several data of Category 2, in which the ratio $\boldsymbol{O}/\boldsymbol{O}_{\widehat{I}}$ (the 1st value /4th value in `list2_FP[j]`) is equal to 2. It should be noted that we put $\mathrm{E} = \mathrm{D} = 0$.

It should be noted that we have $\mathrm{D} = 0$ always in the case of Category 2. Thus, if $\boldsymbol{O}/\boldsymbol{O}_{\widehat{I}} = 2$, all $\boldsymbol{O}_{\widehat{I}}$ is scleral and there are no ascleral derivatives, so as to give $\mathrm{D} = 0$ and $\mathrm{E} = 0$.

4.5.4 Examples of calculation data of category 2

To examine the validity of the factor-group method proposed in the present article, let us testify several data of type-itemized enumerations of Category 2 collected in Tables 6 and 7.

Derivatives with Composition $\mathrm{H}_4\mathrm{ABp}\overline{\mathrm{p}}$

As a typical Category-2 case, let us examine the values collected in the 24th row of Table 6 (`list2_partitions[24]` $= [4,1,1,0,0,0,1,1,0,0]$), which corresponds to the derivatives with composition $\mathrm{H}_4\mathrm{ABp}\overline{\mathrm{p}}$. The top 5 values $[70,41,38,35,22]$ have been already used during the half-size-subgroup method (Subsubsection 4.4.2). The next 5 values $[70,12,6,0,0]$ extracted and listed under the name `list2_FPCat2B[24]` in Table 6 are used in the present factor-group method. In the following GAP code, the set of extracted values `list2_FPCat2B[24]`[6]–[10] ($[70,12,6,0,0]$) is stored temporarily under the name `templist`. Then, this list is multiplied by the inverse matrix of a mark table (`tom_matrix`). The resulting values for `list2_III_V_II_I_Vtype[24]` are stored in the temporary list `list_temp`.

```
gap> tom_matrix :=
> [[4,0,0,0,0],
> [2,2,0,0,0],
> [2,0,2,0,0],
> [2,0,0,2,0],
> [1,1,1,1,1]];;
```

Table 6. Type-Itemized Enumerations by the Factor-Group Method (Category 2, Part 1)

j	list2_partitions	list2_FPCat2 $\left[\begin{matrix}\mathbf{A} & \mathbf{B} & \mathbf{C} & \mathbf{D} \\ \text{(Eq. 40)}, & \text{(Eq. 41)}, & \text{(Eq. 42)}, & \text{(Eq. 43)}, \end{matrix} \mathrm{E}\right]$	[III_V_II_I_IV]type
1	[7, 0, 0, 0, 0, 0, 1, 0, 0, 0]	[1, 0, 1, 0, 0]	[0, 0, 1/2, 0, 0]
2	[6, 1, 0, 0, 0, 0, 1, 0, 0, 0]	[3, 0, 3, 0, 0]	[0, 0, 3/2, 0, 0]
3	[6, 0, 0, 0, 0, 0, 2, 0, 0, 0]	[3, 0, 3, 0, 0]	[0, 0, 3/2, 0, 0]
4	[6, 0, 0, 0, 0, 0, 1, 0, 1, 0]	[3, 0, 3, 0, 0]	[0, 0, 3/2, 0, 0]
5	[5, 2, 0, 0, 0, 0, 1, 0, 0, 0]	[7, 0, 5, 0, 0]	[1/2, 0, 5/2, 0, 0]
6	[5, 1, 1, 0, 0, 0, 1, 0, 0, 0]	[14, 0, 6, 0, 0]	[2, 0, 3, 0, 0]
7	[5, 1, 0, 0, 0, 0, 2, 0, 0, 0]	[7, 0, 5, 0, 0]	[1/2, 0, 5/2, 0, 0]
8	[5, 1, 0, 0, 0, 0, 1, 1, 0, 0]	[14, 4, 6, 0, 0]	[1, 2, 3, 0, 0]
9	[5, 1, 0, 0, 0, 0, 1, 0, 1, 0]	[14, 0, 6, 0, 0]	[2, 0, 3, 0, 0]
10	[5, 0, 0, 0, 0, 0, 3, 0, 0, 0]	[3, 0, 3, 0, 0]	[0, 0, 3/2, 0, 0]
11	[5, 0, 0, 0, 0, 0, 2, 1, 0, 0]	[7, 0, 5, 0, 0]	[1/2, 0, 5/2, 0, 0]
12	[5, 0, 0, 0, 0, 0, 1, 1, 1, 0]	[14, 0, 6, 0, 0]	[2, 0, 3, 0, 0]
13	[4, 0, 0, 0, 0, 0, 4, 0, 0, 0]	[7, 0, 5, 0, 0]	[1/2, 0, 5/2, 0, 0]
14	[4, 3, 0, 0, 0, 0, 1, 0, 0, 0]	[13, 0, 7, 0, 0]	[3/2, 0, 7/2, 0, 0]
15	[4, 0, 0, 0, 0, 0, 3, 1, 0, 0]	[13, 0, 7, 0, 0]	[3/2, 0, 7/2, 0, 0]
16	[4, 0, 0, 0, 0, 0, 3, 0, 1, 0]	[13, 0, 7, 0, 0]	[3/2, 0, 7/2, 0, 0]
17	[4, 2, 0, 0, 0, 0, 2, 0, 0, 0]	[22, 0, 10, 0, 0]	[3, 0, 5, 0, 0]
18	[4, 0, 0, 0, 0, 0, 2, 0, 2, 0]	[22, 0, 10, 0, 0]	[3, 0, 5, 0, 0]
19	[4, 2, 1, 0, 0, 0, 1, 0, 0, 0]	[35, 0, 9, 0, 0]	[13/2, 0, 9/2, 0, 0]
20	[4, 2, 0, 0, 0, 0, 1, 0, 1, 0]	[35, 0, 9, 0, 0]	[13/2, 0, 9/2, 0, 0]
21	[4, 0, 0, 0, 0, 0, 2, 1, 1, 0]	[35, 0, 9, 0, 0]	[13/2, 0, 9/2, 0, 0]
22	[4, 0, 0, 0, 0, 0, 2, 0, 1, 1]	[35, 0, 9, 0, 0]	[13/2, 0, 9/2, 0, 0]
23	[4, 1, 1, 1, 0, 0, 1, 0, 0, 0]	[70, 0, 6, 0, 0]	[16, 0, 3, 0, 0]
24	[4, 1, 1, 0, 0, 0, 1, 1, 0, 0]	[70, 12, 6, 0, 0]	[13, 6, 3, 0, 0]
25	[4, 1, 1, 0, 0, 0, 2, 0, 0, 0]	[35, 0, 9, 0, 0]	[13/2, 0, 9/2, 0, 0]
26	[4, 1, 0, 0, 0, 0, 1, 1, 1, 0]	[70, 0, 6, 0, 0]	[16, 0, 3, 0, 0]
27	[3, 3, 1, 0, 0, 0, 1, 0, 0, 0]	[48, 0, 12, 0, 0]	[9, 0, 6, 0, 0]
28	[3, 3, 0, 0, 0, 0, 1, 1, 0, 0]	[48, 8, 12, 0, 0]	[7, 4, 6, 0, 0]
29	[3, 3, 0, 0, 0, 0, 1, 0, 1, 0]	[48, 0, 12, 0, 0]	[9, 0, 6, 0, 0]
30	[3, 3, 0, 0, 0, 0, 2, 0, 0, 0]	[24, 0, 10, 0, 0]	[7/2, 0, 5, 0, 0]
31	[3, 2, 2, 0, 0, 0, 1, 0, 0, 0]	[70, 0, 14, 0, 0]	[14, 0, 7, 0, 0]
32	[3, 2, 0, 0, 0, 0, 2, 1, 0, 0]	[70, 0, 14, 0, 0]	[14, 0, 7, 0, 0]
33	[3, 2, 1, 1, 0, 0, 1, 0, 0, 0]	[140, 0, 12, 0, 0]	[32, 0, 6, 0, 0]
34	[3, 2, 1, 0, 0, 0, 1, 1, 0, 0]	[140, 16, 12, 0, 0]	[28, 8, 6, 0, 0]
35	[3, 2, 0, 0, 0, 0, 1, 1, 1, 0]	[140, 0, 12, 0, 0]	[32, 0, 6, 0, 0]
36	[3, 1, 1, 1, 1, 0, 1, 0, 0, 0]	[280, 0, 0, 0, 0]	[70, 0, 0, 0, 0]
37	[3, 1, 1, 1, 0, 0, 1, 1, 0, 0]	[280, 24, 0, 0, 0]	[64, 12, 0, 0, 0]
38	[3, 1, 1, 1, 0, 0, 1, 0, 1, 0]	[280, 0, 0, 0, 0]	[70, 0, 0, 0, 0]
39	[3, 1, 1, 0, 0, 0, 1, 1, 1, 0]	[280, 0, 0, 0, 0]	[70, 0, 0, 0, 0]
40	[3, 1, 0, 0, 0, 0, 1, 1, 1, 1]	[280, 8, 0, 0, 0]	[68, 4, 0, 0, 0]

Table 7. Type-Itemized Enumerations by the Factor-Group Method (Category 2, Part 2)

j	list2_partitions	list2_FPCat2 $\left[\underset{\text{(Eq. 40)}}{\text{A}}, \underset{\text{(Eq. 41)}}{\text{B}}, \underset{\text{(Eq. 42)}}{\text{C}}, \underset{\text{(Eq. 43)}}{\text{D}}, \text{E}\right]$	[III_V_II_I_IV]type
41	[3, 0, 0, 0, 0, 0, 3, 2, 0, 0]	[24, 0, 10, 0, 0]	[7/2, 0, 5, 0, 0]
42	[3, 0, 0, 0, 0, 0, 3, 1, 1, 0]	[48, 0, 12, 0, 0]	[9, 0, 6, 0, 0]
43	[3, 0, 0, 0, 0, 0, 3, 0, 1, 1]	[48, 0, 12, 0, 0]	[9, 0, 6, 0, 0]
44	[3, 0, 0, 0, 0, 0, 2, 2, 1, 0]	[70, 0, 14, 0, 0]	[14, 0, 7, 0, 0]
45	[3, 0, 0, 0, 0, 0, 2, 1, 1, 1]	[140, 0, 12, 0, 0]	[32, 0, 6, 0, 0]
46	[2, 2, 2, 0, 0, 0, 2, 0, 0, 0]	[114, 0, 22, 0, 0]	[23, 0, 11, 0, 0]
47	[2, 0, 0, 0, 0, 0, 3, 2, 1, 0]	[70, 0, 14, 0, 0]	[14, 0, 7, 0, 0]
48	[2, 0, 0, 0, 0, 0, 3, 1, 2, 0]	[70, 0, 14, 0, 0]	[14, 0, 7, 0, 0]
49	[2, 0, 0, 0, 0, 0, 3, 1, 1, 1]	[140, 0, 12, 0, 0]	[32, 0, 6, 0, 0]
50	[2, 0, 0, 0, 0, 0, 2, 2, 2, 0]	[114, 0, 22, 0, 0]	[23, 0, 11, 0, 0]
51	[2, 0, 0, 0, 0, 0, 2, 1, 2, 1]	[210, 0, 18, 0, 0]	[48, 0, 9, 0, 0]
52	[2, 2, 2, 1, 0, 0, 1, 0, 0, 0]	[210, 0, 18, 0, 0]	[48, 0, 9, 0, 0]
53	[2, 2, 2, 0, 0, 0, 1, 0, 1, 0]	[210, 0, 18, 0, 0]	[48, 0, 9, 0, 0]
54	[2, 2, 1, 0, 0, 0, 2, 1, 0, 0]	[210, 0, 18, 0, 0]	[48, 0, 9, 0, 0]
55	[2, 2, 1, 0, 0, 0, 2, 0, 1, 0]	[210, 0, 18, 0, 0]	[48, 0, 9, 0, 0]
56	[2, 2, 0, 0, 0, 0, 2, 1, 1, 0]	[210, 0, 18, 0, 0]	[48, 0, 9, 0, 0]
57	[2, 2, 1, 1, 1, 0, 1, 0, 0, 0]	[420, 0, 12, 0, 0]	[102, 0, 6, 0, 0]
58	[2, 2, 1, 1, 0, 0, 2, 0, 0, 0]	[210, 0, 18, 0, 0]	[48, 0, 9, 0, 0]
59	[2, 2, 1, 1, 0, 0, 1, 1, 0, 0]	[420, 24, 12, 0, 0]	[96, 12, 6, 0, 0]
60	[2, 2, 1, 1, 0, 0, 1, 0, 1, 0]	[420, 0, 12, 0, 0]	[102, 0, 6, 0, 0]
61	[2, 2, 1, 0, 0, 0, 1, 1, 1, 0]	[420, 0, 12, 0, 0]	[102, 0, 6, 0, 0]
62	[2, 1, 1, 1, 1, 0, 2, 0, 0, 0]	[420, 0, 12, 0, 0]	[102, 0, 6, 0, 0]
63	[2, 1, 1, 1, 0, 0, 2, 1, 0, 0]	[420, 0, 12, 0, 0]	[102, 0, 6, 0, 0]
64	[2, 1, 1, 1, 0, 0, 2, 0, 1, 0]	[420, 0, 12, 0, 0]	[102, 0, 6, 0, 0]
65	[2, 1, 1, 1, 1, 1, 1, 0, 0, 0]	[840, 0, 0, 0, 0]	[210, 0, 0, 0, 0]
66	[2, 1, 1, 1, 1, 0, 1, 1, 0, 0]	[840, 24, 0, 0, 0]	[204, 12, 0, 0, 0]
67	[2, 1, 1, 1, 1, 0, 1, 0, 1, 0]	[840, 0, 0, 0, 0]	[210, 0, 0, 0, 0]
68	[2, 1, 1, 1, 0, 0, 1, 1, 1, 0]	[840, 0, 0, 0, 0]	[210, 0, 0, 0, 0]
69	[2, 1, 1, 0, 0, 0, 1, 1, 1, 1]	[840, 24, 0, 0, 0]	[204, 12, 0, 0, 0]
70	[1, 1, 1, 1, 1, 1, 2, 0, 0, 0]	[840, 0, 0, 0, 0]	[210, 0, 0, 0, 0]
71	[1, 1, 1, 1, 1, 0, 3, 0, 0, 0]	[280, 0, 0, 0, 0]	[70, 0, 0, 0, 0]
72	[1, 1, 1, 1, 1, 0, 2, 1, 0, 0]	[840, 0, 0, 0, 0]	[210, 0, 0, 0, 0]
73	[1, 1, 1, 1, 1, 0, 2, 0, 1, 0]	[840, 0, 0, 0, 0]	[210, 0, 0, 0, 0]
74	[1, 1, 1, 1, 0, 0, 2, 1, 1, 0]	[840, 0, 0, 0, 0]	[210, 0, 0, 0, 0]
75	[1, 1, 1, 0, 0, 0, 2, 1, 1, 1]	[840, 0, 0, 0, 0]	[210, 0, 0, 0, 0]
76	[1, 1, 1, 1, 1, 1, 1, 1, 0, 0]	[1680, 0, 0, 0, 0]	[420, 0, 0, 0, 0]
77	[1, 1, 1, 1, 1, 0, 1, 1, 1, 0]	[1680, 0, 0, 0, 0]	[420, 0, 0, 0, 0]
78	[1, 1, 1, 1, 0, 0, 1, 1, 1, 1]	[1680, 48, 0, 0, 0]	[408, 24, 0, 0, 0]
79	[0, 0, 0, 0, 0, 0, 6, 2, 0, 0]	[3, 0, 3, 0, 0]	[0, 0, 3/2, 0, 0]
80	[0, 0, 0, 0, 0, 0, 4, 3, 1, 0]	[13, 0, 7, 0, 0]	[3/2, 0, 7/2, 0, 0]
81	[0, 0, 0, 0, 0, 0, 4, 2, 2, 0]	[22, 0, 10, 0, 0]	[3, 0, 5, 0, 0]
82	[0, 0, 0, 0, 0, 0, 4, 2, 1, 1]	[35, 0, 9, 0, 0]	[13/2, 0, 9/2, 0, 0]
83	[0, 0, 0, 0, 0, 0, 3, 2, 2, 1]	[70, 0, 14, 0, 0]	[14, 0, 7, 0, 0]
84	[0, 0, 0, 0, 0, 0, 3, 1, 3, 1]	[48, 0, 12, 0, 0]	[9, 0, 6, 0, 0]

```
gap>
gap> list2_partitions :=[];;
gap> list2_FP := [];;
gap> list2_III_V_II_I_Vtype := [];;
gap>
gap> list2_partitions[24] := [ 4, 1, 1, 0, 0, 0, 1, 1, 0, 0 ];;
gap> list2_FP[24] := [70, 41, 38, 35, 22, 70, 12, 6, 0, 0];;
gap> templist :=
 >[list2_FP[24][6],list2_FP[24][7],list2_FP[24][8],list2_FP[24][9],list2_FP[24][10]];;
gap> list_temp := templist * tom_matrix^(-1);;
gap> Print("list1_III_V_II_I_Vtype[", 24, "] := ", list_temp, "; \n");
list2_III_V_II_I_Vtype[24] := [ 13, 6, 3, 0, 0 ];
gap>
```

Thus, the composition $H_4ABp\overline{p}$ permits the presence of 13 cubane derivatives, each having a type-III stereoisogram, 6 cubane derivatives, each having a type-V stereoisogram, and 3 cubane derivatives, each having a type-II stereoisogram. The resulting type list `[III_V_II_I_IV]type[24]` ($[13, 6, 3, 0, 0]$) is consistent with the previous list `[I, II, III, IV, V]` $= [0, 3, 13, 0, 6]$ which is calculated as Category 2 by means of the half-size-subgroup method (Subsubsection 4.4.2).

Among the enumerated stereoisograms of the composition $H_4ABp\overline{p}$, Figure 10 collects thirteen type-III stereoisograms, where the top twelve type-III stereoisograms are depicted in full form, while the last one type-III stereoisogram is depicted in simplified form.

The simplified form of Figure 10 can be referred to by using an in-line expression such as $([\mathbf{48}\ \overline{\mathbf{48}}]\quad[\mathbf{49}\ \overline{\mathbf{49}}])_{\mathrm{III}}$, where each of two pairs of enantiomers is surrounded by a pair of square brackets ($[\mathbf{48}\ \overline{\mathbf{48}}]$ and $[\mathbf{49}\ \overline{\mathbf{49}}]$). Each pair of enantiomers is counted separately under the point group $\boldsymbol{O}_h$, and two pairs of enantiomers are counted as a single quadruplet of *RS*-stereoisomers, as surrounded by a pair of parentheses with subscript III. According to this formulation, such an in-line expression as $([\mathbf{48}\ \overline{\mathbf{48}}]\ [\mathbf{49}\ \overline{\mathbf{49}}])_{\mathrm{III}}$ can be recovered into the original type-III stereoisogram. Inversely, a type-III stereoisogram in a full format, e.g., the third one of Figure 10, can be transformed into a simplified format and into its in-line expression such as $([\mathbf{28}\ \overline{\mathbf{28}}]\quad[\mathbf{29}\ \overline{\mathbf{29}}])_{\mathrm{III}}$. Because **28** and **48** are convertible to each other by exchanging ligand A and ligand B, the simplified format corresponding to the in-line expression $([\mathbf{28}\ \overline{\mathbf{28}}]\quad[\mathbf{29}\ \overline{\mathbf{29}}])_{\mathrm{III}}$ can be easily depicted.

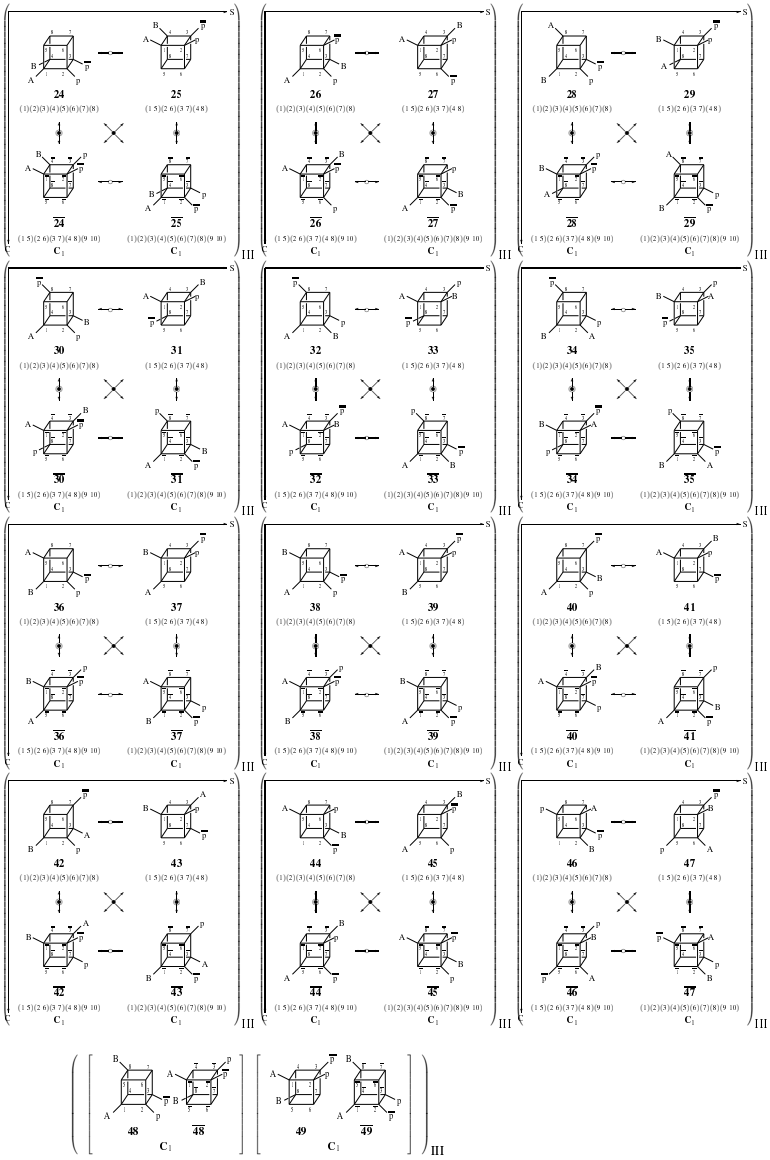

Figure 10. Type-Itemized Enumeration of cubane derivatives with the composition $H_4ABp\overline{p}$ (Part 1). Top twelve type-III stereoisograms are depicted in full form, while the last one type-III stereoisogram is depicted in simplified form.

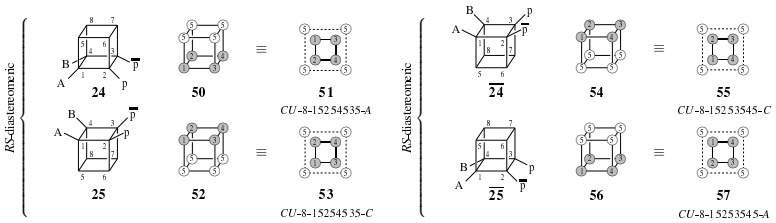

Figure 11. Assignment of *C/A*-descriptors to cubane derivatives of the composition $H_4ABp\overline{p}$, which are characterized by type-III stereoisograms (Part 1). The priority sequence is presumed to be A① > B② > p③ > $\overline{p}$④ > H⑤.

Among the type-III stereoisograms listed in Figure 10, let us select the top diagram ([**24** $\overline{\mathbf{24}}$] [**25** $\overline{\mathbf{25}}$])$_{\mathrm{III}}$ as an example of assigning *C/A*-descriptors. Figure 11 indicates the assignment of *C/A*-descriptors to these type-III cubane derivatives with the composition $H_4ABp\overline{p}$.

The reference cubane derivative **24** is converted into **50** by attaching priority numbers, where the priority sequence is presumed to be A ① > B ② > p ③ > $\overline{p}$ ④ > H ⑤, as shown in the upper-left row of Figure 11. The bottom face of **50** is determined to be the most preferred face, as shown by the four ligands with a grayed priority number. The cubane derivative is re-oriented to give **51** having a top preferred face. The configuration number is obtained to be 15254535, which shows an anti-clockwise citation. Hence, the *CA*-descriptor *CU*-8-15254535-*A* is assigned to **24**, where a last letter *A* is the label for indicating the anti-clockwise citation.

On the other hand, the corresponding *RS*-diastereomer **25** is converted into **52** by attaching priority numbers, where the priority sequence is presumed to be A ① > B ② > p ③ > $\overline{p}$ ④ > H ⑤, as shown in the lower-left row of Figure 11. The top face of **52** is determined to be the most preferred face, as shown by the four ligands with a grayed priority number. The corresponding graphic expression **53** gives the configuration number to be 15254535, which shows a clockwise citation. Hence, the *CA*-descriptor *CU*-8-15254535-*C* is assigned to **25**, where a last uppercase letter *C* is the label for indicating the clockwise citation.

In a similar way, the cubane derivative $\overline{\mathbf{24}}$ is characterized by the *CA*-descriptor *CU*-8-15253545-*C*, while its *RS*-diastereomer $\overline{\mathbf{25}}$ is character-

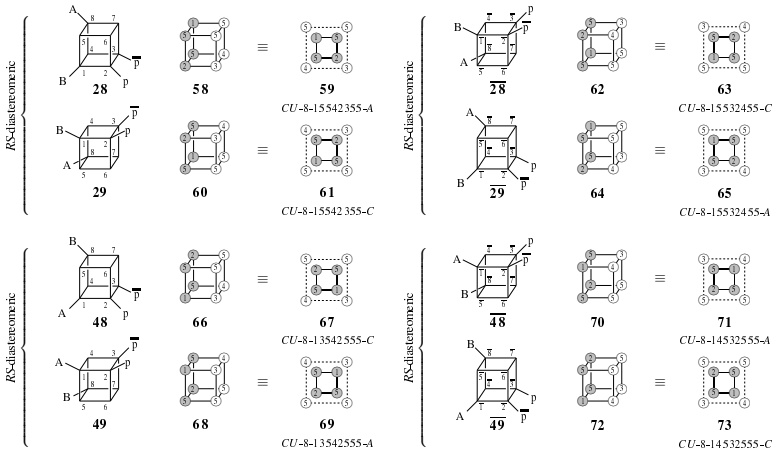

Figure 12. Assignment of *C/A*-descriptors to cubane derivatives of the composition $H_4ABp\overline{p}$, which are characterized by type-III stereoisograms (Part 2). The priority sequence is presumed to be A① > B② > p③ > $\overline{p}$④ > H⑤.

ized by the *CA*-descriptor *CU*-8-15253545-*A*.

It should be emphasized that the pair of *RS*-diastereomers **24**/**25** is characterized by a pair of the *CA*-descriptors *CU*-8-15254535-*A*/*CU*-8-15254535-*C*, while the pair of *RS*-diastereomers $\overline{\mathbf{24}}$/$\overline{\mathbf{25}}$ is characterized by a pair of the *CA*-descriptors *CU*-8-15253545-*C*/*CU*-8-15253545-*A*. The*RS*-diastereomers of each pair are characterized by the same configuration number but contra-rotating *CA*-descriptors.

Figure 12 illustrates the difference of *CA*-descriptors between **28** and **48**, which are convertible to each other by exchanging ligand A and ligand B. As for the type-III stereoisogram represented by ([**28** $\overline{\mathbf{28}}$] [**29** $\overline{\mathbf{29}}$])$_{\mathrm{III}}$, the pair of *RS*-diastereomers **28**/**29** is characterized by a pair of the *CA*-descriptors *CU*-8-15542355-*A*/*CU*-8-15542355-*C*. In contrast, as for the type-III stereoisogram represented by ([**48** $\overline{\mathbf{48}}$] [**49** $\overline{\mathbf{49}}$])$_{\mathrm{III}}$, the pair of *RS*-diastereomers **48**/**49** is characterized by a pair of the *CA*-descriptors *CU*-8-13542555-*C*/*CU*-8-13542555-*A*. Compare between *CU*-8-15542355-*A* for **28** and *CU*-8-13542555-*C* for **48**.

Among the enumerated stereoisograms of the composition $H_4ABp\overline{p}$, Figure 13 collects three Type-II stereoisograms and six Type-V stereoiso-

grams of cubane derivatives, where they are depicted in full format.

Each of the three Type-II stereoisograms is characterized by the horizontal equality symbols, so that its self-*RS*-diastereomeric nature (*RS*-astereogenicity) is specified by its in-line expression, such as $([\mathbf{74}\ \ \overline{\mathbf{74}}])_{\mathrm{II}}$, $([\mathbf{76}\ \ \overline{\mathbf{76}}])_{\mathrm{II}}$, and $([\mathbf{78}\ \ \overline{\mathbf{78}}])_{\mathrm{II}}$, where the description on one pair of enantiomers is sufficient to specify the type-II stereoisogram because the pair [**74** $\overline{\mathbf{74}}$], for example, is equivalent to [**75** $\overline{\mathbf{75}}$].

Six type-V stereoisograms of the composition $\mathrm{H_4ABp\overline{p}}$, which are shown in the bottom part of Figure 13, exhibits the nature of the extended versions of "pseudoasymmetry" [62]. Each of the type-V stereoisogram is characterized of vertical equality symbols to give type index $[a, -, -]$, which exhibits achirality, *RS*-stereogenicity, and sclerality. The "pseudoasymmetry" is expressed by the corresponding in-line expression such as $([\mathbf{80}]\ \ [\mathbf{81}])_{\mathrm{V}}$, where a single membership [**80**] in a pair of square brackets represents an achiral cubane derivative (a pair of self-enantiomers), and where two achiral derivatives [**80**] and [**81**] are distinguished by a lower pair of *a/c*-descriptors under the CIP (Cahn-Ingold-Prolog) system giving *A/C*-descriptors.

It should be noted that the three type-II stereoisograms shown in the top row of Figure 13 cannot be attached with *C/A*-descriptors, although they are chiral. Thus, the preferred face cannot be selected or clockwise/anti-clockwise direction cannot be differentiated in the assignment procedure. This failed procedure reflects another reasoning for the fact that the assignment of *C/A*-descriptors is not based on chirality.

On the other hand, the six type-V stereoisograms shown in the lower part of Figure 13 can be attached with *C/A*-descriptors, even though they are achiral. This point also reflects the other reasoning for the fact that the assignment of *C/A*-descriptors is not based on chirality, but on *RS*-stereogenicity.

Figure 14 shows assignment of *C/A*-descriptors to cubane derivatives of the composition $\mathrm{H_4ABp\overline{p}}$, which are characterized type-V stereoisograms. They are chirality-unfaithful cases represented by a lower-case letters *c/a*. The detaild discussions on Figure 14 will appear in Section 5 (Type-V Stereoisograms for Elucidating "Extended Pseudoasymmetry"),

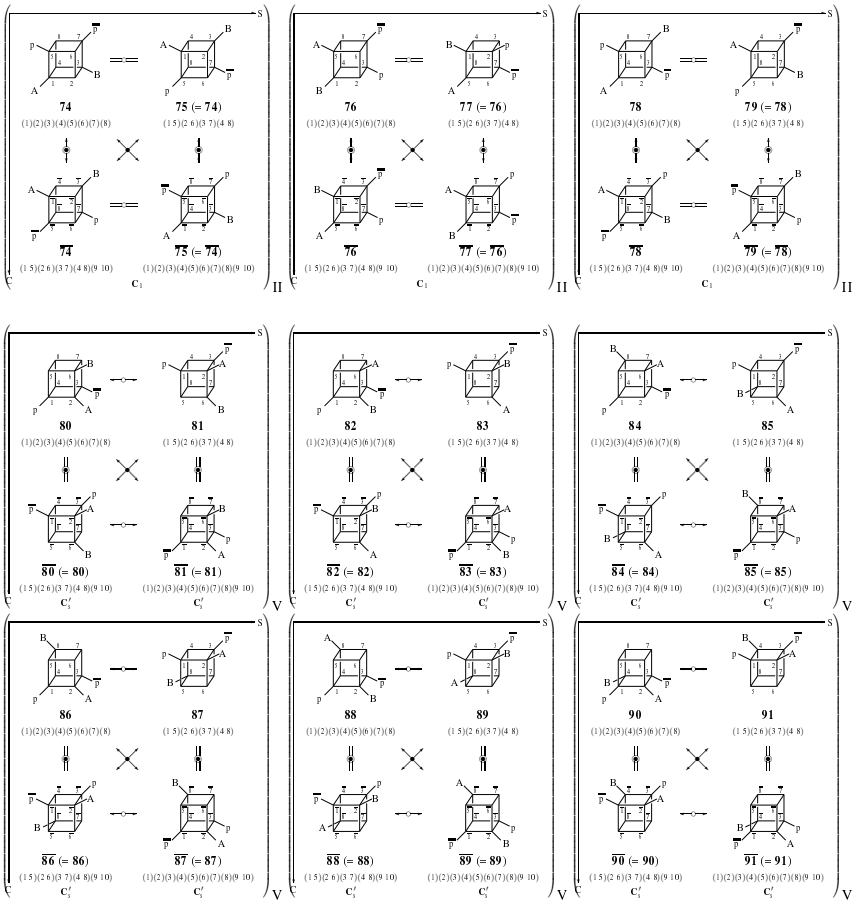

Figure 13. Type-Itemized Enumeration of cubane derivatives with the composition $H_4ABp\overline{p}$ (Part 2). Three Type-II stereoisograms and six Type-V stereoisograms of cubane derivatives with the composition $H_4ABp\overline{p}$.

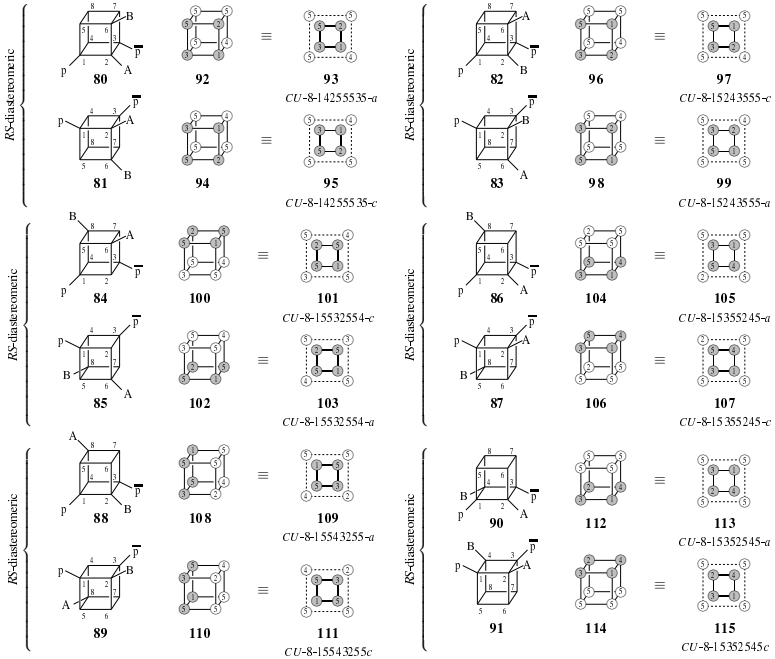

Figure 14. Assignment of *C/A*-descriptors to cubane derivatives of the composition $H_4ABp\overline{p}$, which are characterized type-V stereoisograms. The priority sequence is presumed to be A① > B② > p③ > $\overline{p}$④ > H⑤.

The symmetry-itemized enumerations of cubane derivatives under the point group $\boldsymbol{O}_h$ have been reported by Fujita [33], where the partial-cycle-index method of Fujita's USCI approach was adopted. Table 1 of the report [33] has listed cubane derivatives with the composition $H_4ABp\overline{p}$, which are assigned to be 19 derivatives of the point group $\boldsymbol{C}_1$ and 12 derivatives of the point group $\boldsymbol{C}_s'$. The present type-itemized enumeration indicates that each of the 13 type-III stereoisograms (Figure 10) contains two pairs of enantiomers, while each of the three type-II stereoisograms (the top row of Figure 13) contains one pair of enantiomers. Hence, we have totally $13 \times 2 + 3 \times 1 = 29$, which is consistent with 29 $\boldsymbol{C}_1$-derivatives. Moreover, each of the six type-V stereoisograms shown in the lower part of Figure 13 contains two achiral cubane derivatives, so that we have totally $6 \times 2 = 12$, which is consistent with 12 $\boldsymbol{C}_s'$-derivatives.

4.5.5 The factor-group method applied to category-3 cases — Coexistence of categories 1 and 2

Category-3 stereoisograms are determined if the ratio $\boldsymbol{O}/\boldsymbol{O}_{\widehat{I}}$ in `list_FP[j]` is neither equal to 1 nor equal to 2. The data examined in the present article are collected in Table 4. For applying the factor-group method to these data, the values listed in the E-column should be estimated. The E-value in each row of Table 4 is estimated by (a) drawing type-V stereoisograms manually and count the number x of type-V stereoisograms; (b) then E = A - 2 × x, where A represents the number of achiral promolecule and 2 × x is the total number of achiral promolecules contained in x type-V stereoisograms. Then, the values of E's are calculated to be as follows:

E = 6−0 = 6 for `list3_FPCat3B`[1], E = 11−2×3 = 5 for `list3_FPCat3B`[2],
E = 10−2×2 = 6 for `list3_FPCat3B`[3], E = 14−2×4 = 6 for `list3_FPCat3B`[4],
E = 16−2×6 = 4 for `list3_FPCat3B`[5], E = 26−2×12 = 2 for `list3_FPCat3B`[6],
and E = 28−2×12 = 4 for `list3_FPCat3B`[7].

These values are listed in the `list3_FPCat3B`-[E]-column of Table 8.

In order to execute the factor-group method, the 6th to 10th values listed in the intersection between each j-th row and the `list3_FP`-column of Table 4 are extracted to give `templist`. The resulting five-membered list `templist` is regarded as a fixed-point vector `list3_FP`[j], which is

Table 8. Type-Itemized Enumerations by the Factor-Group Method (Category 3: Coexistence of Category 1 and Category 2)

j	list3_partitions	list3_FPCat3B $\left[\underset{\text{(Eq. 40)}}{\text{A}}, \underset{\text{(Eq. 41)}}{\text{B}}, \underset{\text{(Eq. 42)}}{\text{C}}, \underset{\text{(Eq. 43)}}{\text{D}}, \text{E}\right]$	[III_V_II_I_IV]type
1	$[4,0,0,0,0,0,2,2,0,0]$	$[22,6,10,10,6]$	$[2,0,2,2,6]$
2	$[4,2,0,0,0,0,1,1,0,0]$	$[35,11,9,9,5]$	$[4,3,2,2,5]$
3	$[4,0,0,0,0,0,1,1,1,1]$	$[70,10,6,18,6]$	$[12,2,0,6,6]$
4	$[2,2,0,0,0,0,2,2,0,0]$	$[114,14,22,18,6]$	$[18,4,8,6,6]$
5	$[2,0,0,0,0,0,2,2,1,1]$	$[210,16,18,36,4]$	$[37,6,7,16,4]$
6	$[2,2,2,0,0,0,1,1,0,0]$	$[210,26,18,18,2]$	$[38,12,8,8,2]$
7	$[2,2,0,0,0,0,1,1,1,1]$	$[420,28,12,36,4]$	$[88,12,4,16,4]$

multiplied by the inverse of the mark table `tom_matrix` of the factor group $\boldsymbol{O}\backslash\boldsymbol{O}_{h\widetilde{\sigma}\widehat{I}}$. For example, the first row of Table 4 gives the list `templist` $= [22,6,10,10,6]$ (`list3_FP`[j] of Table 8, $j = 1$), which is multiplied by `tom_matrix`$^{(-1)}$, as shown in the following GAP code:

```
gap> tom_matrix :=
> [[4,0,0,0,0],
> [2,2,0,0,0],
> [2,0,2,0,0],
> [2,0,0,2,0],
> [1,1,1,1,1]];;
gap> list3_partitions :=[];;
gap> list3_FP := [];;
gap> list3_III_V_II_I_Vtype := [];;
gap> list3_partitions[1] := [ 4, 0, 0, 0, 0, 0, 2, 2, 0, 0 ];; ############22/16
gap> list3_FP[1] :=
> [ 22, 14, 16, 16, 12, 22, 6, 10, 10, 6];; ### E = 6-0 = 6
gap> templist :=
> [list3_FP[1][6],list3_FP[1][7],list3_FP[1][8],list3_FP[1][9],list3_FP[1][10]];
[ 22, 6, 10, 10, 6 ]
gap> list_temp := templist * tom_matrix^(-1);;
gap> Print("list3_III_V_II_I_Vtype[", 1, "] := ", list_temp, "; \n");
list3_III_V_II_I_Vtype[1] := [ 2, 0, 2, 2, 6 ];
gap>
```

The resulting `list3_III_V_II_I_Vtype`[1] $(= [2,0,2,2,6])$ is the type list to be calculated. Similar procedures can be executed to calculate the other cases, where we can obtain the lists appearing in the intersection between each j-th row and the `[III_V_II_I_IV]type`-column of Table 8.

4.5.6 Examples of calculation data of category 3

To examine the validity of the factor-group method proposed in the present article, let us testify several data of type-itemized enumerations of Category 3 (Coexistence of Category 1 and 2) collected in Table 8.

Derivatives with Composition $H_4p^2\overline{p}^2$

As for cubane derivatives with composition $H_4p^2\overline{p}^2$, let us first examine the values collected in the first row of Table 8 (`list3_partitions`[1] = $[4, 0, 0, 0, 0, 0, 2, 2, 0, 0]$). As discussed in the preceding subsection, the resulting `[III_V_II_I_IV]type`[1] is obtained to be $[2, 0, 2, 2, 6]$, which indicates the appearance of two type-III stereoisograms, two type-II stereoisograms, two type-I stereoisograms, and six type-IV stereoisograms. No appearance of the type-V stereoisograms is consistent with the preestimated setting of E-value.

Among the derivatives (`[III_V_II_I_IV]type`[1] = $[2, 0, 2, 2, 6]$) of the composition $H_4p_2\overline{p}_2$, six chiral derivatives (i.e., two type-III stereoisograms, two type-II stereoisograms, and two type-I stereoisograms) are depicted in Figure 15. Their point-group symmetries are consistent with the previous paper [63], where the symmetry-itemized enumeration under the point group $\boldsymbol{O}_h$ (Table 2) has reported the appearance of six $\boldsymbol{C}_1$-derivatives, two $\boldsymbol{C}_2'$-derivatives, one $\boldsymbol{C}_s$-derivative, one $\boldsymbol{S}_4$-derivative, one $\boldsymbol{C}_{2v}$-derivative, one $\boldsymbol{C}_{2v}''$-derivative, one $\boldsymbol{C}_{2h}$-derivative, and one $\boldsymbol{C}_{2h}'$-derivative.

As for the first type-III stereoisogram shown in the top row of Figure 15, both the chiral derivatives **116** and **117** belong to the point group $\boldsymbol{C}_2'$, where the presence of two $\boldsymbol{C}_2'$-derivatives is consistent with the previous symmetry-itemized enumeration [63]. The second type-III stereoisogram contains the chiral derivatives **118** and **119** both belonging to the point group $\boldsymbol{C}_1$, where the contribution of two $\boldsymbol{C}_1$-derivatives to the totally six $\boldsymbol{C}_1$-derivatives is consistent with the previous symmetry-itemized enumeration [63].

As for the type-II stereoisograms collected in the middle row of Figure 15, each of reference promolecules **120** and **122** belongs to the point group $\boldsymbol{C}_1$, where each of them contributes to the totally six $\boldsymbol{C}_1$-derivatives so as to be consistent with the previous symmetry-itemized enumeration [63].

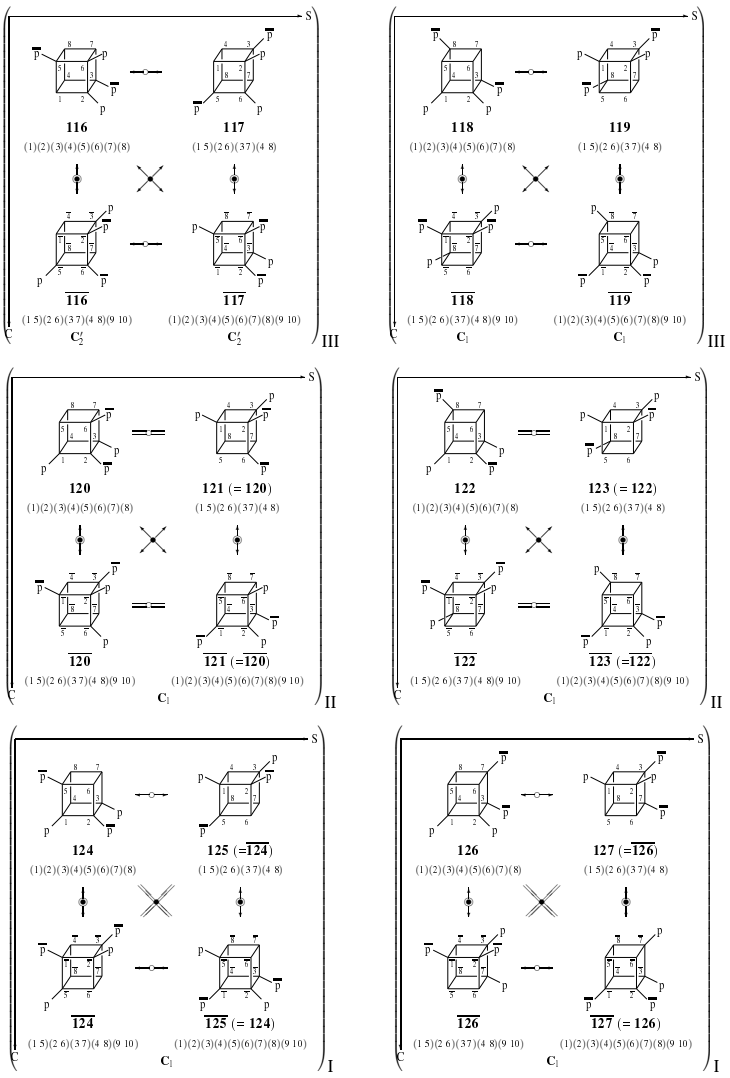

Figure 15. Type-Itemized Enumeration of cubane derivatives with the composition $H_4p_2\overline{p}_2$ (Part 1). Chiral cubane derivatives (two type-III stereoisograms, two type-II stereoisograms, and two type-I stereoisograms) with the composition $H_4p_2\overline{p}_2$.

As for the type-I stereoisograms collected in the bottom row of Figure 15, each of reference promolecules **124** and **126** belongs to the point group $\boldsymbol{C}_1$, where each of them contributes one to the six $\boldsymbol{C}_1$-derivatives. Totally, the value six for $\boldsymbol{C}_1$ [63] is consistent with the summation $6 = 2 \times 1$ (from the one type-III stereoisogram) + $1\times$ 2 (from the two type-II stereoisograms) + $1\times$ 2 (from the two type-I stereoisograms).

Let us next examine the assignability of *A*/*C*-descriptors to the chiral derivatives listed in Figure 15. The procedures of the assignments are collected in Figure 16. It should be noted again that a pair of *A*/*C*-descriptors is assigned not to a pair of enantiomers (due to chirality), but to a pair of *RS*-diastereomers (due to *RS*-stereogenicity).

As for the first type-III stereoisogram collected in the top row of Figure 16, the front face of **128** derived from **116** is determined to be the most preferred face, as shown by the four ligands with a grayed priority number. The cubane derivative is re-oriented to give **129** having a top preferred face so as to give the configuration number 12132333 to **116**, which shows an anti-clockwise configuration. In a similar way, the corresponding *RS*-diastereomer **117** is characterized the configuration number 12132333 in a clockwise fashion. On the other hand, their enantiomers are characterized by an anti-clockwise configuration number 13232133 to $\overline{\mathbf{116}}$, and by a clockwise configuration number 13232133 to $\overline{\mathbf{117}}$. Because the enantiomers **116** and $\overline{\mathbf{116}}$ are characterized to be anti-clockwise, so that they are chirality-unfaithful. In a parallel way, because the enantiomers **117** and $\overline{\mathbf{117}}$ are characterized to be clockwise, so that they are chirality-unfaithful. The chirality-unfaithful nature forces us to be characterized by lowercase letters *c*/*a*. Hence, a pair of enantiomers **116**/ $\overline{\mathbf{116}}$ is specified by the codes *CU*-8-12132333-*a*/*CU*-8-13232133-*a*, while a pair of enantiomers **117**/ $\overline{\mathbf{117}}$ is specified by the codes *CU*-8-12132333-*c*/*CU*-8-13232133-*c*.

The type-III stereoisogram collected in the second row of Figure 16 indicates another example of chirality-unfaithful assignment of *C*/*A*-descriptors. Thus, a pair of enantiomers **118**/$\overline{\mathbf{118}}$ is specified by the codes *CU*-8-13132332-*c*/*CU*-8-12321333-*c*, while a pair of enantiomers **119**/ $\overline{\mathbf{119}}$ is specified by the codes *CU*-8-13132332-*a* / *CU*-8-12321333-*a*.

Because the assignability of *A*/*C*-descriptors depends on the *RS*-ste-

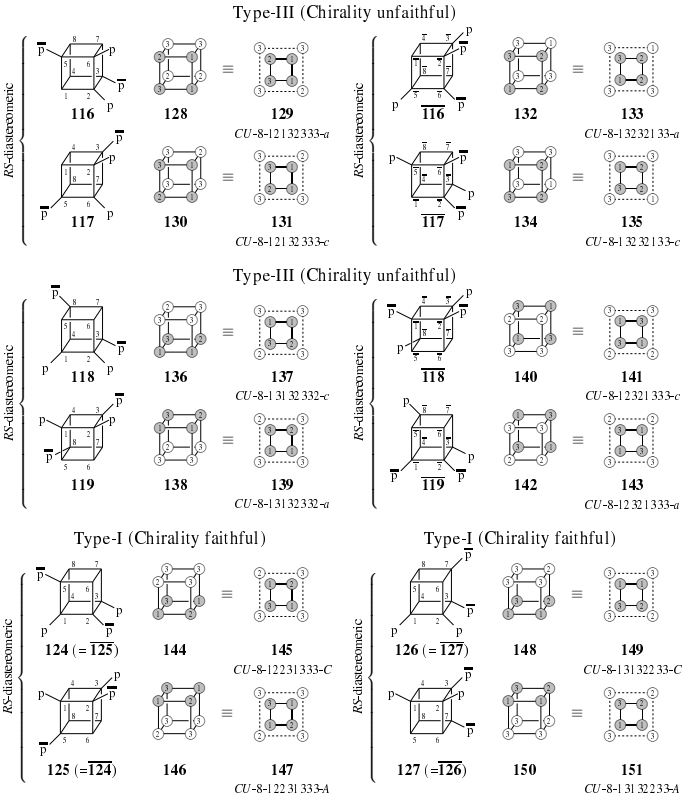

Figure 16. Assignment of *C/A*-descriptors to chiral cubane derivatives of the composition $H_4p_2\overline{p}_2$, which are characterized type-III or type-I stereoisograms. The priority sequence is presumed to be p① > $\overline{\text{p}}$② > H③.

reogenicity and exhibits no dependence on chirality, *A/C*-descriptors cannot be assigned to type-II stereoisograms having type index $[-, a, -]$ (chiral, *RS*-astereogenic, an scleral). This feature of *RS*-astereogenicity is confirmed by the type-II stereoisograms collected in the second row of Figure 15. For example, the horizontal equality symbol between **120** and **121** (or between **122** and **123**) provides us with no means of specifying the second kind of handedness. Even if we apply the selection of the most preferred face according to Figure 16, the ambiguity of selecting clockwise/anti-clockwise directions occurs during the selection step.

As for the left type-I stereoisograms shown in the bottom line of Figure 16, the diagonal equality symbols in each type-I stereoisogram ($[-, -, a]$ in Figure 15) assure the coincidence between a pair of *RS*-diastereomers and a pair of enantiomers. Hence, the pair of the *C/A*-descriptors given to the pair of *RS*-diastereomers, i.e., *CU*-8-12231333-*C* for **124** and *CU*-8-12231333-*A* for **125**, can be regarded to be given to the pair of enantiomers, i.e., *CU*-8-12231333-*C* for **124** and *CU*-8-12231333-*A* for $\overline{\mathbf{124}}$ in a chirality-faithful fashion.

In a similar way, as shown in the right type-I stereoisograms of the bottom line of Figure 16, the pair of the *C/A*-descriptors given to the pair of *RS*-diastereomers, i.e., *CU*-8-13132233-*C* for **126** and *CU*-8-13132233-*A* for **127**, can be regarded to be given to the pair of enantiomers, i.e., *CU*-8-13132233-*C* for **126** and *CU*-8-13132233-*A* for $\overline{\mathbf{126}}$ in a chirality-faithful fashion.

Among the derivatives of the composition $H_4p_2\overline{p}_2$ collected in the first row of Table 8 (`[III_V_II_I_IV]type`$[1] = [2, 0, 2, 2, 6]$), there appear no type-V derivatives. The remaining achiral derivatives (i.e., six type-IV stereoisograms) are depicted in Figure 17. The point groups of these achiral derivatives can be confirmed by referring to the previous symmetry-itemized enumerations [63], i.e., the first type-IV derivative **152** belongs to the $\boldsymbol{C}_s$-point group (the mirror plane running through the midpoint of the edge 1–2, 1–4, 5–6, and 7–8), the second type-IV derivative **154** belongs to the $\boldsymbol{S}_4$-point group (the 4-fold S_4-axis through the centers of the top and bottom planes), the third type-IV derivative **156** belongs to the $\boldsymbol{C}_{2v}$-point group (the two-fold axis through the centers of the top and

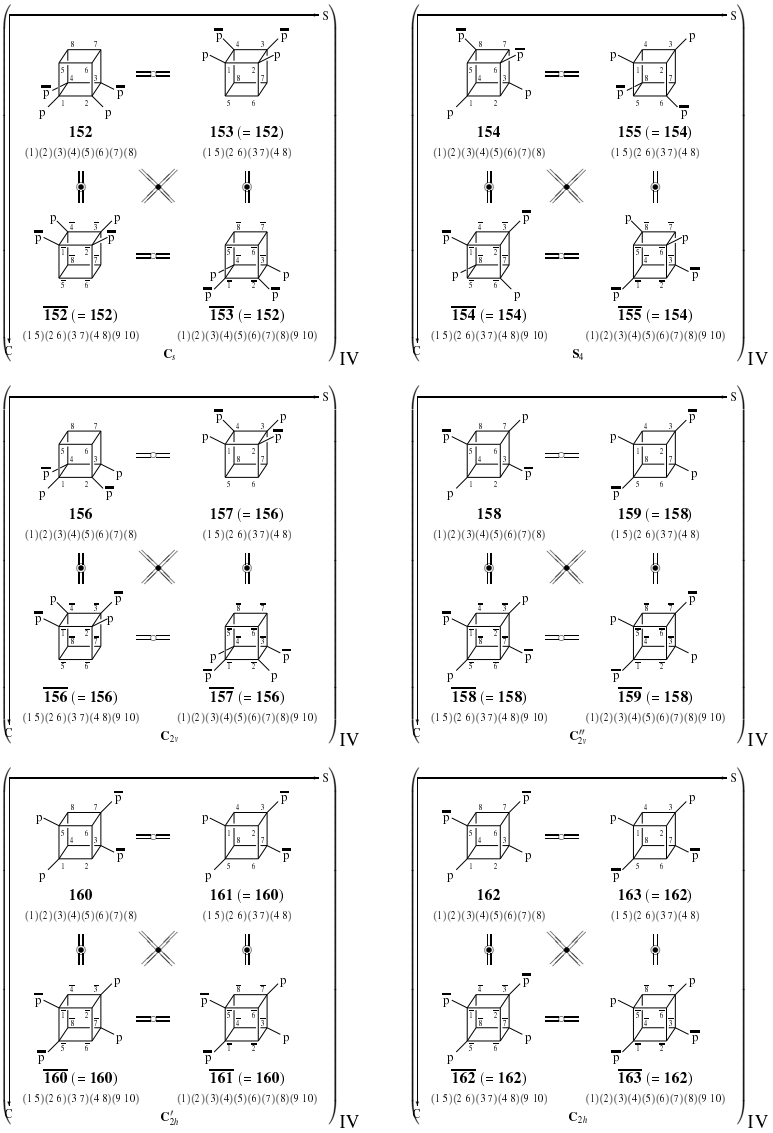

Figure 17. Type-Itemized Enumeration of cubane derivatives with the composition $H_4p_2\overline{p}_2$ (Part 2). Achiral cubane derivatives (six type-IV stereoisograms with the composition $H_4p_2\overline{p}_2$).

the bottom planes, as well as two vertical planes intersecting to give the two-fold axis), the 4th type-IV derivative **158** belongs to the $\boldsymbol{C}''_{2v}$-point group (the two-fold axis through the midpoints of the edges 2–6 and 4–8, as well as two vertical planes intersecting to give the two-fold axis), the 5th type-IV derivative **160** belongs to the $\boldsymbol{C}'_{2h}$-point group (the two-fold axis through the midpoints of the edges 1–5 and 3–7, as well as the horizontal mirror plane 2–4–8–6 perpendicular to the two-fold axis), and the 6th type-IV derivative **162** belongs to the $\boldsymbol{C}_{2h}$-point group (the two-fold axis through the centers of the top and bottom planes, as well as the horizontal mirror plane perpendicular to the two-fold axis).

Derivatives with Composition $\mathbf{H_4A^2p\overline{p}}$

As a next example of type-itemized enumerations of Category 3 (Coexistence of Category 1 and 2) by means of the factor-group method, let us examine the values collected in the second row of Table 8. The partition represented as `list3_partitions`$[2] = [4, 2, 0, 0, 0, 0, 1, 1, 0, 0]$ in the second row corresponds to the derivatives with the composition $H_4A_2p\overline{p}$. The resulting list `[III_V_II_I_IV]type`$[2]$ is obtained to be $[4, 3, 2, 2, 5]$, which indicates the appearance of four type-III stereoisograms, three type-V stereoisograms, two type-II stereoisograms, two type-I stereoisograms, and five type-IV stereoisograms. The appearance of three type-V stereoisograms is consistent with the pre-estimated setting of E-value.

Among these cubane derivatives of the composition $H_4A_2p\overline{p}$, Figure 18 collects chiral derivatives with the composition $H_4A_2p\overline{p}$: i.e., four type-III stereoisograms $(([\mathbf{164}\ \overline{\mathbf{164}}]\ \ [\mathbf{165}\ \overline{\mathbf{165}}])_{\mathrm{III}}$, $([\mathbf{166}\ \overline{\mathbf{166}}]\ \ [\mathbf{166}\ \overline{\mathbf{167}}])_{\mathrm{III}}$, $([\mathbf{168}\ \overline{\mathbf{168}}]\ \ [\mathbf{168}\ \overline{\mathbf{169}}])_{\mathrm{III}}$, and $([\mathbf{170}\ \overline{\mathbf{170}}]\ \ [\mathbf{171}\ \overline{\mathbf{171}}])_{\mathrm{III}})$, two type-II stereoisograms $(([\mathbf{172}\ \overline{\mathbf{172}}])_{\mathrm{II}}$ and $([\mathbf{174}\ \overline{\mathbf{174}}])_{\mathrm{II}})$, as well as two type-I stereoisograms $(([\mathbf{176}\ \overline{\mathbf{176}}])_{\mathrm{I}}$ and $([\mathbf{178}\ \overline{\mathbf{178}}])_{\mathrm{I}})$. They are all chiral so as to be characterized by the presence of vertical double-headed arrows.

Their point-group symmetries are consistent with the previous paper [33, 63], where the symmetry-itemized enumerations under the point group $\boldsymbol{O}_h$ conducted by means of the Maple system (Table 1 of Ref. [33]) and by means of the GAP system (Table 2 of Ref. [63]) have reported the appearance of twelve $\boldsymbol{C}_1$-derivatives, three $\boldsymbol{C}_s$-derivatives, seven $\boldsymbol{C}'_s$-derivatives, and one $\boldsymbol{C}_i$-derivative. The stereoisograms collected in Figure

18 reveals that the sum of 8 (= 2 × 4 for four type-III stereoisograms) + 2 (= 1 × 2 for two type-II stereoisograms) + 2 (= 1 × 2 for two type-I stereoisograms) is equal to 12, which is equal to the value of the twelve $\boldsymbol{C}_1$-derivatives.

Among the enumerated derivatives with the composition $H_4A_2p\overline{p}$ listed in the column `[III_V_II_I_IV]type`[2] = [4, 3, 2, 2, 5], Figure 19 collects stereoisograms of achiral derivatives, i.e., five type-IV stereoisograms (i.e, ([**180**])$_{\rm IV}$, ([**182**])$_{\rm IV}$, ([**184**])$_{\rm IV}$, ([**186**])$_{\rm IV}$, and ([**188**])$_{\rm IV}$) along with three unusual type-V stereoisograms (i.e., ([**190**] [**191**])$_{\rm V}$, ([**192**] [**193**])$_{\rm V}$, and ([**194**] [**195**])$_{\rm V}$), They are characterized by vertical equality symbols, because they are all achiral.

Their point-group symmetries are consistent with the previous paper [33, 63]. The symmetry-itemized enumerations under the point group $\boldsymbol{O}_h$ have been conducted by means of the Maple system (Table 1 of Ref. [33]) and by means of the GAP system (Table 2 of Ref. [63]). As achiral derivatives of the composition $H_4A_2p\overline{p}$, the presence of three $\boldsymbol{C}_s$-derivatives, seven $\boldsymbol{C}'_s$-derivatives, and one $\boldsymbol{C}_i$-derivative has been reported.

Among the derivatives collected in Figure 19, one type-IV stereoisogram ([**180**])$_{\rm IV}$ (one achiral cubane derivative) and one type-V stereoisogram ([**190**] [**191**])$_{\rm V}$ (two achiral cubane derivatives forming one pair of *RS*-diastereomers) correspond to the three $\boldsymbol{C}_s$-derivatives. In addition, three type-IV stereoisograms (i.e., ([**182**])$_{\rm IV}$, ([**184**])$_{\rm IV}$, and ([**186**])$_{\rm IV}$) as well as two type-V stereoisograms (i.e., ([**192**] [**193**])$_{\rm V}$ and ([**194**] [**195**])$_{\rm V}$) correspond to the seven $\boldsymbol{C}'_s$-derivatives. Finally, one type-IV stereoisogram ([**188**])$_{\rm IV}$) corresponds to the one $\boldsymbol{C}_i$-derivative.

Moreover, the three type-V stereoisograms shown in the lower part of Figure 19 can be attached with *C/A*-descriptors, even though they are achiral, as shown later in Figure 20. This point also reflects the other reasoning for the fact that the assignment of *C/A*-descriptors is not based on chirality, but on *RS*-stereogenicity. They are chirality-unfaithful cases represented by a lower-case letters *c/a*.

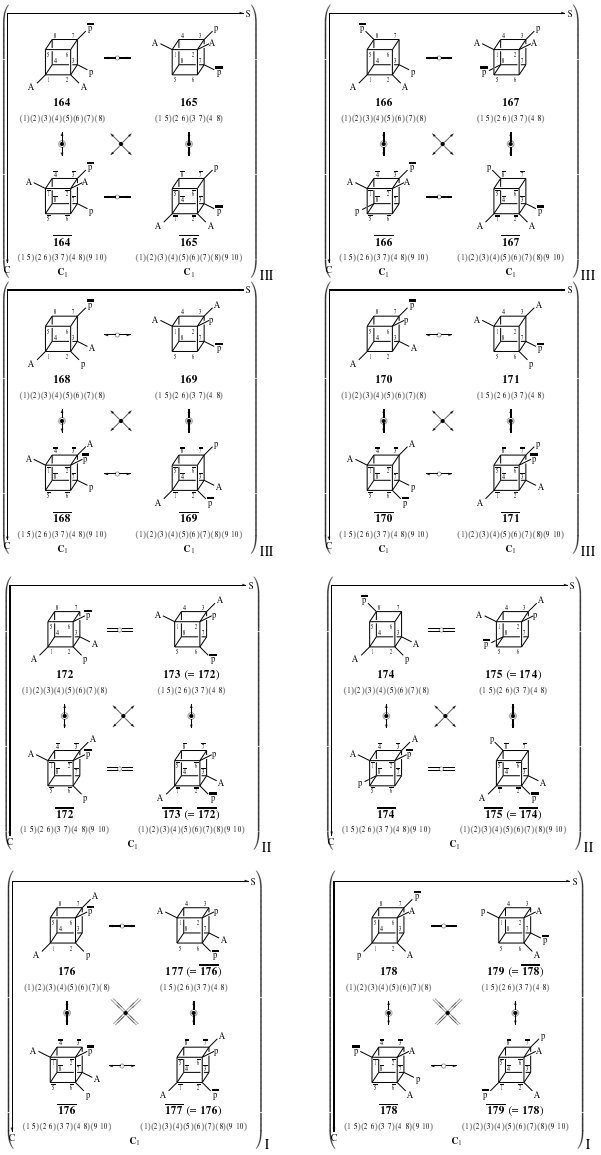

Figure 18. Type-Itemized Enumeration of cubane derivatives with the composition $H_4A_2p\overline{p}$ (Part 1). Chiral cubane derivatives (four type-III stereoisograms, two type-II stereoisograms, and two type-I stereoisograms) with the composition $H_4A_2p\overline{p}$.

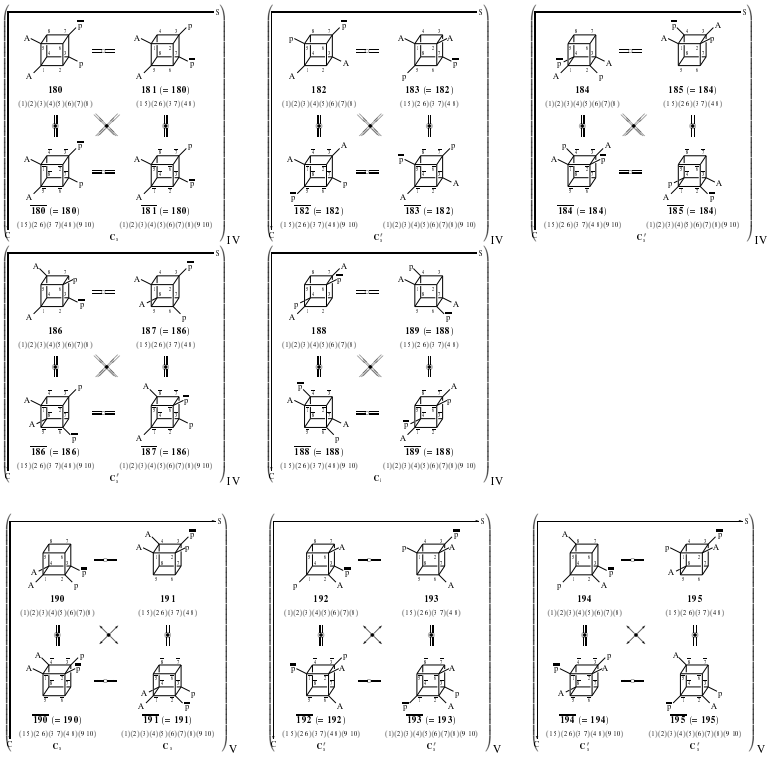

Figure 19. Type-Itemized Enumeration of cubane derivatives with the composition $H_4A_2p\overline{p}$ (Part 2). Achiral cubane derivatives (five type-IV stereoisograms, and three type-V stereoisograms) with the composition $H_4A_2p\overline{p}$.

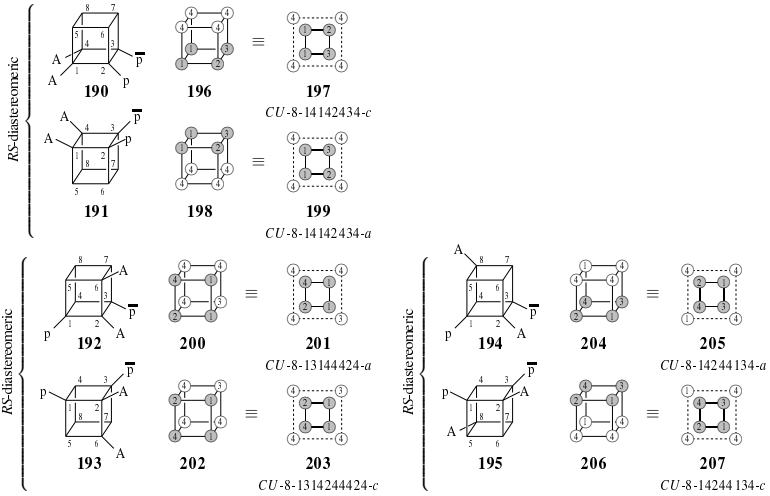

Figure 20. Assignment of *C/A*-descriptors to cubane derivatives of the composition $H_4A_2p\overline{p}$, which are characterized to be type-V stereoisograms. The priority sequence is presumed to be A① > p② > $\overline{p}$③ > H④.

5 Type-V stereoisograms for elucidating "extended pseudoasymmetry"

5.1 Importance of the proligand-promolecule model in enumerations under point groups

For discussing the characteristics of type-V stereoisograms on the basis of Fujita's stereoisogram approach, we should again emphasize the importance of the *proligand-promolecule model* (See Subsection 1.3, Item No. 1) proposed also by Fujita.

According to IUPAC 1996 [10], the term "pseudo-asymmetric carbon atom" is defined that "The traditional name for a tetrahedrally coordinated carbon atom bonded to four different entities, two and only two of which have the same constitution but opposite chirality sense." and that "The *r/s* descriptors of pseudoasymmetric carbon atoms are invariant on reflection in a mirror (i.e. *r* remains *r*, and *s* remains *s*), but are reversed by the exchange of any two entities (i.e. *r* becomes *s*, and *s* becomes

r). Because IUPAC 1996 [10] also defines elsewhere that "An asymmetric atom (chirality centre) is the traditional example of this stereogenic unit.", the term "pseudoasymmetric stereogenic unit" can be produced as an extension by starting the term "pseudoasymmetric carbon atom". At the same time, we can say that "the c/a-descriptors of the newly-defined "pseudoasymmetric stereogenic units" may be defined to be invariant on reflection in a mirror (i.e. c remains c, and a remains a)", if we adopt the C/A-descriptors of a cube [60] according to the indexing system Chemical Abstracts [61]. This extension can be a promising way, only if the "four different entities" described above are defined more distinctively, otherwise than "two and only two of which have the same constitution but opposite chirality sense."

To establish the concrete basis of gross enumerations and symmetry-itemized enumerations of 3D structures under point groups, the author (Fujita) has developed the *proligand-promolecule model* (See Subsection 1.3, Item No. 1) [64–66] and applied to gross-enumerations of alkyl derivatives and alkanes as 3D structures [40, 67–69]. In the process of these enumerations under point groups, the concept of a proligand, which is a structureless but having chirality/achirality for constituting Fujita's proligand-promolecule model, is defined in place of "four different entities" described above (IUPAC 1996 [10]). The nature of structureless should be stressed as a key concept of Fujita's proligand-promolecule model. Thereby, a promolecule is defined as a skeleton with an appropriate number of such achiral or chiral proligands, where the concepts of *sphericity* and *chirality fittingness* are proposed as essential requisites for characterizing substitution modes of proligands (See Subsection 1.3, Item No. 2).

Fujita's USCI approach has been developed to give the four methods of symmetry-itemized enumerations, which is briefly discussed in Subsection 1.3 (Item No. 3) by using cubane derivatives under the point group $\boldsymbol{O}_h$.

5.2 Importance of the proligand-promolecule model in type-itemized enumerations of stereoisograms

Fujita's proligand method (for gross enumerations of 3D structures) and Fujita's USCI approach (for symmetry-itemized enumerations of 3D structures) under point groups have been extended to propose Fujita's stereoisogram approach (for type-itemized enumerations of *RS*-stereoisomers), which is also based on the proligand-promolecule model, but extended to be based on *RS*-stereoisomeric groups (See Figure 2).

The importance of the proligand-promolecule model in Fujita's stereoisogram approach has been discussed as above, during the introduction of type-itemized enumerations of stereoisograms by the half-size-subgroup method (Subsection 4.4) and by the factor-group method (Subsection 4.5). The calculated numbers of types are classified into type-I to type-V. Among the five types, type-V stereoisograms provide us with important clues for discussing pseudoasymmetry base on Fujita's stereoisogram approach (See Figure 2 and compare this figure with Figure 1).

The six type-V stereoisograms of the composition $H_4ABp\overline{p}$ have been depicted in the bottom part of Figure 13. Their features of "extended pseudoasymmetry" [62] can be found by comparing two achiral promolecules contained in each type-V stereoisogram, which is characterized by the presence of equality symbols along the vertical direction. These two achiral promolecules can be differentiated by *a/c*-descriptors collected in Figure 14. For example, the first type-V stereoisogram shown in the second row of Figure 13 is differentiated to be $([\mathbf{80}]\ \ [\mathbf{81}])_V$, where the pair of achiral *RS*-diastereomers, i.e., [**80**] and [**81**], is designated by the pair of *a/c*-descriptors, i.e., *CU*-8-14255535-*a* and *CU*-8-14255535-*c*. Because being chirality-unfaithful due to vertical equality symbols, this pair cannot be used in place of a pair of enantiomers, so that the lowercase letters *a/c* are adopted in place of the uppercase letters *A/C*. The remaining achiral pairs of *RS*-diastereomers collected in Figure 13, i.e., $([\mathbf{82}]\ \ [\mathbf{83}])_V$, $([\mathbf{84}]\ \ [\mathbf{85}])_V$, $([\mathbf{86}]\ \ [\mathbf{87}])_V$, $([\mathbf{88}]\ \ [\mathbf{89}])_V$, and $([\mathbf{90}]\ \ [\mathbf{91}])_V$, are also referred to by the pairs of *a/c*-descriptors obtained by the procedures of Figure 14.

On the other hand, the three type-V stereoisograms of the composition $H_4A_2p\overline{p}$ have been depicted in the bottom part of Figure 19, where each type-V nature is characterized by the presence of equality symbols along the vertical direction. Their features of "extended pseudoasymmetry" [62] can be also found by comparing two achiral promolecules contained in each type-V stereoisogram. These two achiral promolecules can be differentiated by *a/c*-descriptors collected in Figure 20. For example, the first type-V stereoisogram shown in the third row of Figure 19, is differentiated to be $([\mathbf{190}]\ \ [\mathbf{191}])_V$, where the pair of achiral *RS*-diastereomers, i.e., [**190**] and [**191**], is designated by the pair of *a/c*-descriptors, i.e., *CU*-8-14142434-*c* and *CU*-8-14142434-*a*.

The remaining achiral pairs of *RS*-diastereomers collected in Figure 19, i.e., $([\mathbf{192}]\ \ [\mathbf{193}])_V$ and $([\mathbf{194}]\ \ [\mathbf{195}])_V$, are also referred to by the pairs of *a/c*-descriptors obtained by the procedures of Figure 20.

5.3 Cubanes vs. cubic complexes

Among all 12 model polyhedra for 7-, 8-, and 9-coordinate complexes cited in E. STEREOCHEMISTRY AND STEREOPARENTS (III. Coordination compounds. (g) Stereochemical descriptors) of Chem. Abstr. Index Guide [61], cubic complexes (No. 4) are discussed by means of their configuration numbers. As found in the example shown in Figure 21, such a cubic complex as **208** is characterized by the configuration number and the *CA*-descriptor, i.e., *CU*-8-13242542-*A*. On the other hand, its stereoisomer **209** produced by neighboring exchange is a stereoisomer of **208** but not an *RS*-stereoisomer, where **209** is also characterized by the configuration number and the *CA*-descriptor, i.e., *CU*-8-13242542-*A*.

If we obey Figure 2, Figure 21 is regarded to be controlled by the *RS*-stereoisomeric group $\boldsymbol{O}_{h\widetilde{\sigma}\widehat{I}}$ (order $|\boldsymbol{O}_{h\widetilde{\sigma}\widehat{I}}| = 96$) and the stereoisomeric group $\boldsymbol{S}^{[8]}_{\boldsymbol{O}_{h\widetilde{\sigma}\widehat{I}}}$ (order $|\boldsymbol{S}^{[8]}_{\boldsymbol{O}_{h\widetilde{\sigma}\widehat{I}}}| = \boldsymbol{S}^{[8]} \times 2 = 40320 \times 2 = 80640$). Hence, there appear the maximum number $|\boldsymbol{S}^{[8]}_{\boldsymbol{O}_{h\widetilde{\sigma}\widehat{I}}}|/|\boldsymbol{O}_{h\widetilde{\sigma}\widehat{I}}|$ $(= 80640/96 = 840)$ of cosets to explain the isomerization processes of **208** to **209** depicted by such as Figure 21. Because we adopt Figure 2, we should treat cubic complexes (based on an octacoordinated skeleton) by means of the following

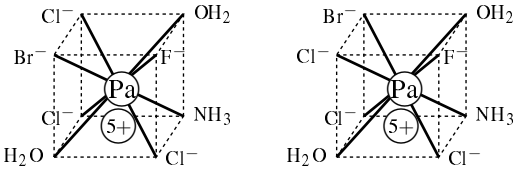

CU-8-13242542-*A* **208**

CU-8-14234225-*C* **209**

Figure 21. Assignment of *C/A*-descriptors to hexahedral protoactinium complexes with the composition $Pa(NH_3)(H_2O)_2Cl_3^-Br^-F^-$. These two complexes are stereoisomeric but not *RS*-stereoisomeric to each other. The priority sequence is presumed to be $Br^-① > Cl^-② > F^-③ > H_2O④ > NH_3⑤$.

scheme:

$$RS\text{-stereoisomerism} \underset{\neq}{\subset} \text{stereoisomerism} \tag{51}$$

In contrast, for referring to cubane derivatives (based on a cubane skeleton), we should obey the following scheme:

$$RS\text{-stereoisomerism} = \text{stereoisomerism} \tag{52}$$

It should be emphasized again that the theoretical framework of the *RS*-stereoisogram approach based on the *RS*-stereoisomeric group $\boldsymbol{O}_{h\widetilde{\sigma}\widehat{I}}$ is commonly effective, even if select either cubane derivatives (Eq. 52) or cubic complexes (Eq. 51). Although the behaviors of cubane derivatives are different from cubic complexes, cubane derivatives are also designated by the configuration number and the *CA*-descriptor.

5.4 Skeletons for the proligand-promolecule model: the concept for covering stereogenic units

The term "stereogenic units" (rather than "stereogenicity") is used widely in IUPAC Recommendations 2013 (P-92.1.1) [55] in accord with Mislow-Siegel's stereogenicity, mainly on the basis of the theoretical framework of Figure 1.

If we re-use the term "stereogenic units" as it is in the theoretical frame-

work of Figure 2, unnecessary verbal transmutations [70, 71] may be induced unconsciously. Hence, the term "stereogenic units" will be replaced by the term "skeletons" in the context of the proligand-promolecule model, although the term "stereogenic" or "stereogenicity" will be maintained in the the theoretical framework of Figure 2 after "*RS*-stereogenicity" is extracted as a key concept. Thereby, we are able to differentiate between Eq. 51 for cubic complexes (based on an octacoordinated skeleton) and Eq. 52 for cubane derivatives (based on a cubane skeleton). This course has merit to have a regard for IUPAC Recommendations 2013 (P-92.1.1) [55] which depend highly on the term "stereogenic units". In addition, it has merit to permit the flexible usage of the term "skeleton" of the proligand-promolecule model during the practices of Fujita's stereoisogram approach.

Finally, it is important to understand the difference between chirality and *RS*-stereogenicity by paying attention to the difference between reflections and permutations of proligands during the processes of applying the proligand-promolecule model to Fujita's stereoisogram approach. Although a reflection operation on an orbit of proligands (along the vertical direction of a stereoisogram) converts a chiral promolecule ($\supset$ molecule) into its enantiomer (mirror image), the reflection operation requires no bond breaking but with the inversion of chirality sence of each proligand ($\supset$ ligand). In contrast, a permutation operation on an orbit of proligands (along the horizontal direction of a stereoisogram) converts an *RS*-stereogenic promolecule ($\supset$ molecule) into its *RS*-diastereomer, where the operation necessitates bond breaking but with no inversion of chirality sence of each proligand ($\supset$ ligand). Note that the resulting enantiomer (according to chirality as the first kind of handedness) and the resulting *RS*-diastereomer (according to *RS*-stereogenicity as the second kind of handedness) would be identical only if a type-I case $[-, -, a]$ [54].

6 Conclusions

Van't Hoff's way and Le Bel's way are compared as two ways of investigation of organic stereochemistry. For emphasizing Le Bel's way, combinatorial enumerations of 3D structures under point groups are first discussed to

develop Fujita's proligand method and Fujita's USCI approach, where (1) the proligand-promolecule model based on a given skeleton, (2) the concept of sphericity of an orbit and chirality fittingness, (3) the concept of the USCI-CF of an orbit, (4) the concept of sphericity of a cycle and chirality fittingness, (5) the emphasis on equivalence relationships and equivalence classes (orbits), and (6) the application of the GAP system after the development of combined-permutation representations (CPRs) as computer-oriented utilities are listed as foundations for further developments. On the basis of these foundations, the concepts of *RS*-stereoisomerism and stereoisomerism have been developed to support synthetic studies of stereoisomers for emphasizing van't Hoff's way. By selecting a cubane skeleton of the point group $\boldsymbol{O}_h$ as probes, *RS*-stereoisomeric groups $\boldsymbol{O}_{h\tilde{\sigma}\hat{I}}$ and stereoisograms as their diagrammatic expressions are developed. After five types (type I to type V) of stereoisograms are classified into three categories (i.e., Category 1 (types I/IV), Category 2 (types II/III/V), and the co-existence case), the half-size-subgroup method and the factor-group method have been developed for type-itemized enumerations of stereoisograms. The enumeration results based on the factor-group method discussed mainly. Type-V stereoisograms for characterizing "extended pseudoasymmetry" are discussed by assigning their configuration numbers and *CA*-descriptors. Importance of the proligand-promolecule model is emphasized in enumerations under point groups (Fujita's proligand method and Fujita's USCI approach) as well as in enumerations of *RS*-stereoisomeric groups (Fujita's stereoisogram approach).

Appendix A

The following CI-CFs are used in the respective calculations of itemized numbers:

CI-CF($\boldsymbol{O}, b_d$) (Eq. 35)	`CICF_O_cube`
CI-CF($\boldsymbol{O}_h, \$_d$) (Eq. 36)	`CICF_Oh_cubeX`
CI-CF($\boldsymbol{O}_{\widetilde{\sigma}}, b_d$ (Eq. 37)	`CICF_Os_cubeX`
CI-CF($\boldsymbol{O}_{\widehat{\sigma}}, \$_d$) (Eq. 38)	`CICF_OI_cubeX`
CI-CF($\boldsymbol{O}_{h\widetilde{\sigma}\widehat{I}}, \$_d$) (Eq. 39)	`CICF_OhsI_cube`

CI-CF(**A**) (Eq. 40)	`CICF_O_cube`
CI-CF(**B**) (Eq. 41)	`CICF_Oh_cubeX_net`
CI-CF(**C**) (Eq. 42)	`CICF_Os_cubeX_nets`
CI-CF(**D**) (Eq. 43)	`CICF_OI_cubeX_netI`

The ligand inventory is changed from the original symbols [H,A,B,X,Y,-Z, p,$\overline{\text{p}}$,q,$\overline{\text{q}}$] to the symbols [A,B,C,D,V,W,p,P,q,Q] for sake of easiness of typesetting. The results of type-itemized enumerations are collected in Table 1 (Category 1), Tables 2 and 3 (Category 2), as well as Table 4 (Category 3: Coexistence of Category 1 and 2).

```
#Read("c:/fujita000/fujita2021/cubaneTypeK4/gap2/enumOh_Os_OI_cubaneK4C.gap");
LogTo("c:/fujita000/fujita2021/cubaneTypeK4/gap2/enumOh_Os_OI_cubaneK4Clog.txt");

#Read("c:/fujita00/fujita2018/subductionOh/gap/CICFgenCC.gapfunc"); #Loading of CICFgenCC.gapfunc
Read("c:/fujita000/fujita2021/cubaneTypeK4/gap2/CICFgenCC.gapfunc"); #Loading of CICFgenCC.gapfunc

b_1 := Indeterminate(Rationals, "b_1"); b_2 := Indeterminate(Rationals, "b_2");
b_3 := Indeterminate(Rationals, "b_3"); b_4 := Indeterminate(Rationals, "b_4");
b_5 := Indeterminate(Rationals, "b_5"); b_6 := Indeterminate(Rationals, "b_6");
b_7 := Indeterminate(Rationals, "b_7"); b_8 := Indeterminate(Rationals, "b_8");
a_1 := Indeterminate(Rationals, "a_1"); a_2 := Indeterminate(Rationals, "a_2");
a_3 := Indeterminate(Rationals, "a_3"); a_4 := Indeterminate(Rationals, "a_4");
a_5 := Indeterminate(Rationals, "a_5"); a_6 := Indeterminate(Rationals, "a_6");
a_7 := Indeterminate(Rationals, "a_7"); a_8 := Indeterminate(Rationals, "a_8");
c_2 := Indeterminate(Rationals, "c_2"); c_4 := Indeterminate(Rationals, "c_4");
c_6 := Indeterminate(Rationals, "c_6"); c_8 := Indeterminate(Rationals, "c_8");



###From FatorG-CICF-typeDlog.txt###############
#################### O ####
CICF_O_cube := 1/24*b_1^8+1/3*b_1^2*b_3^2+3/8*b_2^4+1/4*b_4^2;
################### enantiomeric ############
CICF_Oh_cubeX :=
1/48*b_1^8+1/8*a_1^4*c_2^2+1/6*b_1^2*b_3^2+3/16*b_2^4+1/12*c_2^4+1/8*b_4^2+1/6*c_2*c_6+1/8*c_4^2;
CICF_Oh_cubeX_net := 1/4*a_1^4*c_2^2+1/6*c_2^4+1/3*c_2*c_6+1/4*c_4^2;
################### diasteromeric ############
CICF_Os_cubeX :=
1/48*b_1^8+1/8*b_1^4*b_2^2+1/6*b_1^2*b_3^2+13/48*b_2^4+1/6*b_2*b_6+1/4*b_4^2;
```

```
CICF_Os_cubeX_nets := 1/4*b_1^4*b_2^2+1/6*b_2^4+1/3*b_2*b_6+1/4*b_4^2;
#################### holantimeric ##############
CICF_OI_cubeX :=
1/48*b_1^8+1/48*a_1^8+1/6*b_1^2*b_3^2+3/16*b_2^4+1/6*a_1^2*a_3^2+3/16*c_2^4+1/8*b_4^2+1/8*c_4^2;
CICF_OI_cubeX_netI := 1/24*a_1^8+1/3*a_1^2*a_3^2+3/8*c_2^4+1/4*c_4^2;
#################### OhsI ####
CICF_OhsI_cube :=
1/96*b_1^8+1/96*a_1^8+1/16*b_1^4*b_2^2+1/16*a_1^4*c_2^2+1/12*b_1^2*b_3^2+13/96*b_2^4
+1/12*a_1^2*a_3^2+13/96*c_2^4+1/12*b_2*b_6+1/8*b_4^2+1/12*c_2*c_6+1/8*c_4^2;


A := Indeterminate(Rationals, "A"); B := Indeterminate(Rationals, "B");
C := Indeterminate(Rationals, "C"); D := Indeterminate(Rationals, "D");
V := Indeterminate(Rationals, "V"); W := Indeterminate(Rationals, "W");
p := Indeterminate(Rationals, "p"); P := Indeterminate(Rationals, "P");
q := Indeterminate(Rationals, "q"); Q := Indeterminate(Rationals, "Q");

 aa_1 := A + B + C + D + V + W;
 aa_2 := A^2 + B^2 + C^2 + D^2 + V^2 + W^2;
 aa_3 := A^3 + B^3 + C^3 + D^3 + V^3 + W^3;
 aa_4 := A^4 + B^4 + C^4 + D^4 + V^4 + W^4;
 aa_5 := A^5 + B^5 + C^5 + D^5 + V^5 + W^5;
 aa_6 := A^6 + B^6 + C^6 + D^6 + V^6 + W^6;
 aa_7 := A^7 + B^7 + C^7 + D^7 + V^7 + W^7;
 aa_8 := A^8 + B^8 + C^8 + D^8 + V^8 + W^8;
 bb_1 := A + B + C + D + V + W + p + q + P + Q;
 bb_2 := A^2 + B^2 + C^2 + D^2 + V^2 + W^2 + p^2 + q^2 + P^2 + Q^2;
 bb_3 := A^3 + B^3 + C^3 + D^3 + V^3 + W^3 + p^3 + q^3 + P^3 + Q^3;
 bb_4 := A^4 + B^4 + C^4 + D^4 + V^4 + W^4 + p^4 + q^4 + P^4 + Q^4;
 bb_5 := A^5 + B^5 + C^5 + D^5 + V^5 + W^5 + p^5 + q^5 + P^5 + Q^5;
 bb_6 := A^6 + B^6 + C^6 + D^6 + V^6 + W^6 + p^6 + q^6 + P^6 + Q^6;
 bb_7 := A^7 + B^7 + C^7 + D^7 + V^7 + W^7 + p^7 + q^7 + P^7 + Q^7;
 bb_8 := A^8 + B^8 + C^8 + D^8 + V^8 + W^8 + p^8 + q^8 + P^8 + Q^8;
 cc_2 := A^2 + B^2 + C^2 + D^2 + V^2 + W^2 + 2*p*P + 2*q*Q;
 cc_4 := A^4 + B^4 + C^4 + D^4 + V^4 + W^4 + 2*p^2*P^2 + 2*q^2*Q^2;
 cc_6 := A^6 + B^6 + C^6 + D^6 + V^6 + W^6 + 2*p^3*P^3 + 2*q^3*Q^3;
 cc_8 := A^8 + B^8 + C^8 + D^8 + V^8 + W^8 + 2*p^4*P^4 + 2*q^4*Q^4;

f_O_cube := Value(CICF_O_cube,
[a_1, a_2, a_3, a_4, a_5, a_6, a_7, a_8, b_1, b_2, b_3, b_4, b_5, b_6, b_7, b_8, c_2, c_4, c_6, c_8],
[aa_1, aa_2, aa_3, aa_4, aa_5, aa_6, aa_7, aa_8,
 bb_1, bb_2, bb_3, bb_4, bb_5, bb_6, bb_7, bb_8, cc_2, cc_4, cc_6, cc_8]);;

f_Oh_cube := Value(CICF_Oh_cubeX,
[a_1, a_2, a_3, a_4, a_5, a_6, a_7, a_8, b_1, b_2, b_3, b_4, b_5, b_6, b_7, b_8, c_2, c_4, c_6, c_8],
[aa_1, aa_2, aa_3, aa_4, aa_5, aa_6, aa_7, aa_8,
 bb_1, bb_2, bb_3, bb_4, bb_5, bb_6, bb_7, bb_8, cc_2, cc_4, cc_6, cc_8]);;

f_Os_cube := Value(CICF_Os_cubeX ,
[a_1, a_2, a_3, a_4, a_5, a_6, a_7, a_8, b_1, b_2, b_3, b_4, b_5, b_6, b_7, b_8, c_2, c_4, c_6, c_8],
[aa_1, aa_2, aa_3, aa_4, aa_5, aa_6, aa_7, aa_8,
 bb_1, bb_2, bb_3, bb_4, bb_5, bb_6, bb_7, bb_8, cc_2, cc_4, cc_6, cc_8]);;


f_OI_cube := Value(CICF_OI_cubeX,
[a_1, a_2, a_3, a_4, a_5, a_6, a_7, a_8, b_1, b_2, b_3, b_4, b_5, b_6, b_7, b_8, c_2, c_4, c_6, c_8],
[aa_1, aa_2, aa_3, aa_4, aa_5, aa_6, aa_7, aa_8,
 bb_1, bb_2, bb_3, bb_4, bb_5, bb_6, bb_7, bb_8, cc_2, cc_4, cc_6, cc_8]);;

f_OhsI_cube := Value(CICF_OhsI_cube,
[a_1, a_2, a_3, a_4, a_5, a_6, a_7, a_8, b_1, b_2, b_3, b_4, b_5, b_6, b_7, b_8, c_2, c_4, c_6, c_8],
[aa_1, aa_2, aa_3, aa_4, aa_5, aa_6, aa_7, aa_8,
 bb_1, bb_2, bb_3, bb_4, bb_5, bb_6, bb_7, bb_8, cc_2, cc_4, cc_6, cc_8]);;

################################
f_O_cubeX_net := Value(CICF_O_cube,
[a_1, a_2, a_3, a_4, a_5, a_6, a_7, a_8, b_1, b_2, b_3, b_4, b_5, b_6, b_7, b_8, c_2, c_4, c_6, c_8],
```

```
[aa_1, aa_2, aa_3, aa_4, aa_5, aa_6, aa_7, aa_8,
 bb_1, bb_2, bb_3, bb_4, bb_5, bb_6, bb_7, bb_8, cc_2, cc_4, cc_6, cc_8]);;

f_Oh_cubeX_net := Value(CICF_Oh_cubeX_net,
[a_1, a_2, a_3, a_4, a_5, a_6, a_7, a_8, b_1, b_2, b_3, b_4, b_5, b_6, b_7, b_8, c_2, c_4, c_6, c_8],
[aa_1, aa_2, aa_3, aa_4, aa_5, aa_6, aa_7, aa_8,
 bb_1, bb_2, bb_3, bb_4, bb_5, bb_6, bb_7, bb_8, cc_2, cc_4, cc_6, cc_8]);;

f_Os_cubeX_nets := Value(CICF_Os_cubeX_nets,
[a_1, a_2, a_3, a_4, a_5, a_6, a_7, a_8, b_1, b_2, b_3, b_4, b_5, b_6, b_7, b_8, c_2, c_4, c_6, c_8],
[aa_1, aa_2, aa_3, aa_4, aa_5, aa_6, aa_7, aa_8,
 bb_1, bb_2, bb_3, bb_4, bb_5, bb_6, bb_7, bb_8, cc_2, cc_4, cc_6, cc_8]);;


f_OI_cubeX_netI := Value(CICF_OI_cubeX_netI,
[a_1, a_2, a_3, a_4, a_5, a_6, a_7, a_8, b_1, b_2, b_3, b_4, b_5, b_6, b_7, b_8, c_2, c_4, c_6, c_8],
[aa_1, aa_2, aa_3, aa_4, aa_5, aa_6, aa_7, aa_8,
 bb_1, bb_2, bb_3, bb_4, bb_5, bb_6, bb_7, bb_8, cc_2, cc_4, cc_6, cc_8]);;


j := 0;
list_partitions :=[];
calcCoeffGentype := function(list_partitions)
local list_ligand_L, l_pp;
list_ligand_L := [A,B,C,D,V,W,p,P,q,Q];
l_pp := list_partitions;
j := j + 1;
Print("list_partitions[", j, "] := ", l_pp, "; \n list_FP[", j, "] := [ ",
calcCoeffGen(f_O_cube,list_ligand_L, list_partitions), ", ",
calcCoeffGen(f_Oh_cube,list_ligand_L, list_partitions), ", ",
calcCoeffGen(f_Os_cube,list_ligand_L, list_partitions), ", ",
calcCoeffGen(f_OI_cube,list_ligand_L, list_partitions), ", ",
calcCoeffGen(f_OhsI_cube,list_ligand_L, list_partitions), ", ",
calcCoeffGen(f_O_cubeX_net,list_ligand_L, list_partitions), ", ",
calcCoeffGen(f_Oh_cubeX_net,list_ligand_L, list_partitions), ", ",
calcCoeffGen(f_Os_cubeX_nets,list_ligand_L, list_partitions), ", ",
calcCoeffGen(f_OI_cubeX_netI,list_ligand_L, list_partitions), ", E]; \n");
end;


calcCoeffGentype([8,0,0,0,0,0,0,0,0]);
calcCoeffGentype([7,1,0,0,0,0,0,0,0]);
calcCoeffGentype([6,2,0,0,0,0,0,0,0]);
calcCoeffGentype([6,1,1,0,0,0,0,0,0]);
calcCoeffGentype([5,3,0,0,0,0,0,0,0]);
calcCoeffGentype([5,2,1,0,0,0,0,0,0]);
calcCoeffGentype([5,1,1,1,0,0,0,0,0]);
calcCoeffGentype([4,4,0,0,0,0,0,0,0]);
calcCoeffGentype([4,3,1,0,0,0,0,0,0]);
calcCoeffGentype([4,2,2,0,0,0,0,0,0]);
calcCoeffGentype([4,2,1,1,0,0,0,0,0]);
calcCoeffGentype([4,1,1,1,1,0,0,0,0]);
calcCoeffGentype([3,3,2,0,0,0,0,0,0]);
calcCoeffGentype([3,3,1,1,0,0,0,0,0]);
calcCoeffGentype([3,2,2,1,0,0,0,0,0]);
calcCoeffGentype([3,2,1,1,1,0,0,0,0]);
calcCoeffGentype([2,2,2,2,0,0,0,0,0]);
calcCoeffGentype([2,2,2,1,1,0,0,0,0]);
calcCoeffGentype([2,2,1,1,1,1,0,0,0]);

calcCoeffGentype([7,0,0,0,0,0,1,0,0]);
calcCoeffGentype([6,1,0,0,0,0,1,0,0]);
calcCoeffGentype([6,0,0,0,0,0,2,0,0]);
calcCoeffGentype([6,0,0,0,0,0,1,1,0]);
calcCoeffGentype([6,0,0,0,0,0,1,0,1]);
calcCoeffGentype([5,2,0,0,0,0,1,0,0]);
calcCoeffGentype([5,1,1,0,0,0,1,0,0]);
```

```
calcCoeffGentype([5,1,0,0,0,0,2,0,0,0]);
calcCoeffGentype([5,1,0,0,0,0,1,1,0,0]);
calcCoeffGentype([5,1,0,0,0,0,1,0,1,0]);
calcCoeffGentype([5,0,0,0,0,0,3,0,0,0]);
calcCoeffGentype([5,0,0,0,0,0,2,1,0,0]);
calcCoeffGentype([5,0,0,0,0,0,1,1,1,0]);
calcCoeffGentype([4,0,0,0,0,0,4,0,0,0]);
calcCoeffGentype([4,3,0,0,0,0,1,0,0,0]);
calcCoeffGentype([4,0,0,0,0,0,3,1,0,0]);
calcCoeffGentype([4,0,0,0,0,0,3,0,1,0]);
calcCoeffGentype([4,2,0,0,0,0,2,0,0,0]);
calcCoeffGentype([4,0,0,0,0,0,2,2,0,0]);
calcCoeffGentype([4,0,0,0,0,0,2,0,2,0]);
calcCoeffGentype([4,2,1,0,0,0,1,0,0,0]);
calcCoeffGentype([4,2,0,0,0,0,1,1,0,0]);
calcCoeffGentype([4,2,0,0,0,0,1,0,1,0]);
calcCoeffGentype([4,0,0,0,0,0,2,1,1,0]);
calcCoeffGentype([4,0,0,0,0,0,2,0,1,1]);
calcCoeffGentype([4,1,1,1,0,0,1,0,0,0]);
calcCoeffGentype([4,1,1,0,0,0,1,1,0,0]);
calcCoeffGentype([4,1,1,0,0,0,2,0,0,0]);
calcCoeffGentype([4,1,0,0,0,0,1,1,1,0]);
calcCoeffGentype([4,0,0,0,0,0,1,1,1,1]);
calcCoeffGentype([3,3,1,0,0,0,1,0,0,0]);
calcCoeffGentype([3,3,0,0,0,0,1,1,0,0]);
calcCoeffGentype([3,3,0,0,0,0,1,0,1,0]);
calcCoeffGentype([3,3,0,0,0,0,2,0,0,0]);
calcCoeffGentype([3,2,2,0,0,0,1,0,0,0]);
calcCoeffGentype([3,2,0,0,0,0,2,1,0,0]);
calcCoeffGentype([3,2,1,1,0,0,1,0,0,0]);
calcCoeffGentype([3,2,1,0,0,0,1,1,0,0]);
calcCoeffGentype([3,2,0,0,0,0,1,1,1,0]);
calcCoeffGentype([3,1,1,1,1,1,1,0,0,0]);
calcCoeffGentype([3,1,1,1,1,0,1,0,0,0]);
calcCoeffGentype([3,1,1,1,0,0,1,1,0,0]);
calcCoeffGentype([3,1,1,1,0,0,1,0,1,0]);
calcCoeffGentype([3,1,1,0,0,0,1,1,1,0]);
calcCoeffGentype([3,1,0,0,0,0,1,1,1,1]);
calcCoeffGentype([3,0,0,0,0,0,3,2,0,0]);
calcCoeffGentype([3,0,0,0,0,0,3,1,1,0]);
calcCoeffGentype([3,0,0,0,0,0,3,0,1,1]);
calcCoeffGentype([3,0,0,0,0,0,2,2,1,0]);
calcCoeffGentype([3,0,0,0,0,0,2,1,1,1]);
calcCoeffGentype([2,2,2,0,0,0,2,0,0,0]);
calcCoeffGentype([2,2,0,0,0,0,2,2,0,0]);
calcCoeffGentype([2,0,0,0,0,0,3,2,1,0]);
calcCoeffGentype([2,0,0,0,0,0,3,1,2,0]);
calcCoeffGentype([2,0,0,0,0,0,3,1,1,1]);
calcCoeffGentype([2,0,0,0,0,0,2,2,2,0]);
calcCoeffGentype([2,0,0,0,0,0,2,2,1,1]);
calcCoeffGentype([2,0,0,0,0,0,2,1,2,1]);
calcCoeffGentype([2,2,2,1,0,0,1,0,0,0]);
calcCoeffGentype([2,2,2,0,0,0,1,1,0,0]);
calcCoeffGentype([2,2,2,0,0,0,1,0,1,0]);
calcCoeffGentype([2,2,1,0,0,0,2,1,0,0]);
calcCoeffGentype([2,2,1,0,0,0,2,0,1,0]);
calcCoeffGentype([2,2,0,0,0,0,2,1,1,0]);
calcCoeffGentype([2,2,1,1,1,0,1,0,0,0]);
calcCoeffGentype([2,2,1,1,0,0,2,0,0,0]);
calcCoeffGentype([2,2,1,1,0,0,1,1,0,0]);
calcCoeffGentype([2,2,1,1,0,0,1,0,1,0]);
calcCoeffGentype([2,2,1,0,0,0,1,1,1,0]);
calcCoeffGentype([2,2,0,0,0,0,1,1,1,1]);
calcCoeffGentype([2,1,1,1,1,0,2,0,0,0]);
calcCoeffGentype([2,1,1,1,0,0,2,1,0,0]);
calcCoeffGentype([2,1,1,1,0,0,2,0,1,0]);
calcCoeffGentype([2,1,1,1,1,1,1,0,0,0]);
```

```
calcCoeffGentype([2,1,1,1,1,0,1,1,0,0]);
calcCoeffGentype([2,1,1,1,1,1,0,1,0,1,0]);
calcCoeffGentype([2,1,1,1,0,0,1,1,1,0]);
calcCoeffGentype([2,1,1,0,0,0,1,1,1,1]);

calcCoeffGentype([1,1,1,1,1,1,2,0,0,0]);
calcCoeffGentype([1,1,1,1,1,1,0,3,0,0,0]);
calcCoeffGentype([1,1,1,1,1,1,0,2,1,0,0]);
calcCoeffGentype([1,1,1,1,1,1,0,2,0,1,0]);
calcCoeffGentype([1,1,1,1,1,0,0,2,1,1,0]);
calcCoeffGentype([1,1,1,0,0,0,0,2,1,1,1]);
calcCoeffGentype([1,1,1,1,1,1,1,1,1,1,0,0]);
calcCoeffGentype([1,1,1,1,1,1,0,1,1,1,0]);
calcCoeffGentype([1,1,1,1,1,0,0,1,1,1,1]);
calcCoeffGentype([0,0,0,0,0,0,0,6,2,0,0]);

calcCoeffGentype([0,0,0,0,0,0,0,4,4,0,0]);
calcCoeffGentype([0,0,0,0,0,0,0,4,3,1,0]);
calcCoeffGentype([0,0,0,0,0,0,0,4,2,2,0]);
calcCoeffGentype([0,0,0,0,0,0,0,4,2,1,1]);
calcCoeffGentype([0,0,0,0,0,0,0,3,3,1,1]);
calcCoeffGentype([0,0,0,0,0,0,0,3,2,2,1]);
calcCoeffGentype([0,0,0,0,0,0,0,3,1,3,1]);


LogTo();
```

References

[1] S. Fujita, Stereogenicity revisited. Proposal of holantimers for comprehending the relationship between stereogenicity and chirality, *J. Org. Chem.* **69** (2004) 3158–3165.

[2] S. Fujita, *Mathematical Stereochemistry*, De Gruyter, Berlin, 2015.

[3] S. Fujita, *Mathematical Stereochemistry, 2nd Ed.*, De Gruyter, Berlin, 2021.

[4] J. H. van't Hoff, Voorstel tot Uitbreiding der tegenwoordig in de scheikunde gebruikte Structure-Formules in de ruimte; benevens een daarmee samenhangende opmerking omtrent het verband tusschen optisch Vermogen en Chemische Constitutie van Organische Verbindingen, *Archives Néerlandaises des Sciences Exactes et Naturelles* **9** (1874) 445–454.

[5] J. H. van't Hoff, A Suggestion looking to the extension into space of the structural formulas at present used in chemistry. And a Note upon the relation between the optical activity and the chemical constitution of organic compounds, in: G. M. Richardson (Ed.), *Foundations of Stereochemistry, Memoirs of Pasteur, van't Hoff, Le Bel and Wislicenus*, American Book Co., New York, 1901, pp. 35–46.

[6] K. Mislow and J. Siegel, Stereoisomerism and local chirality, *J. Am. Chem. Soc.* **106** (1984) 3319–3328.

[7] J. A. Le Bel, Sur les Relations qui existent entre les Formules atomiques des Corps organique et le Pouvoir rotatoire de leurs Dissolutions, *Bull. Soc. Chim. Fr. II* **22** (1874) 337–347.

[8] J. A. Le Bel, On the relations which exist between the atomic formulas of organic compounds and the rotatory power of their solutions, in: O. T. Benfey (Ed.), *Classics in the Theory of Chemical Combination*, Dover, New York, 1963, pp. 161–171.

[9] W. T. Kelvin, The baltimore lectures on molecular dynamics and the wave theory of light, Appendix H, *C. J. Clay & Sons, London* (1904) 619–619.

[10] G. P. Moss, IUPAC Organic Chemistry Division, Basic terminology of stereochemistry (IUPAC recommendations 1996), *Pure Appl. Chem.* **68** (1996) 2193–2222.

[11] S. Fujita, Systematic comparison between three-dimensional structures and graphs (part 1). the fate of asymmetry and pseudoasymmetry in the enumeration of monosubstituted alkanes, *MATCH Commun. Math. Comput. Chem.* **62** (2009) 23–64.

[12] S. Fujita, Systematic comparison between three-dimensional structures and graphs (Part 2). The fate of asymmetry and pseudoasymmetry in the enumeration of alkanes, *MATCH Commun. Math. Comput. Chem.* **62** (2009) 65–104.

[13] S. Fujita, Stereoisograms for specifying chirality and *RS*-stereogenicity. A versatile tool for avoiding the apparent inconsistency between geometrical features and *RS*-nomenclature in stereochemistry, *MATCH Commun. Math. Comput. Chem.* **61** (2009) 11–38.

[14] S. Fujita, Stereoisograms for reorganizing the theoretical foundations of stereochemistry and stereoisomerism: II. Rational avoidance of misleading standpoints for *R/S*-stereodescriptors of the Cahn-Ingold-Prelog system, *Tetrahedron: Asymmetry* **25** (2014) 1169–1189.

[15] S. Fujita, Pseudoasymmetry, stereogenicity, and the *RS*-nomenclature comprehended by the concepts of holantimers and stereoisograms, *Tetrahedron* **60** (2004) 11629–11638.

[16] S. Fujita, Complete settlement of long-standing confusion on the term "prochirality" in stereochemistry. Proposal of pro-*RS*-stereogenicity and integrated treatment with prochirality, *Tetrahedron* **62** (2006) 691–705.

[17] S. Fujita, Stereoisograms for reexamining the concept of prochirality, *Yuki Gosei Kagaku Kyokai-Shi/J. Synth. Org. Chem. Jpn.* **66** (2008) 995–1004.

[18] S. Fujita, Importance of the proligand-promolecule model in stereochemistry. I. the Unit-Subduced-Cycle-Index (USCI) approach to geometric features of prismane derivatives, *J. Math. Chem.* **50** (2012) 2202–2222.

[19] S. Fujita, Importance of the proligand-promolecule model in stereochemistry. II. the stereoisogram approach to stereoisomeric features of prismane derivatives, *J. Math. Chem.* **50** (2012) 2168–2201.

[20] O. E. Polansky, Pólya's method for the enumeration of isomers, *MATCH Commun. Math. Comput. Chem.* **1** (1975) 11–31.

[21] G. Pólya, R. C. Read, *Combinatorial Enumeration of Groups, Graphs, and Chemical Compounds*, Springer, New York, 1987.

[22] S. Fujita, Chirality fittingness of an orbit governed by a coset representation. Integration of point-group and permutation-group theories to treat local chirality and prochirality, *J. Am. Chem. Soc.* **112** (1990) 3390–3397.

[23] S. Fujita, *Symmetry and Combinatorial Enumeration in Chemistry*, Springer-Verlag, Berlin, 1991.

[24] S. Fujita, Orbits in a molecule. A novel way of stereochemistry through the concepts of coset representations and sphericities (Part 1), *MATCH Commun. Math. Comput. Chem.* **54** (2005) 251–300.

[25] W. Burnside, *Theory of Groups of Finite Order*, Cambridge Univ. Press, Cambridge, 1911.

[26] S. Fujita, Enumeration of digraphs with a given automorphism group, *J. Math. Chem.* **12** (1993) 173–195.

[27] S. Fujita, Generalization of partial cycle indices and modified bisected mark tables for combinatorial enumeration, *Bull. Chem. Soc. Jpn.* **73** (2000) 329–339.

[28] S. Fujita, Subduction of coset representations. An application to enumeration of chemical structures, *Theor. Chim. Acta* **76** (1989) 247–268.

[29] S. Fujita, Subduction of coset representations. An application to enumeration of chemical structures with achiral and chiral ligands, *J. Math. Chem.* **5** (1990) 121–156.

[30] S. Fujita, Systematic enumeration of high symmetry molecules by means of unit subduced cycle indices with and without chirality fittingness, *Bull. Chem. Soc. Jpn.* **63** (1990) 203–215.

[31] S. Fujita, The USCI approach and elementary superposition for combinatorial enumeration, *Theor. Chim. Acta* **82** (1992) 473–498.

[32] S. Fujita, Symmetry-itemized enumeration of cubane derivatives as three-dimensional entities by the fixed-point matrix method of the USCI approach, *Bull. Chem. Soc. Jpn.* **84** (2011) 1192–1207.

[33] S. Fujita, Symmetry-itemized enumeration of cubane derivatives as three-dimensional entities by the partial-cycle-index method of the USCI approach, *Bull. Chem. Soc. Jpn.* **85** (2012) 793–810.

[34] S. Fujita, Symmetry-itemized enumeration of cubane derivatives as three-dimensional entities by the elementary-superposition method of the USCI approach, *Bull. Chem. Soc. Jpn.* **85** (2012) 811–821.

[35] S. Fujita, Graphs to chemical structures 1. Sphericity indices of cycles for stereochemical extension of Pólya's theorem, *Theor. Chem. Acc.* **113** (2005) 73–79.

[36] S. Fujita, Sphericities of cycles. What Pólya's theorem is deficient in for stereoisomer enumeration, *Croat. Chem. Acta* **79** (2006) 411–427.

[37] S. Fujita, *Combinatorial Enumeration of Graphs, Three-Dimensional Structures, and Chemical Compounds*, Univ. Kragujevac, Kragujevac, 2013.

[38] S. Fujita, Graphs to chemical structures 2. Extended sphericity indices of cycles for stereochemical extension of Pólya's coronas, *Theor. Chem. Acc.* **113** (2005) 80–86.

[39] S. Fujita, Graphs to chemical structures 3. General theorems with the use of different sets of sphericity indices for combinatorial enumeration of nonrigid stereoisomers, *Theor. Chem. Acc.* **115** (2006) 37–53.

[40] S. Fujita, Graphs to chemical structures 4. Combinatorial enumeration of planted three-dimensional trees as stereochemical models of monosubstituted alkanes, *Theor. Chem. Acc.* **117** (2007) 353–370.

[41] S. Fujita, Combinatorial enumeration of cubane derivatives as three-dimensional entities. I. Gross enumeration by the proligand method, *MATCH Commun. Math. Comput. Chem.* **67** (2012) 5–24.

[42] S. Fujita, Combinatorial enumeration of cubane derivatives as three-dimensional entities. II. Gross enumeration by the markaracter method, *MATCH Commun. Math. Comput. Chem.* **67** (2012) 25–54.

[43] S. Fujita, Combinatorial enumeration of cubane derivatives as three-dimensional entities. III. Gross enumeration by the characteristic-monomial method, *MATCH Commun. Math. Comput. Chem.* **67** (2012) 649–668.

[44] S. Fujita, Combinatorial enumeration of cubane derivatives as three-dimensional entities. IV. Gross enumeration by the extended superposition method, *MATCH Commun. Math. Comput. Chem.* **67** (2012) 669–686.

[45] S. Fujita, Combinatorial enumeration of cubane derivatives as three-dimensional entities. V. Gross enumeration by the double coset representation method, *MATCH Commun. Math. Comput. Chem.* **67** (2012) 687–712.

[46] S. Fujita, Orbits among molecules. A novel way of stereochemistry through the concepts of coset representations and sphericities (Part 2), *MATCH Commun. Math. Comput. Chem.* **55** (2006) 5–38.

[47] S. Fujita, Combinatorial enumeration of stereoisomers by linking orbits in molecules with orbits among molecules. A novel way of stereochemistry through the concepts of coset representations and sphericities (Part 3), *MATCH Commun. Math. Comput. Chem.* **55** (2006) 237–270.

[48] S. Fujita, Mandalas and Fujita's proligand method. A novel way of stereochemistry through the concepts of coset representations and sphericities (Part 4), *MATCH Commun. Math. Comput. Chem.* **57** (2007) 5–48.

[49] S. Fujita, Computer-oriented representations of point groups and cycle indices with chirality fittingness (CI-CFs) calculated by the GAP system. enumeration of three-dimensional structures of ligancy 4 by Fujita's proligand method, *MATCH Commun. Math. Comput. Chem.* **76** (2016) 379–400.

[50] https://www.gap-system.org/.

[51] S. Fujita, Computer-oriented representations of $\mathbf{O}_h$-skeletons for supporting combinatorial enumeration by Fujita's proligand method. GAP calculation of cycle indices with chirality fittingness (CI-CFs), *MATCH Commun. Math. Comput. Chem.* **77** (2017) 409–442.

[52] S. Fujita, Concordant generation of mark tables and USCI-CF (unit subduced cycle indices with chirality fittingness) tables on the basis of combined-permutation representations, *MATCH Commun. Math. Comput. Chem.* **82** (2019) 295–326.

[53] S. Fujita, Standardization of mark tables and USCI-CF (unit subduced cycle indices with chirality fittingness) tables derived from different $\mathbf{O}_h$-skeletons, *MATCH Commun. Math. Comput. Chem.* **82** (2019) 327–373.

[54] S. Fujita, Chirality and *RS*-stereogenicity as two kinds of handedness. Their Aufheben by Fujita's stereoisogram approach for giving new insights into classification of isomers, *Bull. Chem. Soc. Jpn.* **89** (2016) 987–1017.

[55] H. A. Favre, W. H. Powell, *Nomenclature of Organic Chemistry: IUPAC Recommendations and Preferred Names 2013*, Royal Soc. Chem., Cambridge, 2013.

[56] S. Fujita, Stereoisograms of octahedral complexes. II. *RS*-stereogenicity vs. stereogenicity as well as *RS*-stereoisomerism vs. stereoisomerism, *MATCH Commun. Math. Comput. Chem.* **71** (2014) 537–574.

[57] S. Fujita, Type-itemized enumeration of *RS*-stereoisomers of octahedral complexes, *Iranian J. Math. Chem.* **7** (2016) 113–153; The symbols $[\theta]^*_{15}$, $[\theta]^*_{19}$, $[\theta]^*_{27}$, $[\theta]^*_{30}$, $[\theta]^*_{40}$, and $[\theta]^*_{45}$ in Table 2 should be corrected to be $[\theta]_{15}$, $[\theta]_{19}$, $[\theta]_{27}$, $[\theta]_{30}$, $[\theta]_{40}$, and $[\theta]_{45}$.

[58] S. Fujita, Type-itemized enumeration of five types of stereoisograms and their simplified diagrams for characterizing cubane derivatives, *Bull. Chem. Soc. Jpn.* **95** (2022) 000–000.

[59] S. Fujita, Stereoisograms of cubane derivatives., *Bull. Chem. Soc. Jpn.* **88** (2015) 1653–1679.

[60] M. F. Brown, B. R. Cook, and T. E. Sloan, Stereochemical notation in coordination chemistry. mononuclear complexes, *Inorg. Chem.* **14** (1975) 1273–1278.

[61] Chemical Abstract Service, *Naming and Indexing of Chemical Substances for Chemical Abstracts, 2007 Edition*, Am. Chem. Soc., Columbus, 2008.

[62] S. Fujita, Extended pseudoasymmetry and geometric prochirality clarifying the scope of the concepts of holantimers and stereoisograms, *Tetrahedron: Asymmetry* **23** (2012) 623–634.

[63] S. Fujita, Application of GAP (Groups, Algorithms and Programming) system to stereoisograms for characterizing *RS*-stereoisomers of cubane derivatives, *MATCH Commun. Math. Comput. Chem.* **87** (2022) 207–270.

[64] S. Fujita, Promolecules for characterizing stereochemical relationships in non-rigid molecules, *Tetrahedron* **47** (1991) 31–46.

[65] S. Fujita, Promolecules with a subsymmetry of $\mathbf{D}_{\infty h}$. combinatorial enumeration and stereochemical properties, *J. Chem. Inf. Comput. Sci.* **32** (1992) 354–363.

[66] S. Fujita, Promolecules with a subsymmetry of $\mathbf{O}_h$. Combinatorial enumeration and stereochemical properties, *Polyhedron* **12** (1993) 95–110.

[67] S. Fujita, Numbers of monosubstituted alkanes as stereoisomers, *J. Comput. Chem. Jpn.* **6** (2007) 59–72.

[68] S. Fujita, Enumeration of primary, secondary, and tertiary monosubstituted alkanes as stereoisomers, *J. Comput. Chem. Jpn.* **6** (2007) 73–90.

[69] S. Fujita, Graphs to chemical structures 5. Combinatorial enumeration of centroidal and bicentroidal three-dimensional trees as stereochemical models of alkanes, *Theor. Chem. Acc.* **117** (2007) 339–351.

[70] E. L. Eliel, Infelicitous sterochemical nomenclature, *Chirality* **9** (1997) 428–430.

[71] K. Mislow, Stereochemical terminology and its discontents, *Chirality* **14** (2002) 126–134.